Alaska Geobotany Center

ALASKA GEOBOTANY CENTER DATA REPORT

AGC 23-02

NATURAL ICE-RICH PERMAFROST OBSERVATORY PRUDHOE BAY, ALASKA: 2022 FIELD ACTIVITIES

DONALD A. WALKER, HELENA BERGSTEDT, AMY L. BREEN, RONALD DAANEN, OLIVIA HOBGOOD, BENJAMIN M. JONES, ANJA KADE, MIKHAIL KANEVSKIY, ANNA KUČEROVÁ, ANNA K. LILJEDAHL, ELIOS MANOS, DMITRY J. NICOLSKY, JANA L. PEIRCE, MARTHA K. RAYNOLDS, VLADIMIR E. ROMANOVSKY, SERGEI RYBAKOV, YURI L. SHUR, EMILY WATSON-COOK, CHANDI WITHARANA

EDITED BY D. A. WALKER AND J. L. PEIRCE

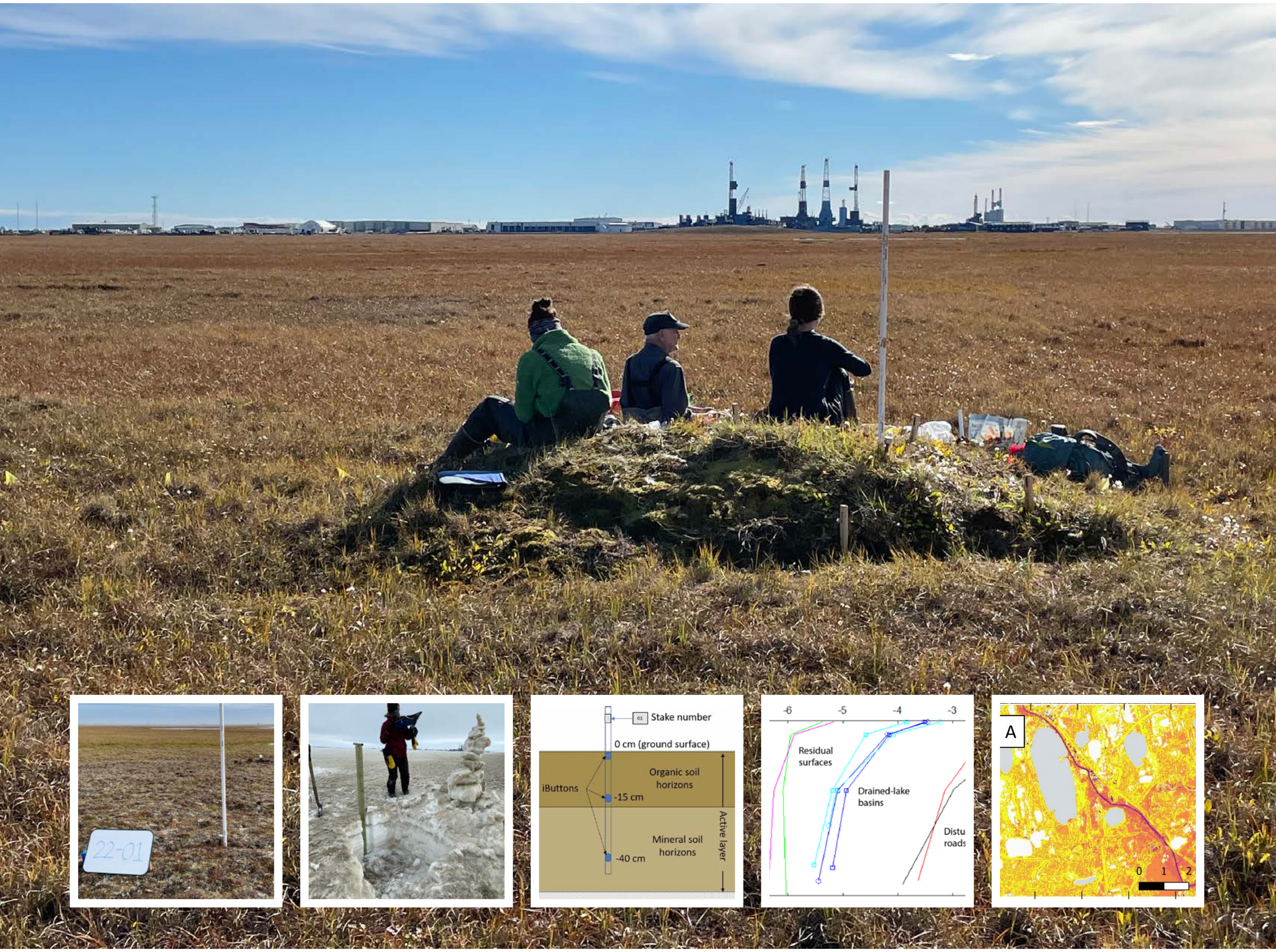

MARCH 2023

NNAIRPS Ice-Rich Permafrost Systems

UAF UNIVERSITY OF ALASKA FAIRBANKS

A PUBLICATION OF THE ALASKA GEOBOTANY CENTER 23-02
INSTITUTE OF ARCTIC BIOLOGY, UNIVERSITY OF ALASKA FAIRBANKS

NATURAL ICE-RICH PERMAFROST OBSERVATORY PRUDHOE BAY, ALASKA: 2022 FIELD ACTIVITIES

ALASKA GEOBOTANY CENTER DATA REPORT 23-02 :: MARCH 2023

Edited by
DONALD A. WALKER AND JANA L. PEIRCE

TABLE OF CONTENTS

Acknowledgments ... ii
Contributors ... iii
Preface ... iv

1 The Prudhoe Bay region and the main NNA-IRPS study area
1.1 NIRPO site ... 1

2 2022 Field Season
2.1 Vegetation studies ... 5
2.2 Snow survey ... 13
2.3 Soil-temperature loggers ... 16
2.4 Thaw depths, water depths, and vegetation heights ... 16
2.5 Greenhouse gas fluxes ... 17
2.6 Permafrost studies ... 21
2.7 Remote-sensing studies ... 30

3 Summary of accomplishments and observations of the 2022 studies and future directions
3.1 The NIRPO research area ... 36
3.2 Vegetation studies ... 36
3.3 Permafrost ... 37
3.4 Remote sensing ... 38
3.5 Future directions and synthesis ... 39

4 References ... 40

Appendices ... 43

UNIVERSITY OF ALASKA FAIRBANKS

Funding acknowledgment

Principal funding for this research is provided by the National Science Foundation (NSF) *Navigationg the New Arctic: Landscape evolution and adapting to change in Ice-Rich Permafrost Systems (NNA-IRPS)* project (RISE Award 1928237). The participation of several team members was supported by additional funding, including NSF awards to Yuri Shur and Mikhail Kanevskiy (OPP Award 1820883); Vladimir Romanovsky and Dmitry Nicolsky (OPP Award 1832238, RISE Award 1927708); Ben Jones and colleagues (OPP Award 1806213); Anna Liljedahl and colleagues (RISE Awards 1927723 and 2052107); and through an intern scholarship from Masaryk University, Czechia, to Anna Kučerová. Logistic support was provided by the Battelle Arctic Research Operations office in Fairbanks and the Institute of Arctic Biology, University of Alaska Fairbanks.

How to cite this volume

Walker, D. A. and J. L. Peirce (editors). 2023. Natural Ice-Rich Permafrost Observatory, Prudhoe Bay, Alaska: 2022 field activities. AGC 23-02 Data Report. Alaska Geobotany Center, Institute of Arctic Biology, University of Alaska, Fairbanks, AK, USA.

On the cover

Lunch on a bird mound along Transet 8 at the NIRPO site, Prudhoe Bay Oilfield (credit: A.L. Breen). **Inset figures from left:** 2022 vegetation studies, see p. 5 (credit: A.L. Breen); snow survey, see p. 13 (credit: A.L. Breen); soil temperature loggers, see p. 16 (credit: D.A. Walker); near-surface permafrost temperatures, see p. 21 (credit: D.J. Nicolsky); remote sensing of dust impacts, see p. 31 (credit: H. Bergstedt).

CONTRIBUTORS

HELENA BERGSTEDT, PHD
b.geos GmbH, Korneburg, Austria

AMY L. BREEN, PHD
Alaska Geobotany Center, Institute of Arctic Biology & International Arctic Research Center, University of Alaska Fairbanks

RONALD P. DAANEN, PHD
Division of Geological & Geophysical Surveys, Department of Natural Resources, State of Alaska

OLIVIA HOBGOOD
Alaska Geobotany Center, Institute of Arctic Biology & Department of Biology and Wildlife, University of Alaska Fairbanks

BENJAMIN M. JONES, PHD
Water Environmental Research Center, Institute of Northern Engineering, University of Alaska Fairbanks

ANJA N. KADE, PHD
Alaska Geobotany Center, Institute of Arctic Biology & Department of Biology and Wildlife, University of Alaska Fairbanks

MIKHAIL KANEVSKIY, PHD
Water Environmental Research Center, Institute of Northern Engineering, University of Alaska Fairbanks

ANNA KUČEROVÁ
Department of Botany and Zoology, Masaryk University, Brno, Czech Republic

ANNA K. LILJEDAHL, PHD
Woodwell Climate Research Center, Falmouth, Massachusetts

ELIAS MANOS
Department of Geography, University of Connecticut

DMITRY J. NICOLSKY, PHD
Permafrost Laboratory, Geophysical Institute, University of Alaska Fairbanks

JANA L. PEIRCE
Alaska Geobotany Center, Institute of Arctic Biology, University of Alaska Fairbanks

MARTHA K. RAYNOLDS, PHD
Alaska Geobotany Center, Institute of Arctic Biology, University of Alaska Fairbanks

VLADIMIR E. ROMANOVSKY, PHD
Permafrost Laboratory, Geophysical Institute, University of Alaska Fairbanks (Emeritus)

SERGEI RYBAKOV
Department of Geosciences, University of Alaska Fairbanks

YURI L. SHUR, PHD, PE
Water Environmental Research Center, Institute of Northern Engineering & Department of Civil, Geological, and Environmental Engineering, University of Alaska Fairbanks

DONALD A. WALKER, PHD
Alaska Geobotany Center, Institute of Arctic Biology & Department of Biology and Wildlife, University of Alaska Fairbanks

EMILY WATSON-COOK
Alaska Geobotany Center, Institute of Arctic Biology & Department of Biology and Wildlife, University of Alaska Fairbanks

CHANDI WITHARANA, PHD
Department of Natural Resources & The Environment, University of Connecticut

Preface

The National Science Foundation's Navigating the New Arctic (NNA) initiative is conducting fundamental convergence research across the social, natural, and built environments to inform our understanding of Arctic change at local to global scales.

The NNA project *Landscape evolution and adapting to change in Ice-Rich Permafrost Systems (NNA-IRPS)* is examinging the cumulative impacts of climate change and infrastructure in the Prudhoe Bay region and Point Lay, Alaska. The umbrella research questions are:

- How are climate change and infrastructure affecting ice-rich permafrost systems (IRPSs)?
- What roles do ecosystems play in the development and degradation of ice-rich permafrost?
- How can people and their infrastructure adapt to changing ice-rich permafrost?

This report focuses on the 2022 field season at Prudhoe Bay, where the main objectives were to: (1) continue to establish a new Natural Ice-Rich Permafrost Observatory (NIRPO), and (2) conduct baseline observations of permafrost, hydrology, vegetation, climate, snow, and trace-gas fluxes at the NIRPO and other sites that are part of the NNA-IRPS cluster of research sites.

The information from these studies is summarized in four sections of this report:

1. Descriptions of the study areas
2. Descriptions of the 2022 field studies divided into seven subsections
3. Summary of accomplishments and future directions
4. Appendices containing the field data

1 The Prudhoe Bay region and the main NNA-IRPS study areas

D.A. Walker and Martha Raynolds

The Prudhoe Bay Oilfield (PBO) was the first major oilfield discovered on Alaska's North Slope. It is now part of the largest industrial complex in the North American Arctic. Its history, geo-ecology, and cumulative impacts of development have been described in several publications (e.g., Brown 1975; Walker 1985, Walker et al. 1980, 1987, 2014, 2022a; Rawlinson 1993; Truett and Johnson 2000; National Research Council 2003; Jorgenson 2011; Raynolds et al. 2014).

The main NNA-IRPS research area (Figure 1) contains the Natural Ice-Rich Permafrost Observatory (NIRPO) and several other long-term permafrost research sites near Deadhorse, including Vladimir Romanovsky's Deadhorse station (Romanovsky and Osterkamp 1995), the Jorgenson site (Jorgenson et al. 2015, Kanevskiy et al. 2017, Koch et al. 2018, Wickland et al. 2020), and the Colleen and Airport roadside sites (Walker et al. 2015, 2016, 2018, 2022a; Kanevskiy et al. 2022) (Figure 1b).

1.1 NIRPO site

The NIRPO site (Figures 2 and 3) is relatively isolated from most infrastructure-related impacts and provides a relatively undisturbed landscape to compare with the disturbed landscapes at the Colleen and Airport sites. Although most changes to the vegetation

Figure 1. ***a.*** *The eastern portion of the Prudhoe Bay oilfield showing study areas of the NNA-IRPS project. A, B, and C are areas of concentrated development where detailed geo-ecological and historical changes have been mapped (Walker et al. 1987, 2014; National Research Council 2003; Raynolds et al. 2014).* ***b.*** *Detail of the main NNA-NIRPO study area. Most field research during 2022 was conducted at the Colleen, NIRPO, Jorgenson and Airport sites. Climate and permafrost borehole temperature data were from the Romanovsky Deadhorse station and the Deadhorse Airport. Ice-wedge degradation studies were conducted at all sites including the Erosion and Culvert sites. (Credit: D.A. Walker. Basemap: Google Earth)*

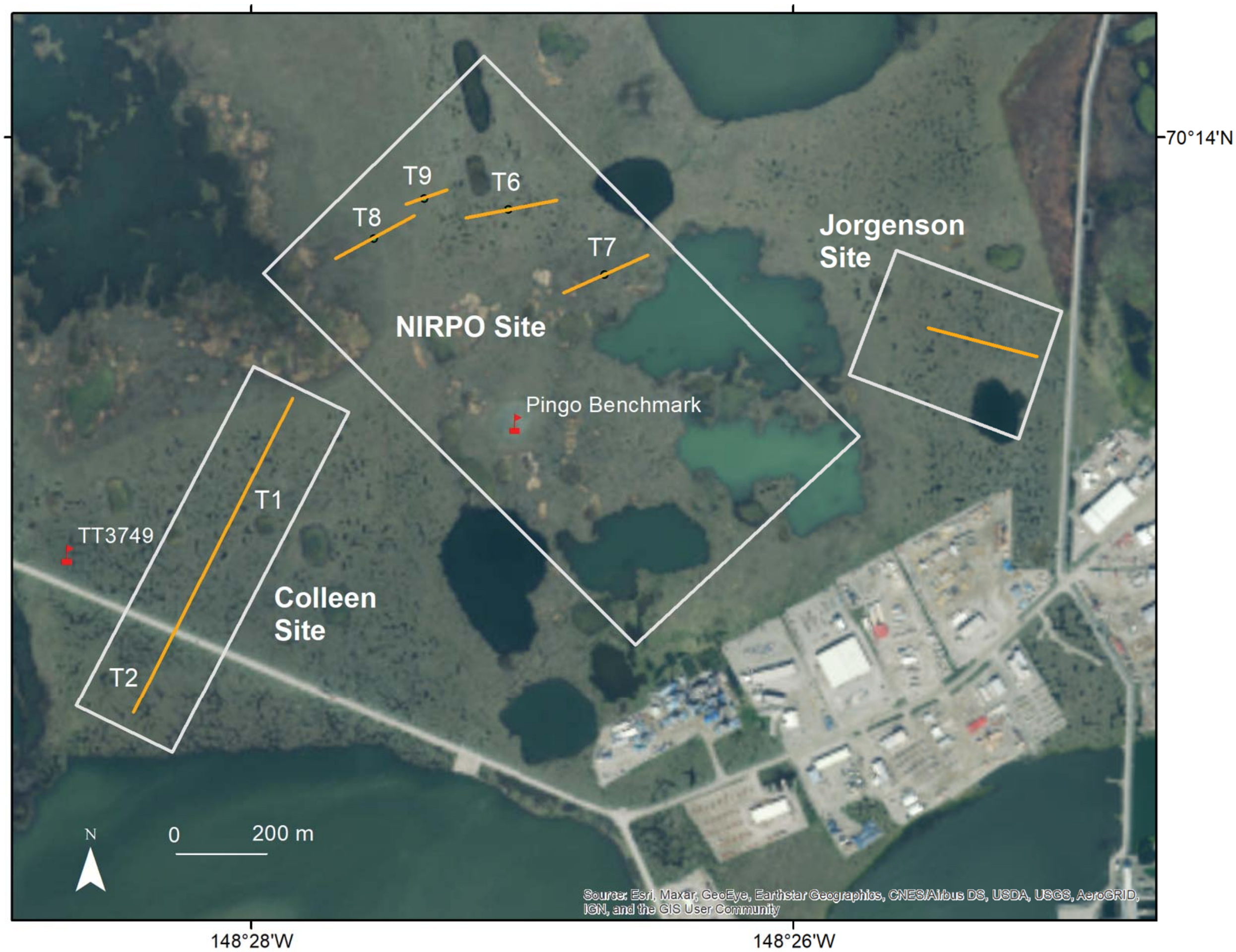

Figure 2. *The Colleen, NIRPO, and Jorgenson sites and research transects at each site. Transects T3, T4, and T5 are located at the Airport site (Figure 1b). See Walker et al. 2016 for Airport site details. (Credit: M.K. Raynolds. Basemap: North Slope Borough, Maxar / ESRI)*

and landforms at the NIRPO site are associated with climate change, there are also impacts that occur widely throughout the PBO, including vehicle trails from past seismic operations and other off-road activities, low levels of road dust from the PBO road network, and atmospheric emissions from industrial activities (Walker et al. 2022a).

In 2022, boundaries of the NIRPO site included four transects, a small pingo, several small lakes, and wetlands in the vicinity of the pingo (Figure 2).

Transect T6 (200 m) (Figure 3a) is on a surface with no evidence of having been affected by thaw lake processes. The surficial geology has been mapped as Quaternary-Period alluvial-plain sand and gravel deposits (Qsg, Rawlinson 1993). The patterned-ground features are mainly well-developed transitional and high-centered polygons with many thermokarst ponds.

Transect T7 (200 m) (Figure 3b) is in a complex drained-lake basin, where the surficial geology is mapped as Ice-Rich Thaw-Lake Deposits (Qti). The east end of T7 is in an area with low-centered polygons and thermokarst features. The west end of T7 is a complex wetland with disjunct polygons and shallow ponds with marl-covered pond bottoms.

Transect T8 (200 m) (Figure 3c) is in a young, drained thaw-lake basin. The east end of T8 is in a somewhat older portion where the surficial geology has been mapped as Ice-Rich Thaw-Lake Deposits (Qti), which has disjunct ice-wedge-polygon features. The west end of T8 is on younger Thaw-Lake Deposits (Qt) with flat wet generally featureless terrain.

Transect T9 (100-m) (Figure 3d) crosses the boundary of the same drained thaw-lake basin that contains T8. The east end is outside of the drained lake basin on a low lake margin with surficial geology mapped as Alluvial-Plain Deposits (Qsg). The surface features include well-drained high-centered polygons and infrequent ice-wedge thermokarst ponds. The west end of T9 is on Ice-Rich Thaw-Lake Deposits (Qti) with weakly developed low-centered ice-wedge polygons.

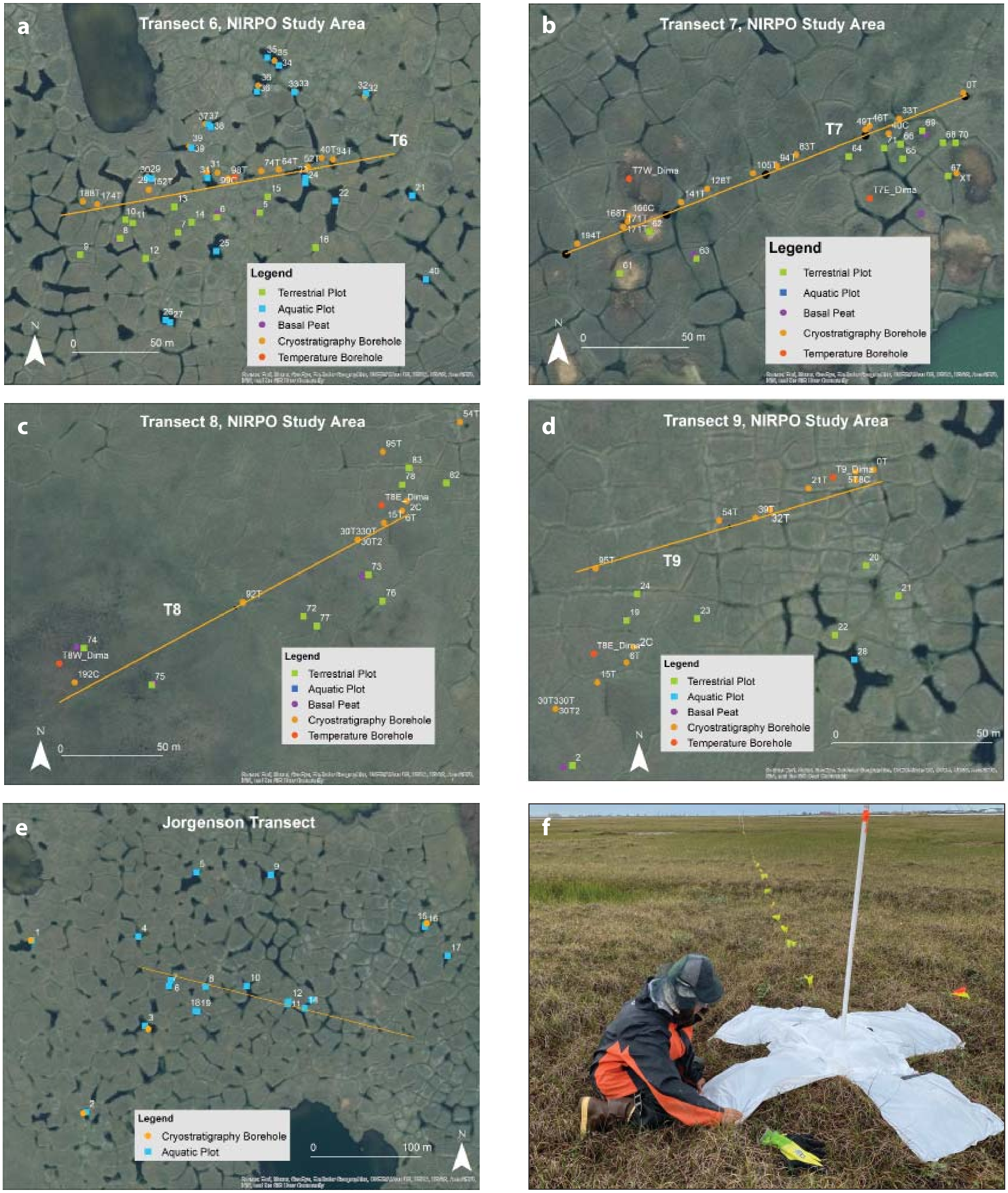

Figure 3. *NIRPO and Jorgenson transects and study plots.* ***a-e.*** *NIRPO transects T6–T9 and the Jorgenson transect with the locations of terrestrial and aquatic vegetation plots, basal peat samples, cryostratigraphy boreholes, and temperature boreholes sampled in 2021. Note: Terrestrial and aquatic plot numbers are abbreviated on the maps. Plot numbers on field markers and cited elsewhere in this report include a prefix starting with the last two digits of the year of sampling, e.g. 21-__ for terrestrial plots and 21A-__ for aquatic plots established in 2021. (Credits: M.K. Raynolds. Basemap: North Slope Borough, Maxar / ESRI).* ***f.*** *The east end of transect T8 with large "X" marking the location for aerial surveys. The pin flags spaced at 1-m intervals along the transect are for monitoring thaw depths, water depths, vegetation type, spectral characteristics, and other site and vegetation factors. (Credit: J.L. Peirce, IMG 4283)*

Photographs of typical terrain along each transect are in AGC 22-01 (Figures 23–26 in Walker et al. 2022b).

Data collected in 2021 at or near plots along transects T6–T9 included:

- Vegetation surveys in 35 terrestrial plots (Figures 3a–d, green squares)
- Vegetation surveys in 39 aquatic plots along transect T6 and the Jorgenson Transect (Figures 3a and 3e, blue squares)
- Trace-gas flux measurements from 33 of the permanent vegetation plots along transects T6 and T7 (see Table 1 in the AGC 22-01 data report, Walker eτ al. 2022b)
- Basal peat samples from a selection of 10 plots along T6–T9 (Figures 3b-f, purple circles)
- 53 cryostratigraphy boreholes in polygon centers, rims, troughs, and thermokarst ponds (Figures 3b-f, orange circles)
- Six permafrost-temperature boreholes along T6–T9 (Figures 3b-e, red circles)

Methods, coordinates, and preliminary data from these studies are in AGC 22-01 (Walker et al. 2022b).

2 2022 Field Studies

2.1 Vegetation studies

The vegetation of the Prudhoe Bay region was first described and classified during the early phases of oilfield exploration and development (Walker 1985, Walker and Everett 1991).

The vegetation structure and composition of the regional vegetation has changed since the original surveys were made due to changes in the local hydrology, local patterned-ground surface forms, climate, and other disturbances, such as road dust, infrastructure-related flooding, and air pollutants. The cumulative effects of these impacts were partially investigated in studies at the Colleen site (Walker et al. 2022a, Kanevskiy et al. 2022).

Changes to the vegetation in more remote areas of the PBO are the topic of ongoing vegetation research at the NIRPO site and are part of Olivia Hobgood's MS thesis and papers in progress by members of the vegetation component of the NNA-IRPS project.

New vegetation studies were conducted in 2022 at the NIRPO site during four field efforts:

- **26 April–3 May:** Late-winter/early-spring snow studies and trace-gas flux measurements
- **13–22 July:** Mid-summer trace-gas-flux measurements and plant collections
- **19 August–1 September:** New vegetation plots, biomass clip harvest, bryophyte life-form study, installation of soil temperature loggers, and late-summer thaw, water, and plant height measurements
- **28–29 November:** Early-winter trace-gas fluxes

Descriptions from these studies are divided into the following subsections:

- New vegetation plots
- Aboveground biomass
- Bryophyte life-form diversity
- Snow survey
- Soil-temperature loggers
- Thaw depths, water depths, and vegetation heights
- Greenhouse gas fluxes

2.1.1 New vegetation plots

Skip Walker, Amy Breen, Olivia Hobgood, Anna Kučerová

2.1.1.1 Introduction

The main goal for the new vegetation plots was to extend NIRPO observations to the dry and aquatic ends of the site-moisture gradient at the NIRPO site.

2.1.1.2 Methods

Fifteen new vegetation plots were surveyed in late summer 2022 (Figure 4). These were added to the 79 plots surveyed at the NIRPO and Jorgenson sites in 2021 (Figure 3).

- Eight plots were established on a small pingo, including six dry plots (22-01 to 22-06); one was on the pingo-top, which had zoogenic vegetation (22-13); and one was in a snowbed on the southwest side of the pingo (22-14). The pingo was informally named "Lemming Pingo" because of the abundance of collared lemmings (*Dicrostonyx groenlandicus*) on the pingo summit.
- Six plots (22-07 to 22-12) were placed in aquatic habitats (three *Carex aquatilis* communities in marl-bottomed ponds, and three in *Arctophila fulva* communities) on lake margins near the pingo.
- Plot 22-15 was placed on a bird mound (see cover photo) with zoogenic plant communities, located approximately 500 m northwest of the pingo near the 100-m marker along transect T8.

All 1-m x 1-m plots (Figure 5a) were marked with plot numbers, which include the last two digits of the sample year and consecutive plot numbers (22-01 to 22-15). The center of each plot was marked with a 5/8-inch (1.6 cm) x 30-cm rebar stake with an aluminum cap stamped with the plot number.

To make the plot visible for summer aerial surveys, a white circular 20-cm-diameter paper plate was centered on the rebar stake and anchored with nails.

For locating the terrestrial plots in winter, a 30-cm x 0.95-cm (3/8-inch) rebar stake was driven next to the center stake to anchor a vertical piece of white 1.5-m x 2.5-cm (1-inch inside diameter) polyvinyl chloride (PVC) pipe, marked at the top with the plot number (Figure 5a).

Environmental site factors, cover-abundance of species, and soils were sampled according to proto-

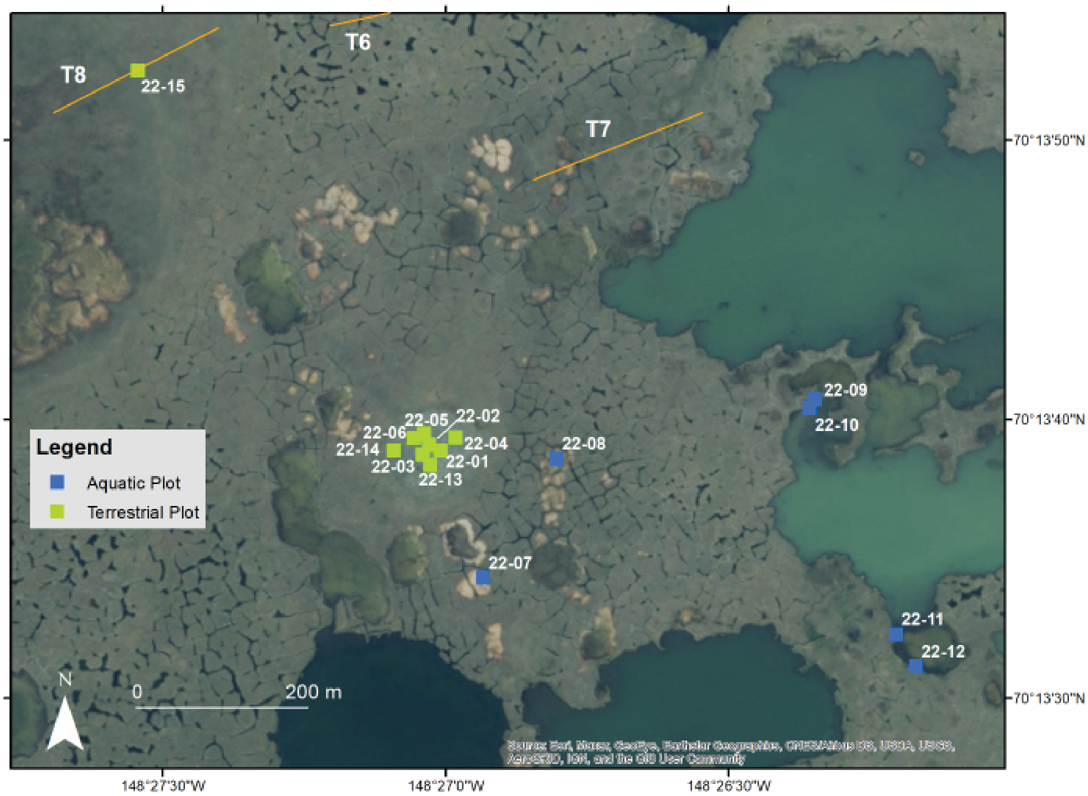

Figure 4. *Vegetation plots established in August 2022 in the vicinity of Lemming Pingo focused on dry and zoogenic habitats (green squares) and lake habitats (blue squares). (Credit: M.K. Raynolds. Basemap: North Slope Borough, Maxar / ESRI)*

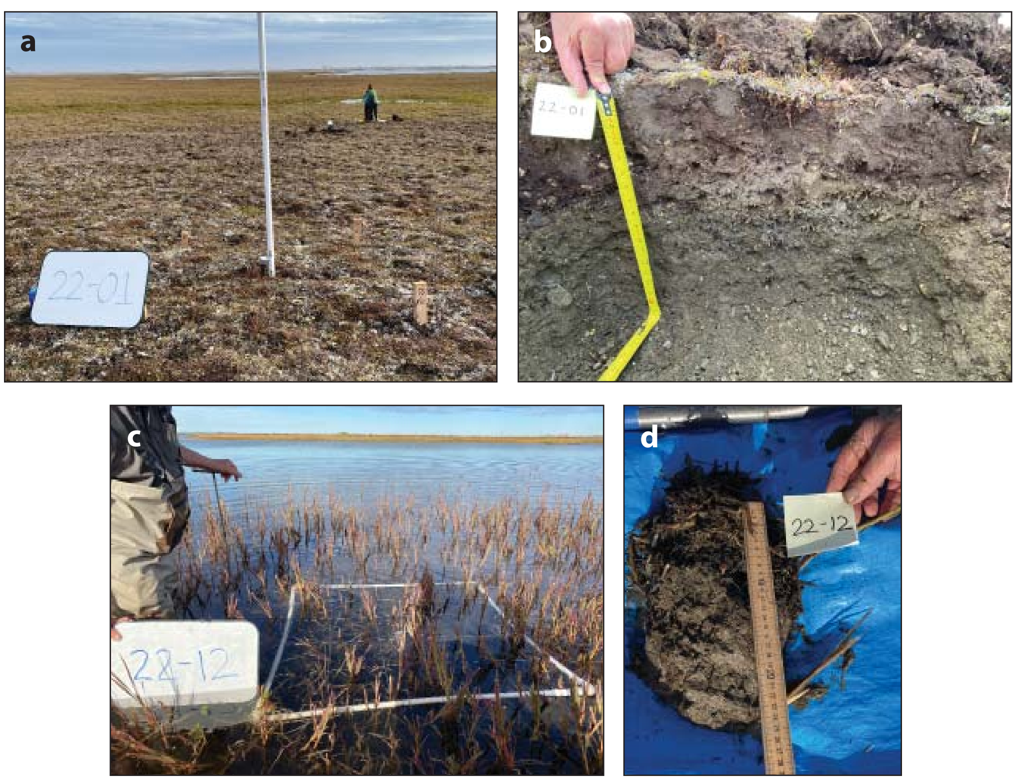

Figure 5. *Vegetation plots.* ***a.*** *Dry plot 22-01 in a* Dryas integrifolia – Oxytropis nigrescens *community on Lemming Pingo.* ***b.*** *Soil pit adjacent to plot 22-01. Nails mark horizon boundaries.* ***c.*** *Aquatic plot 22-12 in an* Arctophila fulva – Scorpidium scorpioides *community. The plastic frame with 20-cm x 20-cm subdivisions marked with string was used for estimating cover-abundance of plant species.* ***d.*** *Soil and biomass sample removed from adjacent to plot 22-12. The plug was removed with a soil corer (see Figure 6c). (Credits: A.L. Breen, IMG 9222, IMG 9226, IMG 9257, IMG 9261)*

cols developed for permanent plots at the Colleen, Airport, and NIRPO sites (Walker et al. 2015, 2016, 2022b). Data sheets used for plot sampling are in Appendix 1 (Table A1.1, site descriptions; Table A1.2, species cover-abundance; and Table A1.3, soil descriptions). Codes used for describing the environmental factors and vegetation are in Appendix 2 (Table A2.1, categorical and scalar environmental variables; Table A2.2, vegetation type codes; and Table A2.3, habitat type codes).

The species surveys included lists and estimated cover-abundance of vascular plants, lichens, mosses, and liverworts. Species nomenclature followed the Pan Arctic Species List (Raynolds et al. 2013).

Soils in the dry plots on the pingo were described in soil pits next to the dry plots (22-01–22-06) (e.g., Figure 5b). Soils of the aquatic plots (22-07 to 22-12) were described and sampled from soil plugs (e.g. Figure 5d) that were removed with a coring device that was developed for sampling soils and biomass in the NIRPO aquatic ponds in 2021(Figure 6c) (Watson-Cook 2022; Walker et al. 2022b). Soils in the snowbed and zoogenic plots (22-13 to 22-15) were described from 40-cm long plugs of soil removed with a tile spade from areas adjacent to the plots (see Appendix 4, Table A4.3).

The major soil horizons were briefly described (Appendix 3, Table A3.1). Soil samples were collected from the top horizon (generally the top mineral horizon at approximately 10-cm depth) using a 180-cm^3 soil can. The soils were analyzed for gravimetric and volumetric soil moisture, bulk density, percentage of sand, silt and clay, pH, and total organic matter (Table A3.2).

2.1.1.3 Preliminary results

Brief descriptions of the 15 new vegetation plots sampled in 2022 are in Table 1. Photographs of the plots are in Appendix 4 (Table A4.1, landscapes; Table A4.2, vegetation; and Table A4.3, soils). Summaries of environmental site factors, including plant-life-form percentage-cover values, are in Appendix 5. A list of plant species recorded in all plots sampled in 2021 and 2022 at the NIRPO site is in Appendix 6. Cover-abundance scores for all species recorded at the new plots established in 2022 are in Appendix 7.

2.1.1.4 Preliminary conclusions

- Observations at the pingo, bird mound, and lake plots provide information on the soils and vegetation from a wider diversity of habitat types than previously sampled to develop a clearer understanding of how the vegetation and total landscapes are evolving under climate change and local sources of disturbance.
- The pingo plots provided insights to vegetation and soil response along meso-topographic gradients associated with well-drained slopes that are common on the pingos but rare elsewhere in the flat thaw-lake landscapes of the PBO. The soils on

Table 1. *Summary of 15 plots sampled in 2022 at the NIRPO site. Veg type codes according to Walker (1985).*

Plot ID	Veg type	Site	Field name (description) of plant community
22-01	B1	Pingo, N-facing slope shoulder	Dry *Dryas integrifolia, Oxytropis nigrescens, Carex rupestris, Thamnolia subuliformis* prostrate dwarf-shrub, lichen tundra
22-02	B1	Pingo, N-facing slope shoulder	Dry *Dryas integrifolia, Oxytropis nigrescens, Carex rupestris, Thamnolia subuliformis* prostrate dwarf-shrub, lichen tundra
22-03	B1	Pingo, N-facing slope shoulder	Dry *Dryas integrifolia, Oxytropis nigrescens, Carex rupestris, Thamnolia subuliformis* prostrate dwarf-shrub, lichen tundra
22-04	B2	Pingo, N-facing slope footslope	Dry *Dryas integrifolia, Saxifraga oppositifolia, Carex rupestris, Thamnolia subuliformis, Ditrichum flexicaule* prostrate dwarf-shrub, lichen tundra
22-05	B2	Pingo, N-facing slope footslope	Dry *Dryas integrifolia, Saxifraga oppositifolia, Carex rupestris, Thamnolia subuliformis* prostrate dwarf-shrub, lichen tundra
22-06	B2	Pingo, N-facing slope footslope	Dry *Dryas integrifolia, Saxifraga oppositifolia, Thamnolia subuliformis* prostrate dwarf-shrub, lichen tundra
22-07	E1	Shallow marl pond	Aquatic *Carex aquatilis* sedge marsh
22-08	E1	Shallow marl pond	Aquatic *Carex aquatilis* sedge marsh
22-09	E1	Shallow marl lake embayment	Aquatic *Carex aquatilis* sedge marsh
22-10	E2	Lake embayment	Aquatic *Arctophila fulva, Scorpidium scropioides* grass marsh
22-11	E2	Lake embayment	Aquatic *Arctophila fulva, Scorpidium scropioides* grass marsh
22-12	E2	Lake embayment	Aquatic *Arctophila fulva, Scorpidium scropioides* grass marsh
22-13	U10	Pingo, summit	Moist/dry *Poa arctica, Festuca baffinensis, Cerastium beeringianum, Abietinella abietina*, grass, forb, moss meadow
22-14	U6	Pingo, SW slope snowbed	Dry *Cassiope tetragona, Dryas integrifolia, Thamnolia subuliformis, Sanionia uncinata*, dwarf-shrub, lichen tundra
22-15	U10	Bird mound, Transect T8	Moist *Arctagrostis latifolia, Plemonium boreale, Dryas integrifolia, Sanionia uncinata*, grass, forb, moss tundra

the upper pingo slopes had very deep thaw (>110 cm) and well-developed A horizons that are like Mollisol soils described by Everett and Parkinson (1977) on other pingos and dry well-developed high-centered polygons in the PBO.

- The soils and vegetation on the pingo summit and bird mound had extensive evidence of animal activity, including large numbers of small mammal bones, feathers, and scat from a variety of bird species including ptarmigan, snowy owls, and jaegers that use these elevated sites as observation points.
- Marl ponds and lakes are a common component of the PBO wetland landscapes and are important nesting sites and foraging areas for a wide variety of shorebirds and waterfowl. Marl ponds have been described in southern Alaska, where they have been studied as a source for Portland Cement (Moxham and Eckhart 1956) and are probably common in other areas of northern Alaska where limestone occurs, but so far these ponds have received little ecological attention in Arctic Alaska.

2.1.2 Aboveground biomass

Olivia Hobgood and Skip Walker

2.1.2.1 Methods

Intact slices of tundra were collected and later clipped in the lab and sorted according to plant growth forms using the methods developed for the NIRPO terrestrial plots sampled in 2021 (Walker et al 2022b). A 50-cm x 20-cm (0.1 m^2) aluminum sampling frame was nailed to the tundra near each plot in an area that matched as closely as possible the composition and structure of the vegetation in the plot (Figure 6a). The tundra within the frame was cut around the inner margin of the frame with a bread knife. An additional cut was made to divide the sample in half, forming two 25-cm x 20-cm subsamples. The frame was then removed, and each half was cut horizontally 2–3 cm beneath the tundra surface. Each half sample was removed from the sample area and placed in 1-quart Ziploc® bag with the plot number, date of harvest, and the sample half (e.g., 1 of 2 or 2 of 2) recorded on the bag and on a Post-it® note placed inside the bag (Figure 6b).

The samples were frozen for transport to UAF, where they were kept frozen until removed for processing and thawed. The aboveground plant parts were clipped with scissors and sorted into growth forms: evergreen shrubs, deciduous shrubs (leaves and woody stems), graminoids (live and dead), horsetails, forbs, mosses, lichens, and litter. Values for the 0.1-m^2 plots were multiplied by 10 to obtain biomass per 1-m^2.

Biomass sampling in aquatic plots used a coring device that was developed for sampling biomass and soils in thermokarst ponds (Figure 6c) (Watson-Cook 2022). The cylindrical cores had a diameter of 15.2 cm (6 in) (cross-section area of approximately 182.3 cm^2). The sample of aboveground biomass was removed by slicing the core with a knife at the sediment surface. The biomass samples were then thoroughly washed in the field to remove trapped mineral sediment and before freezing. Upon thawing in the lab, the core was again washed and then sorted by plant growth forms and dried according to the same procedures as the terrestrial vegetation plots. The samples were dried at 65 °C until a constant mass was obtained (approximately one week). To obtain biomass per 1 m^2, the biomass values for the sample area of plots were multiplied by 54.85 (number of sample areas per m^2). Biomass data for all terrestrial and aquatic plots sampled in 2021 and 2022 are in Appendix 8.

2.1.2.2 Preliminary results

- A summary of the biomass in 70 NIRPO plots sampled in 2021 and 2022 is in Figure 7, sorted by growth form and grouped by vegetation type.
- Mean total biomass ranged from 25 ± 10 (standard error) g/m^2 (n = 2) in marl-bottomed lake plots with scattered *Carex aquatilis* shoots (vegetation type Marl) to 3617 ± 199 g/m^2 in the aquatic moss (*Calliergon richardsonii*) plant communities in ice-wedge thermokarst ponds (type Em, n = 10). Total biomass in the most common terrestrial tundra types (U3, U4, M2, and M4) ranged between 388 ± 57 g/m^2 (n = 5) in M4 (very wet polygon centers) to 1199 ± 42 g/m^2 (n = 7) in U3 (moist high-centered polygons). The *Cassiope tetragona* snowbed (U6) plot had biomass of 1384 g/m^2.
- Moss biomass was a large part of the total biomass in most vegetation types and ranged from 0 g/m^2 in the marl plots to an extreme of 6411 g/m^2 in an aquatic moss plant community in an ice-wedge thermokarst pond. Mean moss biomass in the most common terrestrial vegetation types (U3, U4, M2) ranged from 141 ± 162 g/m^2 in M4 to 495 ± 28 g/m^2 in U3. Very high biomass (3584.6 ± 1784.8 g/m^2) occurred in mossy thermokarst ponds (Em, n=10). Such high biomass has not been found anywhere else in local PBO plant communities. The moss has an important cooling

Figure 6. *Biomass harvest methods.* ***a.*** *Cutting out a 50-cm x 20-cm slice of tundra using a metal frame and a bread knife.* ***b.*** *Ziploc® bag containing one half of the tundra slice.* ***c.*** *Coring device used to sample biomass and soils in aquatic sites. (Credits: J.L. Peirce, IMG 5608, IMG 5602; E. Watson-Cook, IMG 3631)*

effect on pond bottom temperatures and likely helps to stabilize ice-wedge degradation in the thermokarst ponds (Watson-Cook 2022). Future studies will examine the reasons for the high moss biomass in thermokarst ponds.

- The low biomass in the shallow-pond plots (Figure 7, types Marl and E1) is due in part to the abundance of marl, a soft white mud-like deposit rich in calcium carbonate and a diverse assemblage of algae, diatoms, insects, and other organisms (Vreeken 1981).
- Although these ponds are unstudied in Arctic Alaska, marl ponds have been described in other settings in more temperate and semi-tropical regions of North America with limestone bedrock (Vreeken 1981, Schwert et al. 1985, Yang et al. 2001, Guillet et al. 2010; *https://uwaterloo.ca/wat-on-earth/news/marl*). In New York state, marl ponds are considered critically imperiled (State conservation Status: S1) because their total area is very small (New York Natural Heritage Program, *https://guides.nynhp.org/marl-pond*). In south Florida "marl prairies" are common in some areas with limestone bedrock but are considered highly vulnerable to sea-level rise as well as many non-climate-related threats.

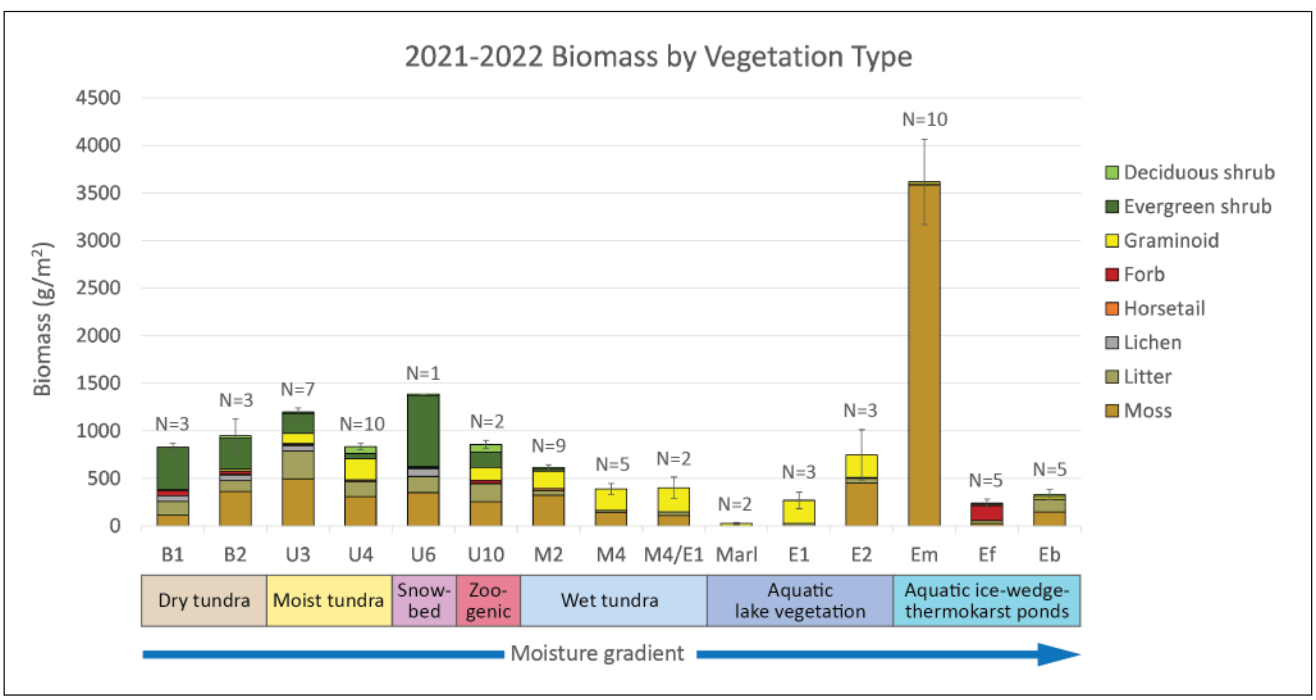

Figure 7. *Summary of NIRPO mean biomass ± SE sorted by plant growth form and vegetation type.*

2.1.3 Bryophyte life-form diversity along a site-moisture gradient

Anna Kučerová and Skip Walker

2.1.3.1 Introduction

This study was conducted by Anna Kučerová (Figure 8), an MS intern visiting the AGC from Masaryk University, Czech Republic. The study examined the distribution of bryophyte (moss and liverwort) life forms that occur across a site-moisture gradient at the NIRPO site.

Because of the flat and wet nature of the terrain at the NIRPO site, most plant communities occur across a small range of site-moisture conditions that vary according to small differences in elevation of microtopographic features. Thanks to specific adaptations, such as a broad ability to recover from desiccation and freezing and low maximum photosynthetic rates, bryophytes can thrive in northern ecosystems and are often a dominant component in tundra landscapes, where bryophytes play an important role in biochemical cycles, energy balance, soil moisture, and soil insulation. They affect tundra ecosystem processes such as permafrost formation, peat accumulation, and development of microtopography. Bryophytes play a particularly important role in insulating the permafrost from thaw and limiting thermal degradation of the permafrost (Turetsky et al. 2012, Lett et al. 2022).

The composition, diversity, and abundance of bryophytes in tundra plant communities vary widely. Unfortunately, identification of bryophytes to the species level in the field is difficult, usually requiring determination of microscopic characters. One approach that could simplify their application for some ecological studies is to use bryophyte life forms—similar in concept to the application of plant functional types in vegetation modelling applications (e.g., Smith et al. 1997). Like vascular plants, mosses respond to environmental factors differentially due to specific morphological and physiological adaptations, so the suite of bryophyte life forms within a given vegetation type can provide insights into how the vegetation type is affecting ecosystem processes.

Figure 8. *Anna Kučerová identifying bryophyte specimens from the NIRPO site. (Credit: A.N. Kade)*

2.1.3.2 Methods

2.1.3.2.1 Bryophyte life-form classification system

The life-form classification system developed here (Table 2) is based on a review of the literature and collections of all identifiable bryophyte species in a subset of dry, moist, wet, and aquatic permanent vegetation plots at the NIRPO site. The system includes three broad bryophyte life-form categories and seven subcategories, including: (1) turfs [species with mainly erect, vertical (orthotropic) stems with limited branching, subdivided into tall turfs (≥ 2 cm tall) and short turfs (< 2 cm tall)]; (2) mats [species with extensive lateral (plagiotropic) branches creeping close to the ground, subdivided into rough, smooth, and thalloid (thalloid liverwort) subcategories]; and (3) solitaires [solitary occurring stems, subdivided into erect (orthotropic) and creeping (plagiotropic) species].

2.1.3.2.2 Field methods

The cover-abundance of bryophytes was surveyed in 19 plots spanning nine vegetation types along the moisture gradient at the NIRPO site in July and August 2022 (Table 3 and Appendix 9).

2.1.3.3 Preliminary results

- A total of 77 bryophyte taxa identified to the species level were included in the analysis. Mean values of total species richness (Figure 9a) and richness grouped by bryophyte life forms (Figure 9b) were calculated for each vegetation type along the site-moisture gradient. The largest numbers of species (mean 24–26) occurred in dry to moist tundra (vegetation types B2, U3, and U4). Moderate numbers of species (mean 12.5–18) occurred in the driest sites (B1 on the exposed shoulder of the pingo) and the wet sites (M2 in partly watered habitats of flat and low-centered polygons and troughs). Low numbers of species (mean 0–4.5) were recorded in the very wet to aquatic plots (M4, M4/E1, E1, and E2).

- Mean cover of bryophytes along the moisture gradient varied from ~ 5 percent in B1 to ~ 75 percent in E2. Low bryophyte cover in types M4 and E1 was due to very high cover of marl (see discussion, Section 2.1.2.2). For the dry-to-wet portion of the moisture gradient (B1–M2), the relative percent cover of all mat subcategories (Mr, Ms, Mt) increases, and the cover of solitaires (Se and Sc) decreases (Figure 9d).

Table 2. *Classification of bryophyte life forms, their definitions, and descriptions.*

Category	Definition	Subcategory	Description	Abbr.	Ilustrations of life-forms (undertaken from Grace 1995)
turfs	many closely packed vertically standing stems with limited branching, usually orthotropic species	tall	>= 2 cm tall	Tt	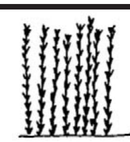
		short	< 2 cm tall	Ts	
mats	main and lateral branches creeping close to the ground, usually plagiotropic species	rough	branches in different directions	Mr	
		smooth	branches in the same direction	Ms	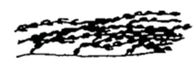
		thallose	thallose liverworts	Mt	
solitaires	solitary occurring stems	solitary erect	solitary standing stems of orthotropic spp.	Se	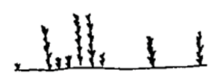
		solitary creeping	solitary creeping stems of plagiotropic spp.	Sc	

Table 3. *Selected vegetation plots for bryophyte survey.*

Veg code	Plot ID	Transect or location	Landform	Microsite	Description of vegetation type
B1	22-01	Lemming pingo	pingo	hill slope shoulder	Dry *Dryas integrifolia, Carex rupestris, Oxytropis nigrescens, Lecanora epibryon* dwarf-shrub, crustose-lichen tundra
	22-02	Lemming pingo	pingo	hill slope shoulder	
B2	22-04	Lemming pingo	pingo	hill foot slope	Dry *Dryas integrifolia, Saxifraga oppositifolia, Lecanora epibryon* dwarf-shrub, crustose-lichen tundra
	22-05	Lemming pingo	pingo	hill foot slope	
U3	21-05	T6	plain, residual surface	high polygon center	Moist *Eriophorum angustifolium, Dryas integrifolia, Tomentypnum nitens, Thamnolia subuliformis* graminoid, prostrate dwarf-shrub, moss, lichen tundra
	21-21	T9	plain, residual surface	high polygon center	
U4	21-09	T6	plain, residual surface	flat polygon center	Moist *Eriophorum angustifolium, Dryas integrifolia, Tomentypnum nitens*, sedge, dwarf-shrub, moss tundra
	21-34	T7	drained lake basin	polygon rim	
M2	21-01	T8	drained lake basin	polygon basin	Wet *Carex aquatilis, Drepanocladus brevifolius* graminoid, moss tundra
	21-16	T6	plain, residual surface	polygon trough	
	21-29	T7	drained lake basin	polygon basin	
M4	21-03	T8	drained lake basin	flat polygon center	Wet Carex aquatilis, Scorpidium scorpioides graminoid, moss tundra
	21-28	T7	drained lake basin	polygon basin	
M4/E1	21-31	T7	drained lake basin	polygon trough	Transitional wet to aquatic *Carex aquatilis, Scorpidium scorpioides* graminoid, moss tundra
	21-35	T7	drained lake basin	polygon trough	
E1	22-07	Lemming pingo vicinity	marl pond	marl pond	Aquatic *Carex aquatilis* sedge tundra
	22-08	Lemming pingo vicinity	marl pond	marl pond	
E2	22-11	Lemming pingo vicinity	lake	lake	Aquatic *Arctophila fulva* grass marsh
	22-12	Lemming pingo vicinity	lake	lake	

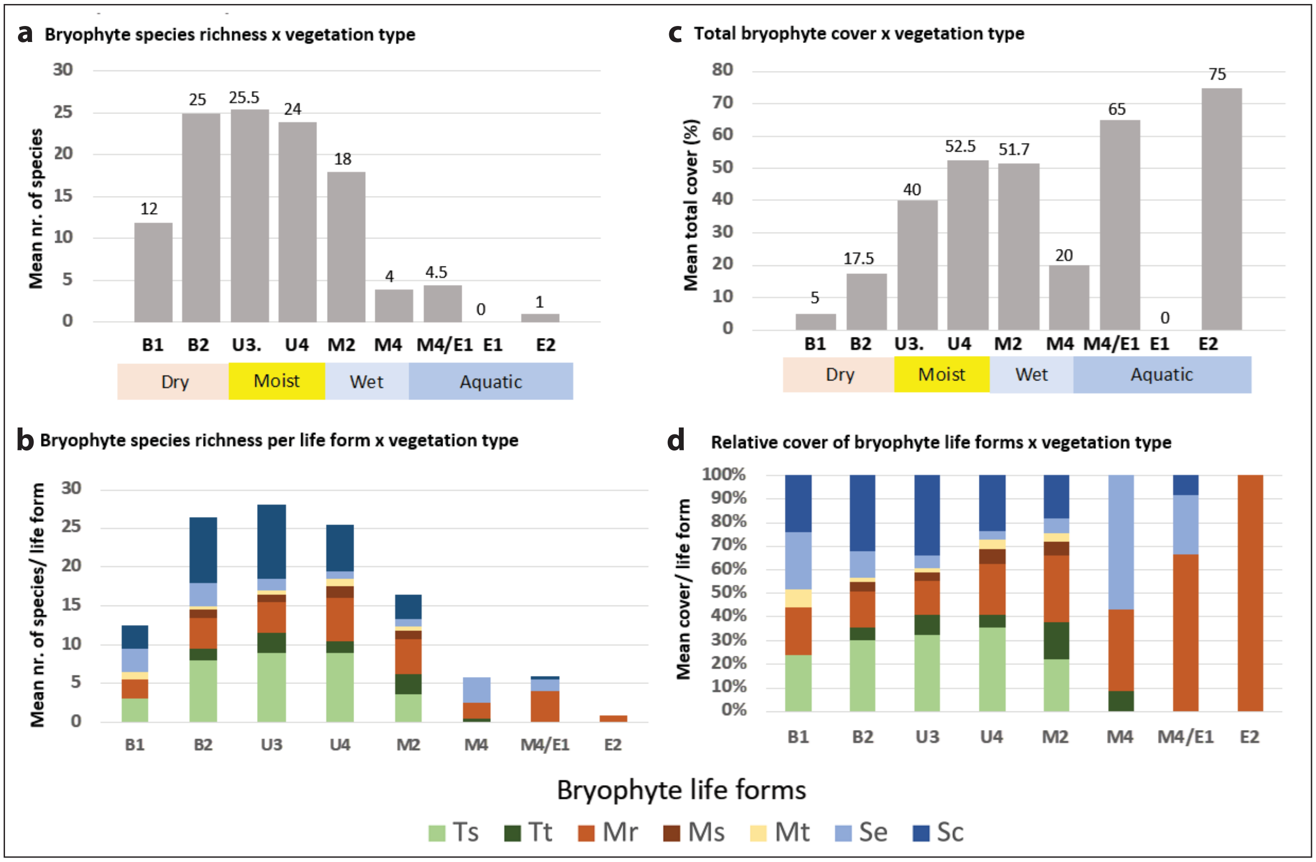

Figure 9. *Bryophyte species richness and cover of bryophyte species in vegetation types along the NIRPO site-moisture gradient.* ***a.*** *Mean number of bryophyte species by vegetation type across the site-moisture gradient.* ***b.*** *Mean total cover of bryophyte layer by vegetation type based on percentage estimates.* ***c.*** *Mean number of species by life-form category and vegetation type.* ***d.*** *Mean relative cover of bryophyte life forms for each vegetation type based on percentage estimates. N=2 plots for all vegetation types except for M2, where N=3. Key to bryophyte life-form abbreviations are in Table 2.*

2.1.3.4 Discussion

The diversity of bryophyte life forms is a reflection of environmental conditions necessary to maximize CO_2 uptake and to minimize water loss (Longton 1988, Proctor 2007, Wang 2016, May 2018). Bryophytes are ectohydric plants, meaning that water movement happens mainly on the external surfaces of most species. To avoid water loss, dense colonies of cushions and turfs are successful strategies to deal with harsh conditions because the water is enveloped in the laminar boundary layer of the aerodynamically shaped colony limiting evaporation (Natkatsubo 1994, Bates 1998).

The most common life forms in this study were turfs. Turf-dominated colonies tended to be more common in the dry-to-moist plots at the NIRPO site (B2–U4) (Figure 9). Short turfs (e.g., *Bryum* spp., *Encalypta* spp., *Pohlia* spp., *Ceratodon purpureus, Meesia triquetra, Catascopium nigritum*) predominated over tall turfs (e.g., *Distichium capillaceum, Flexitrichum* spp.) in both number of occurrences and total cover. Shorter forms are typically more frequent in open habitats possibly due to the impact of high light intensity, which represses the lengthening of the main shoot axes (Mägdefrau 1982). This could be related to the occurrence of stronger winds in the slightly elevated microsites of these types or possibly to the threat of photoinhibition in more open landscapes with 24-hour daylight during the summer, which might favor self-shading forms, such as turfs, over the more sensitive prostrate forms (Bates 1998).

Mat bryophytes increased with soil moisture and were dominate in wet and aquatic sites (Figure 9d). Mats have more open life forms and usually are found in places with low desiccation stress (Bates 1998). Rough-mat forms (e.g., *Tomentypnum nitens, Drepanocladus* spp., *Scorpidium scorpioides, Hypnum spp., Campylium stellatum, Calliergon* spp., *Pseudocalliergon* spp.) were far more common at NIRPO than smooth mats, which were represented only by a few liverworts (e.g., *Scapania simmonsii, Blepharostoma trichophyllum, Platydictya jungermannioides*). This can be expected as smooth mats with shoots oriented in one direction occur more often on vertical substrates or in habitats with slowly moving water. One prevailing rough-mat species, *Tomentypnum nitens*, covered more than 50% of most moist-tundra vegetation plots (U3 and U4). Similarly in wet and aquatic plots, rough-mat species (e.g., *Pseudocalliergon brevifolium, Scorpidium scorpioides, Calliergon giganteum*) were often dominant.

Solitaires decreased along the moisture gradient from type B1 to M2. Here solitaires included two subcategories, "solitary creeping" and "solitary erect", which included a wide variety of moss and liverwort taxa (e.g., *Cephaloziella* spp., *Anastrophyllum minutum, Orthothecium* spp., *Cinclidium* spp., *Brachythecium* spp.). Solitaires were generally more common in drier vegetation types (B1–U3), but one component of the solitaire erect group (leafy liverworts) was especially common, often found creeping among the moss mats. Solitaire species often can be found in mixtures of several species or can be present in an otherwise monospecific colony, erect in turfs, or creeping among mats or turfs. The concept of solitaires is treated variously in the literature and probably needs to be more clearly defined. Some authors (Mägdefrau 1982, Victoria et al. 2009, Lett et al. 2022) do not include solitaires in their grouping systems. Other approaches use "threads" or "thread-like mats" to characterize delicate, sparsely branched, feather-like or solitary creeping shoots growing among other vegetation (Grace 1995). An approach used for British and Irish mosses treats thread-like mats and solitary creeping individuals separately (Hill et al. 2007).

No cushion forms were encountered in the sampled plots. PBO is characterized by strong winds, so cushion forms might be expected as they are considered very common in most windy Arctic and Antarctic regions (Mägdefrau 1982). But most microsites on the flat thaw-lake-plain landscapes in the PBO are also saturated with water, so species do not usually face the threat of drying out. Victoria et al. (2009) showed that on Antarctic islands the occurrence of cushions is restricted to the more exposed sites such as rocks and rocky outcrops, while organic substrates frequently had turfs. This corresponds to the characteristics of the NIRPO site where no rocks were present.

The life forms used in this study showed distinctive trends of richness and abundance along the moisture gradient, but other approaches to dividing bryophytes into functional units should also be explored. For example, a promising 12-category functional grouping approach was published while writing this study (Lett et al. 2022) and should be examined for future studies of the Prudhoe Bay bryophyte flora. It would also be useful to examine if the various bryophyte life forms have distinctive insulating capacities to aid in modeling the effects of bryophytes on permafrost degradation (e.g., Porada et al. 2016).

2.2 Snow survey

Amy Breen, Anja Kade, Olivia Hobgood, Jana Peirce

2.2.1 Introduction

Snow depths were measured on 126 permanent vegetation plots at the NNA-IRPS sites during 28 April–3 May 2022.

2.2.2 Methods

To locate the plots in winter, all plots were previously marked with vertical poles made from white polyvinylchloride (PVC) pipe (2.5-cm inside diameter x 120 cm tall). GPS coordinates were needed to locate some pond plots because deep snow covered the tops of the poles on many of these plots.

Snow depth, snow density, and snow water equivalent (SWE) were measured at the NIRPO site (35 terrestrial plots and 40 aquatic plots that were relatively unimpacted by dust) and the Colleen site (24 plots impacted by road dust). Only snow depth was measured at the Airport site (27 plots).

- Snow depth was measured at five points within 0.5 m of the PVC center poles and averaged per plot. Snow pits were dug adjacent to the plots to photograph the snow stratigraphy.
- Snowpack density and SWE were determined using a plastic ESC30 snow sampling tube (7.1-cm diameter) (shown in Figure 11). Photographs of each snow pit were taken with the tube inserted for reference. Snow depth at the tube location was recorded for each plot. Snow samples from the tube were placed in 1-gallon Ziploc® bags, sealed, and weighed in the lab to determine the mass and SWE.

No snow pits were dug at the Airport site due to time limitations. Data collection was more time consuming than anticipated because the late-winter snowpack was unusually deep, which slowed data collection especially in the thermokarst pond plots where the snow poles were often buried by deep snow. Cold weather with high winds also slowed progress on the first day (28 April) of the survey.

2.2.3 Results

- There was a large contrast in the snow condition at the NIRPO site compared to the Colleen site (Figure 11), where the snow surface and several layers within the snowpack contained large amounts of road dust (Figure 11b). The snow surface had started to melt and had a slushy texture compared to the NIRPO site.
- Snow data from each plot are in Appendix 10 and summarized in Figure 12.
- Snow was deeper in polygon troughs compared to polygon centers at both the NIRPO and Colleen site (CS) plots (Snow depth: NIRPO centers: 38.4 ± 12.2 cm, troughs: 62.8 ±10.5 cm; CS centers: 33.1 ± 18.6 cm; troughs: 58.7 ± 12.7 cm) (Figure 12a).
- Snow density was similar in polygon centers and troughs at both sites (NIRPO: 0.26 g/cm^3; CS: 0.27 g/cm^3) (Figure 12b).
- SWE in the polygon troughs was about double that in polygon centers at both sites (NIRPO centers: 9.8 ± 3.9 cm; troughs: 18.1 ± 3.6 cm. CS centers: 9 ± 6.2 cm; troughs: 17.8 ± 5.7 cm) (Figure 12c).
- At the NIRPO site, snow depth, density, and SWE were compared between surface-form features and vegetation types (Figure 12d–f). Snow depth was deepest in moist-tundra polygon troughs (72 ± 11 cm) and thermokarst ponds (70 ± 11 cm) and shallowest on moist-tundra polygon rims (34.6 ± 5.8 cm) and moist polygon centers (36.2 ± 13.3 cm). Snow density was less variable than snow depth across vegetation types and surface features (0.24–0.3 g/cm^3) (Figure 12e).
- The trends for SWE mirrored snow depth with the greatest SWE in the thermokarst ponds (21.5 ± 4.4 cm) and moist tundra troughs (21.2 ± 4.1 cm) (Figure 12f). The lowest SWE values were from the moist tundra high-centered polygons (9.1 ± 4.2 cm). For the remaining plots, SWE varied between 11.7 ± 2.4 cm for the moist-tundra low-center

Figure 10. *Olivia Hobgood skiing with sled of field equipment during snow measurements at the NIRPO site. (Credit: A.L. Breen)*

Figure 11. *Snow character at a relatively dust-free site and a site with heavy road dust.* ***a.*** *Anja Kade and snow pit at the relatively dust-free NIRPO site in a thermokarst pond with deep snow. Note the top of the 120-cm snow stake, which is anchored in the bottom of the pond; at least half of the stake is below the water level in the pond.* ***b.*** *Olivia Hobgood and snow pit at a dusty polygon-center plot along the Spine Road at the Colleen site. Note the ESC30 snow sampling tube in both photos. Both photos were taken 2 May 2022. (Credits: A.L. Breen, IMG 0192, IMG 0182)*

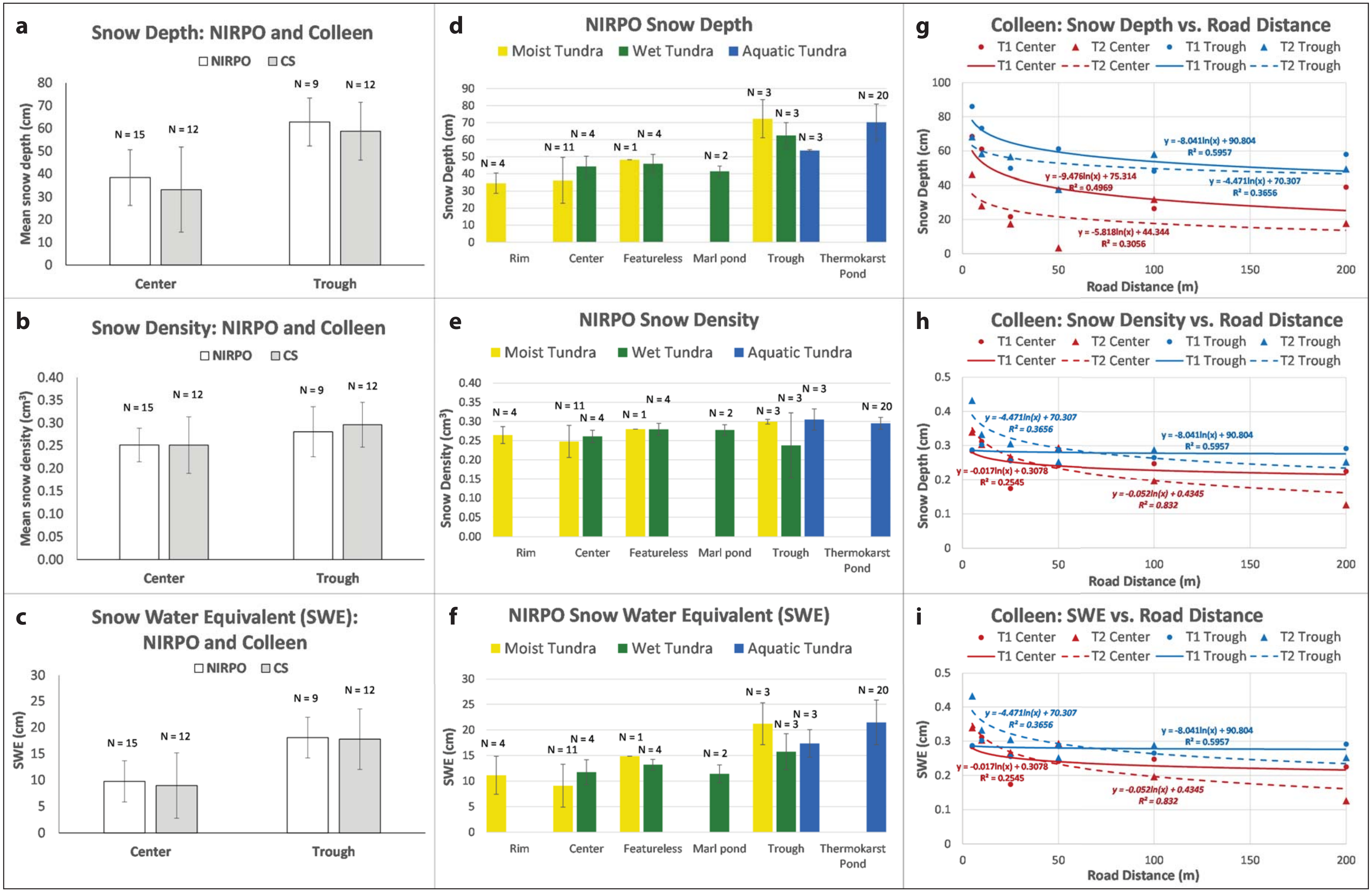

Figure 12. *Snow characteristics at the NIRPO and Colleen sites.* ***a–c:*** *Snow depth, snow density, and snow water equivalent (SWE) in polygon center and trough plots across both sites.* ***d–f:*** *Snow depth, density, and SWE in moist (yellow), wet (green) and aquatic (blue) plots across common microrelief features at the NIRPO site.* ***g–i:*** *Snow depth, density, and SWE in polygon centers (red lines) and troughs (blue lines) along Colleen transect T1 (solid line, dominantly the windward side of road) and T2 (dashed line, dominantly the leeward side of road). Snow was deeper in troughs compared with polygon centers at both sites.*

polygon centers to 17.4 ± 2.7 cm in the aquatic plots in polygon troughs.

- At the road-disturbed Colleen site, snow depth, snow density, and SWE varied logarithmically with distance from the road, with most of the variation occurring within 25 m of the road due to road-related snowdrifts on both sides of the road (Figure 12g–i). Snow depths were deeper on the T1 side of the road in both centers and troughs.

2.3 Soil-temperature loggers

Skip Walker and Olivia Hobgood

2.3.1 Introduction

Temperature loggers were placed in 35 plots to examine the vertical trends of soil temperature in common vegetation types along the soil moisture gradient.

2.3.2 Methods

Three Maxim iButtons® (DS 1922L-F5# Thermochron 8K, resolution ± 0.5˚ C; Figure 13a) were taped to 24-inch (61-cm) PVC stakes for placement in the soil at 0 cm (ground surface), -15 cm, and -40 cm. Each logger was waterproofed by first sealing it in a white rubber coating (Plasti Dip®). It was then labeled with a consecutive iButton field ID number using a black Sharpie marker, tied in a finger from a blue Nitrile glove, and placed in a small Ziploc® bag also marked with the iButton ID (Figure 13b). The iButtons were then taped

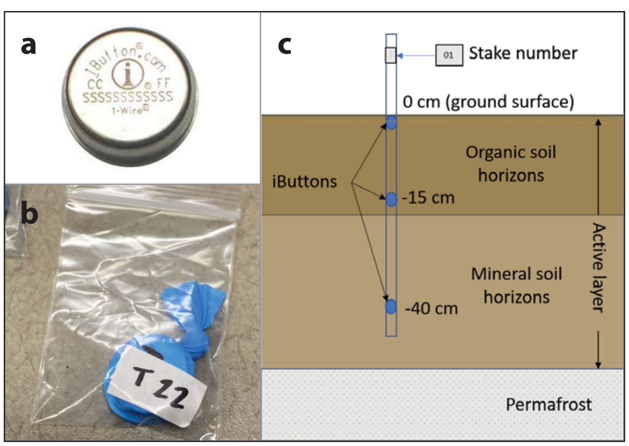

Figure 13. *Ground-temperature data loggers. **a.** Maxim iButton®, DS 1922L-F5# Thermochron 8K, resolution ± 0.5˚. Each iButton has a 12-digit serial number (credit: Mouser Electronics). **b.** Waterproofed iButton placed in a small plastic Ziploc® bag before being taped to a PVC stake using Gorilla Tape® (credit: J.L. Peirce, IMG 4510). **c.** Schematic of a PVC stake with iButtons inserted in the soil so that the loggers are at 0 cm (ground surface), -15 cm and -40 cm depths (credit: D.A. Walker).*

to 150-cm x 0.5-in (1.27-cm inside-diameter) PVC stakes for placement in the ground (Figure 13c).

The temperature stakes were placed next to plots in common PBO habitats along the tundra site-moisture gradient (Appendix 11): four dry-tundra plots (B1 and B2), six moist-tundra plots (U3 and U4), two moist zoogenic-tundra plots (U10), one moist snowbed plot (U6), 10 wet-tundra plots (M2, M4, and M4/E1), four aquatic lake plots (E1 and E2), and eight thermokarst ponds (Em, Ef, and Es).

Soil-temperature loggers were also taped to the top of two vertical snow poles at plots 22-05 and 22-13 to record the air temperatures at the pingo summit and near the base of the pingo. The loggers were set to record temperatures at 4-hr intervals (0:00, 4:00, 8:00, 12:00, 16:00, 20:00) starting 15 September 2022.

2.4 Thaw depths, water depths, and vegetation heights

Skip Walker, Amy Breen, Olivia Hobgood, Anna Kučerová

2.4.1 Methods

Thaw depths and water depths were measured during 27–29 August 2022 at 138 NNA-IRPS permanent vegetation plots, including:

- 70 NIRPO plots (including 15 new pingo and lake plots sampled in 2022, 35 terrestrial plots sampled in 2021, and 20 aquatic thermokarst-pond plots sampled in 2021)
- 19 Jorgenson thermokarst pond plots sampled in 2021
- 24 Colleen terrestrial plots sampled in 2014
- 25 Airport terrestrial plots sampled in 2015

At each plot, five measurements of thaw depth and water depth (one at the plot center and one at each of the four corners) were made and then averaged.

2.4.2 Results

- The thaw-depth and water-depth data collected at permanent vegetation plots in 2022, along with available vegetation-height and 2022 snow-depth data, were compared for the common vegetation types along the soil moisture gradient at the NIRPO site (Figure 14). These data are presented in Appendix 12.
- Mean thaw depths were deepest in the dry tundra plots on the pingo (B1, 113 ± 12 cm; and B2, 85 ± 11 cm) and were shallowest in the aquatic moss vegetation plots in ice-wedge thermokarst ponds (Em, 36 ± 6 cm).

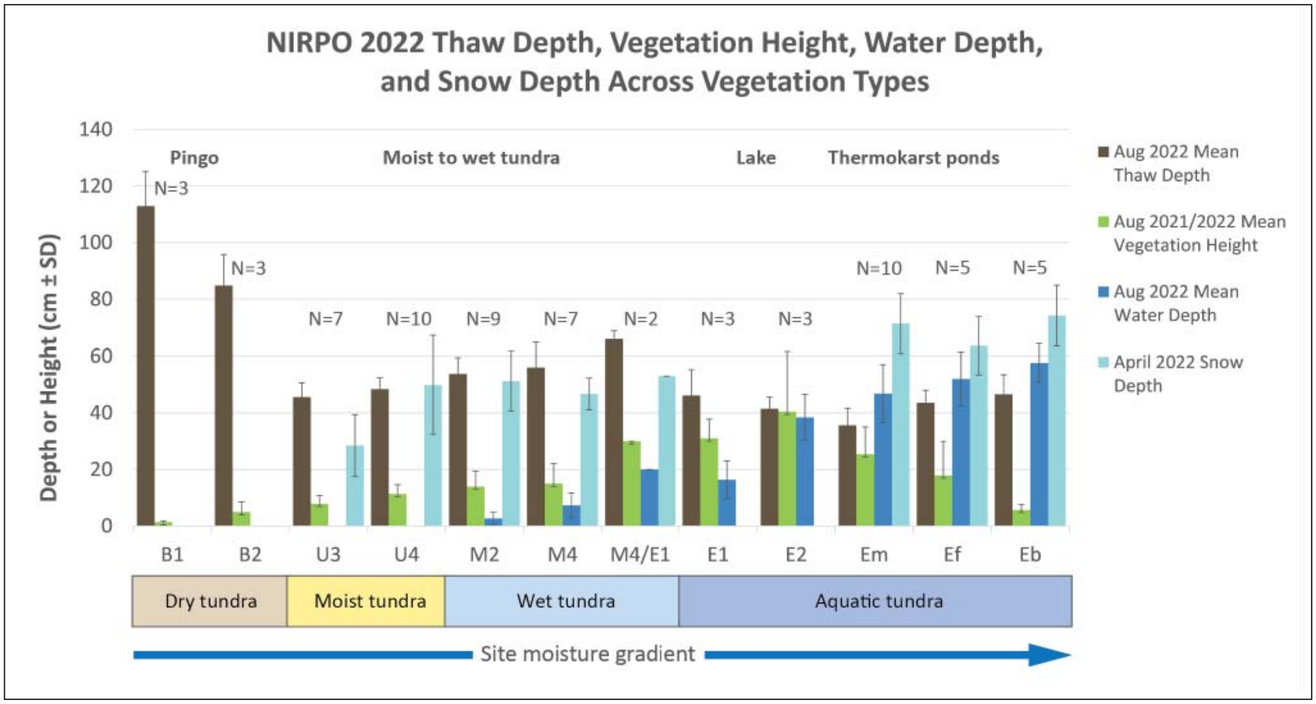

Figure 14. *Summary of thaw depth (8/27–29/2022), vegetation height (August 2021 or 2022), water depth (8/27–29/2022) and snow depth (4/28-5/3/2022) measured at NIRPO permanent vegetation plots. Data for thaw depth and water depth are in Appendix 12. Data for vegetation height are from the original plot surveys in 2021 and 2022. Data for snow measurements are from the Spring 2022 snow survey (Appendix 10).*

- The deepest water and snow depths were in the barren thermokarst ponds (Es, mean water depth 56 ± 2 cm, mean snow depth 74 ± 11 cm).
- Vegetation heights, measured from the soil surface, generally increased with water depth except in thermokarst ponds. Maximum mean vegetation heights occurred in aquatic vegetation type E2 (*Arctophila fulva*) (40 ± 21 cm).
- The non-aquatic moist and wet vegetation types (U3, U4, M2, M4, M4/E1) showed a general pattern of increased water depth, thaw depth, and vegetation height with site moisture.

2.5 Greenhouse gas fluxes

Anja Kade

2.5.1 Introduction

Changes in the distribution of water have impacts to the flux of greenhouse gases to the atmosphere. Fluxes of greenhouse gases were previously measured in degraded ice-wedge polygon troughs in varying states of degradation/stabilization at the Jorgenson site (Wickland et al. 2020). This study is examining seasonal (summer and winter) variation in fluxes across the natural site-moisture gradient at the NIRPO site and along roadside disturbance gradients at the Colleen site.

2.5.2 Methods

In 2021, CO_2 fluxes were measured on 33 vegetation plots that are representative of common landforms, surface forms, and vegetation plots at the relatively unimpacted NIRPO site (see Table 1, p. 24, in AGC 22-01, Walker et al. 2022b).

In 2022, measurements were made along roadside transects T1 and T2 at the Colleen site during three periods:

- **30 April–1 May**: Late-winter ecosystem respiration on Colleen and NIRPO plots
- **13–22 July**: Mid-summer net ecosystem exchange on the Colleen plots
- **28–29 November**: Early winter ecosystem respiration on the Colleen and NIRPO plots.

Appendix 13 contains a summary of the dates on which trace-gas fluxes were measured on plots at the NIRPO and Colleen sites in summer 2021, winter 2022, and summer 2022.

2.5.2.1 Early- and late-winter 2022 CO_2-flux measurements

CO_2 fluxes were measured during periods of snow cover in late-winter (30 April–1 May) and early winter 28–29 November 2022 on the same 33 NIRPO plots where the 2021 summer fluxes were measured, plus

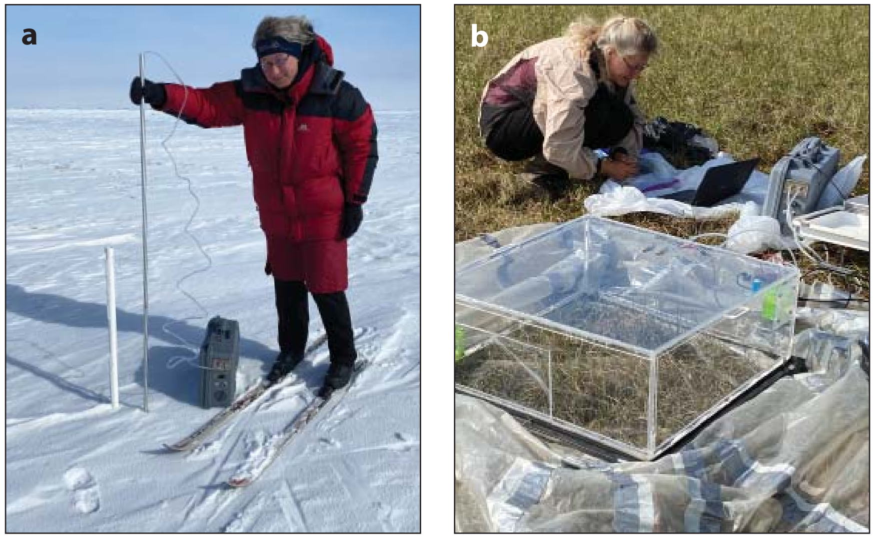

Figure 15. *Trace-gas flux measurements.* ***a.*** *Winter measurement of CO_2 concentration below and above the snowpack using a gas analyzer connected to tubing that is fed through a metal rod.* ***b.*** *Summer trace-gas flux measurements in a wet-tundra plant community using a 0.7-m x 0.7-m chamber and a CO_2 gas analyzer (in the gray case). (Credits: J.L. Peirce, IMG 0309, IMG 4197)*

the 24 plots along Colleen transects T1 and T2. The Colleen plots included paired plots in ice-wedge polygon centers and troughs on both sides of the Spine Road at 5, 10, 25, 50, 100, and 200 m from the road.

Diffusional CO_2 flux through the snowpack to the atmosphere was measured based on Fick's Law of Diffusion as described by Musselman et al. (2005). CO_2 concentrations at the surface and the base of the snowpack were measured with an LI-7810 portable infrared gas analyzer in closed-path configuration (Li-Cor Inc., Lincoln, Nebraska). The gas analyzer was attached to a sturdy, hollow metal probe with a perforated tip that housed 3.2 mm polyethylene tubing (Sullivan 2010) (Figure 15a). The probe was carefully inserted into the snowpack to avoid disturbance. CO_2 concentrations and average snowpack temperature and density were measured, and the diffusion-gradient technique was used to estimate respiration (e.g., Fahnestock et al. 1998, Schindlbacher et al. 2007, Sullivan, 2010).

2.5.2.2 Mid-summer 2022 flux measurements at the Colleen vegetation plots

Midsummer CO_2 and methane fluxes were measured at the 24 Colleen plots along transects T1 and T2 from 13-22 July 2022. Chamber-based methods were used to measure ecosystem respiration (ER) and the light response of net ecosystem exchange (NEE). Midday carbon dioxide, humidity, and methane concentrations were measured by connecting a clear Plexiglas chamber (0.7 m x 0.7 m x 0.25 m) to an LI-7810 portable infrared gas analyzer in closed-path configuration (Li-Cor Inc., Lincoln, Nebraska) and fitting the chamber to a portable rectangular base with an airtight polyethylene skirt (Figure 15b). Two small fans mixed the air within the chamber. The LI-7810 recorded internal trace-gas concentrations, while temperature, barometric pressure, and photosynthetic active radiation (PAR) were logged simultaneously to a Campbell CR-6 data logger every second over a 40-second period.

Two to three measurements were taken at each study plot: under full sunlight, three levels of successive shading, and complete darkness. Shading was provided with layers of fiberglass window screen material (approximately 1.5 mm mesh), and each successive layer of shading reduced the ambient light intensity by approximately 50%. To obtain complete darkness for the ER measurements, the chamber was covered with an opaque tarp. The chamber was ventilated between measurements.

For each dataset, only periods with stable PAR values were used to calculate net CO_2 flux. From these data, a light-response curve was constructed for each plot by interpolating between measured light intensities. Net CO_2 flux (NEE) = (r*V/A)*(dC/dt), where r is air density (mol/m³), V is the chamber volume (m³), dC/dt is the rate of change in CO_2 concentration (µmol/mol/s) and A is the surface area of the chamber (m²). Gross ecosystem productivity (GEP) was calculated as the difference between NEE and ER. NEE values were reported at 600 µmol photons/m²/s, because this light level was achieved consistently in the field and we did not wish to extrapolate beyond the measured values of PAR. GEP was calculated as the difference between NEE and ER. We used negative GEP and NEE values to indicate carbon uptake by the vegetation, according to the micrometeorological sign convention.

2.5.3 Preliminary results

2.5.3.1 Fluxes along the NIRPO site-moisture gradient

- Low levels of ecosystem respiration were measured in all plots across the soil moisture gradient in late winter 2022 as expected due to cold soils and snow cover (Figure 16a). However, small relatively high respiration compared to the other plots occurred in subsiding low-centered polygon trough plots (LPT) with aquatic transitional vegetation (M4/E1) (Figure 16a, dark blue bar).
- These same low-centered polygon trough plots (LPT) showed the largest negative NEE values during flux measurements in summer 2021 (Figure 16b). The trend in summer CO_2 flux across the moist portion of the moisture gradient (U3 to U4) shows generally increasingly negative but low flux values. The plots in ice-wedge-polygon troughs (U4, FPT; M2, FPT; and M4/E1, LPT) show relatively high negative CO_2 flux, indicating that the troughs are fixing relatively high amounts of carbon compared to polygon centers or featureless wet areas in recently drained thaw-lake basins.
- Early-winter 2022 ecosystem respiration (Figure 16c) was low but still two to five times higher than late-winter respiration rates (Figure 16a).

2.5.3.2 Summer net ecosystem exchange along the Colleen road-disturbance transects

- A preliminary analysis of peak-season (July 2022, Figure 17c, d) CO_2 fluxes at the Colleen site also shows generally greater flux in the polygon troughs compared to polygon centers (Figure 17). Midsummer NEE, ER, and GEP were generally greater in polygon troughs than polygon centers on both sides of the Spine Road that intersects the Colleen site. Presumably, nutrient, soil temperatures, and water dynamics in the polygon troughs are more favorable for photosynthesis than in the polygon centers due to greater amounts of water in the troughs.
- Ecosystem respiration in late winter (April 2022) (Figure 17a, b) was generally low (<0.02 µmol/m²/s CO_2), and there was a trend of reduced ecosystem respiration with distance from the road in troughs on the T1 side of the road and both troughs and centers on the T2 side, presumably related to greater snowpack, more disturbance, and warmer soil temperatures near the road.

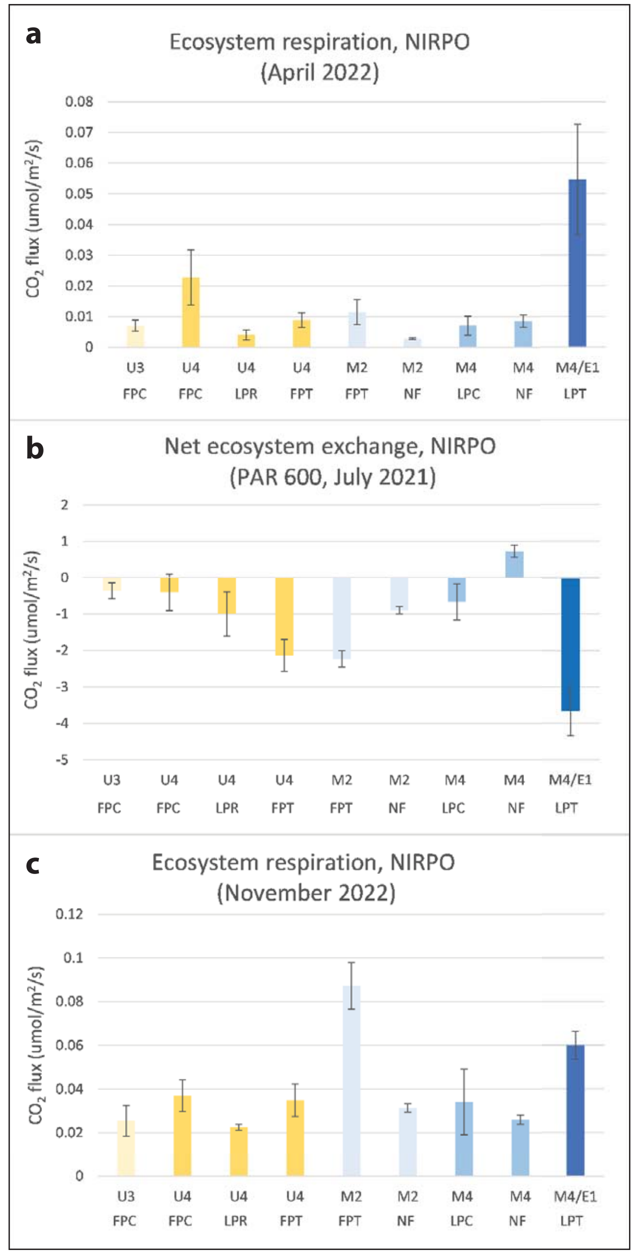

Figure 16. *CO_2 fluxes along the site-moisture gradient at the NIRPO site in late winter, midsummer, and early winter.* ***a.*** *Mean late winter (April 2022) ecosystem respiration (µmol/m²/s ± standard error). FPC = flat-center polygon center, LPR = low-center polygon rim, FPT = flat-polygon trough, NF = no feature, LPC = low-center polygon center, LPT = low-center polygon trough.* ***b.*** *Mean midsummer (July 2021) net ecosystem exchange.* ***c.*** *Mean early-winter (November 2022) ecosystem respiration.*

- However, there were no similar clear trends of either summer net ecosystem exchange (Figure 17c, d) or early-winter ecosystem respiration (Figure 17e, f) related to distance from the road in either polygon centers or troughs. A closer analysis of the timing and degree of flooding at each of the plots would help in assessment of the these results.

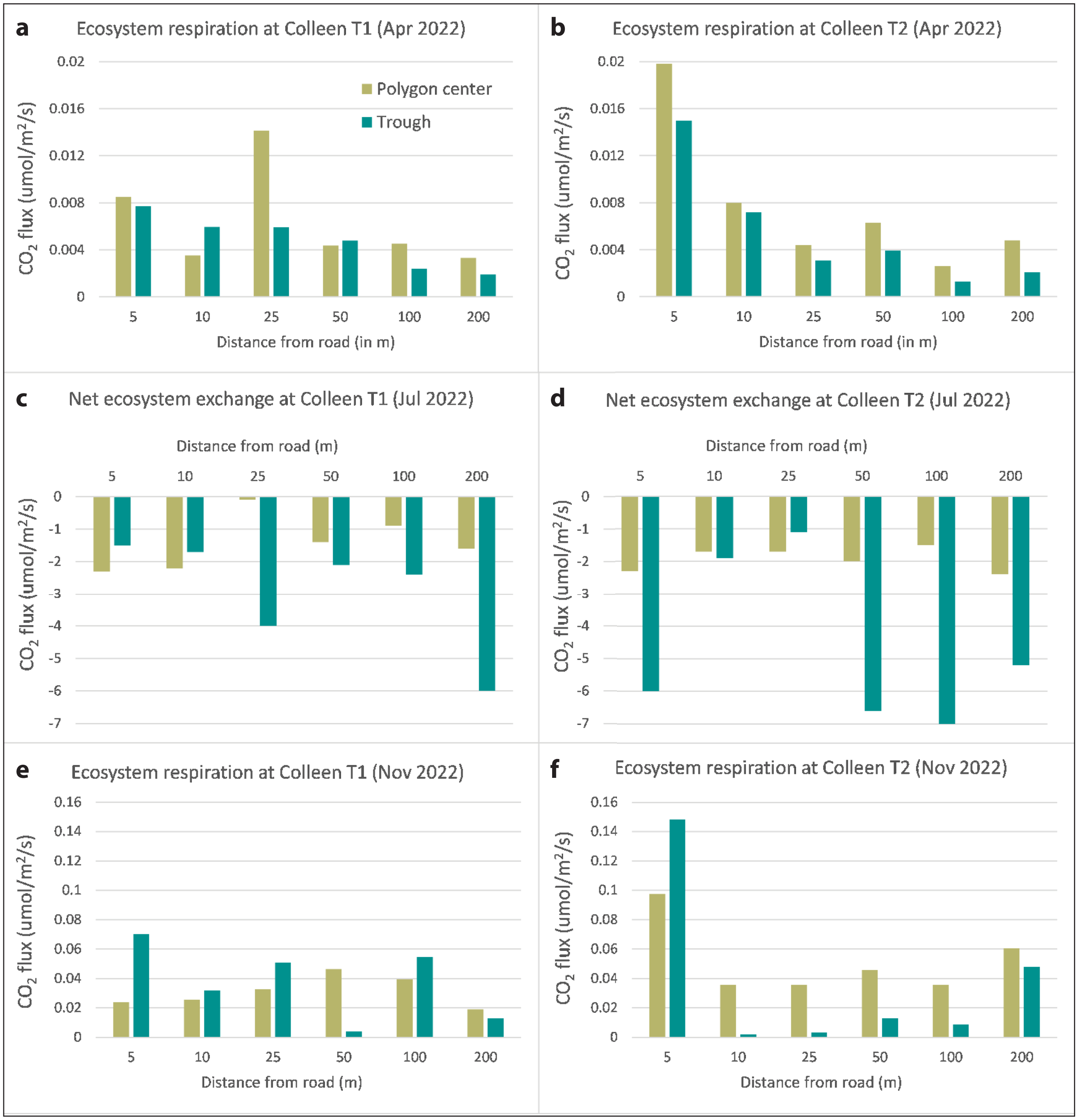

Figure 17. *Summary of CO_2 flux measurements at disturbed Colleen roadside plots. Measurements were made in polygon centers and troughs along transects T1 and T2 at 5, 10, 25, 50, 100, and 200 m from the road.* ***a–b.*** *Ecosystem respiration in late winter at T1 and T2, respectively.* ***c–d.*** *Net ecosystem exchange at 600 PAR in mid-summer at T1 and T2.* ***e–f.*** *Ecosystem respiration in early winter 2022 at T1 and T2.*

2.6 Permafrost studies

2.6.1 Deadhorse snow depths, temperatures, and active-layer thickness

Vladimir Romanovsky

Data for long-term regional snow depths, temperatures, and active layer depths are from the Deadhorse Romanovsky/CALM site (Romanovsky and Osterkamp 1995, Romanovsky et al. 2017). Snow data were collected continuously using a Campbell SR50A-L ultra-sonic snow sensor (*permafrost.gi.alaska.edu/site/dh1*).

- The 2022 maximum snowpack was approximately 80 cm at the Deadhorse site, the deepest in the 2007–2022 record, compared to 50–65 cm in the previous eight years (Figures 18a).
- Mean annual air temperature (MAAT) at the same station was -11.6 ˚C, continuing a trend of colder MAATs for 2020–2022 (Figure 18b, black line). Temperatures at the ground surface and permafrost surface, however, were warmer than in 2021(Figure 18b, red and blue lines), probably related to the deeper snowpack that kept the ground surface relatively warm.
- The 2022 mean active-layer thickness (ALT) was near the mean long-term (1996–2022) ALT at all three CALM grids in the PBO [(2022 ALT)/(mean ALT1995-2022): Deadhorse = 65 cm/65.8 cm; Betty Pingo = 35 cm/38.2 cm; West Dock = 31 cm/31.7 cm]; but as noted in Figure 18b, 2022 was also a relatively cold year compared to recent years between 2011 and 2019, which resulted in thinner ALT in 2021 and 2022 compared to 2019, as well as most years between 2012 and 2019.
- The long-term (1996–2022) mean ALT at the Deadhorse station (Figure 18c) is much thicker than at the other PBO CALM stations (Mean ALT ± SD: Deadhorse 65.8 cm ± 5 cm; Betty Pingo 38.2 cm ± 3.7 cm; West Dock 31.7 cm ± 3.5 cm). Annual variations in the Deadhorse ALT (red line) generally reflect the annual ALT variations at West Dock (purple line) and Betty Pingo (blue line).
- The Deadhorse ALT (Figure 18c, red line) is most like the ALT at Franklin Bluffs (orange line), which is approximately 40 km further inland from the coast with much warmer summer temperatures. The thick active layer at Deadhorse is probably related to its location on an occasionally flooded terrace of the Sagavanirktok River, which has a thin cover of peat and fine-grained soil over alluvial gravels. In contrast, the Happy Valley CALM grid (Figure 18c, green line), which is 115 km inland from the Deadhorse station, has an ALT most like the coastal PBO CALM sites at Betty Pingo (blue line) and West Dock (purple line) due to the thick protective organic layer of tussock tundra and peaty soil at Happy Valley.

2.6.2 Near-surface permafrost temperature monitoring at NNA-IRPS transects

Dmitry Nicolsky

2.6.2.1 Introduction

Near-surface permafrost temperature monitoring sites (Figure 19a, b) were established at each of the NIRPO transects (Figure 19c) and on both sides of the road at the Colleen site (not shown).

2.6.2.2 Methods

Shallow 1-inch diameter boreholes (1.5–2.5 m deep) were drilled at each site, and temperature sensors were then placed at four depths: -0.02 m (just below the ground surface), -0.5 m, -1.0 m, and between -1.5 m and -2.5 m (bottom of the borehole). HOBO® Onset data loggers record temperatures in the boreholes every four hours. Temperature readings were started three days after the installation on 26 August 2021, when temperatures at the bottom of the borehole had stabilized.

Water-depth/temperature loggers (HOBO® Onset U20L) were installed in seven ponds at the NIRPO site (Figure 19c). The loggers were placed on pond bottoms in areas relatively free of vegetation.

A summary of the site locations, depths, and temperature at the borehole bottom are as follows:

NIRPO site

- **T6:** Transect T6. High-center polygon. Vegetation type: U3. Maximum depth: 2.49 m. Temperature at the bottom: -4 ˚C. Coordinates: -148.450731, 70.231876.
- **T7W:** West end of transect T7. Marl site, aquatic tundra, standing water most of the year. Vegetation type: M4. Maximum depth: 2.29 m. Temperature at the bottom: -3.9 ˚C. Coordinates: -148.446651, 70.230452.
- **T7E:** East end of transect T7. Low-centered polygon, wet tundra, no standing water at end of thaw season. Vegetation type: M2. Maximum depth: 2.1 m. Temperature at the bottom: -3 ˚C. Coordinates: -148.443620, 70.230450.

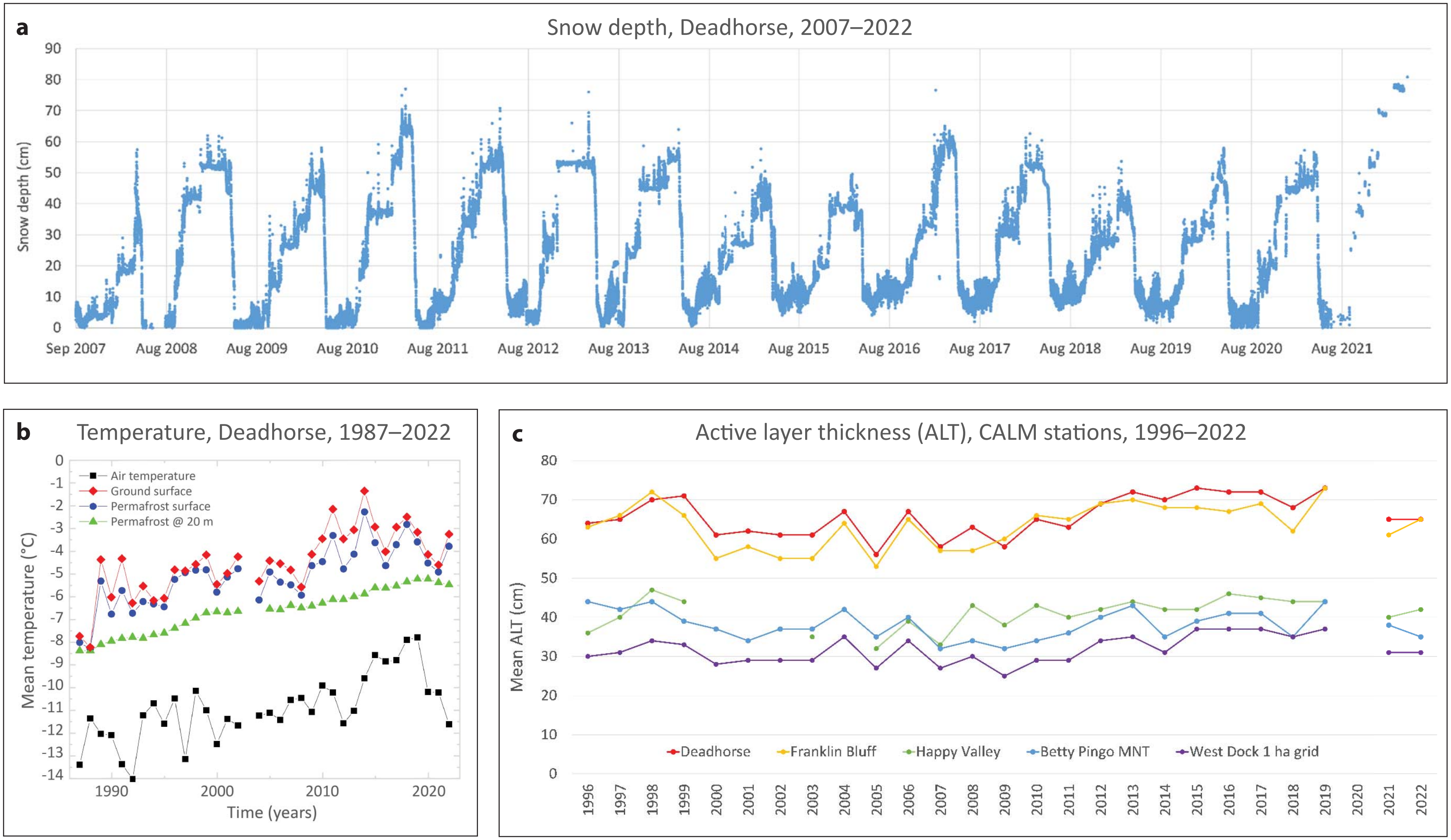

Figure 18. *Climate and active-layer thickness data .* ***a.*** *2007-2022 continuous snow-depths, CALM Deadhorse site. Data were collected using a Campbell SR50A-L ultrasonic snow-depth sensor (Romanovsky Deadhorse CALM station, 2022).* ***b.*** *Mean air temperature, ground-surface temperature, permafrost-surface temperature, and permafrost temperature at 20-m depth (Romanovsky Deadhorse CALM station, 2022).* ***c.*** *Mean annual active layer thickness (1995–2022) at five North Slope CALM grids in the PBO: West Dock (purple), Deadhorse (red), Betty Pingo (blue); and along the Dalton Highway: Franklin Bluffs (orange), Happy Valley (green). (Data from the CALM website: www2.gwu.edu/~calm/data/north.htm).*

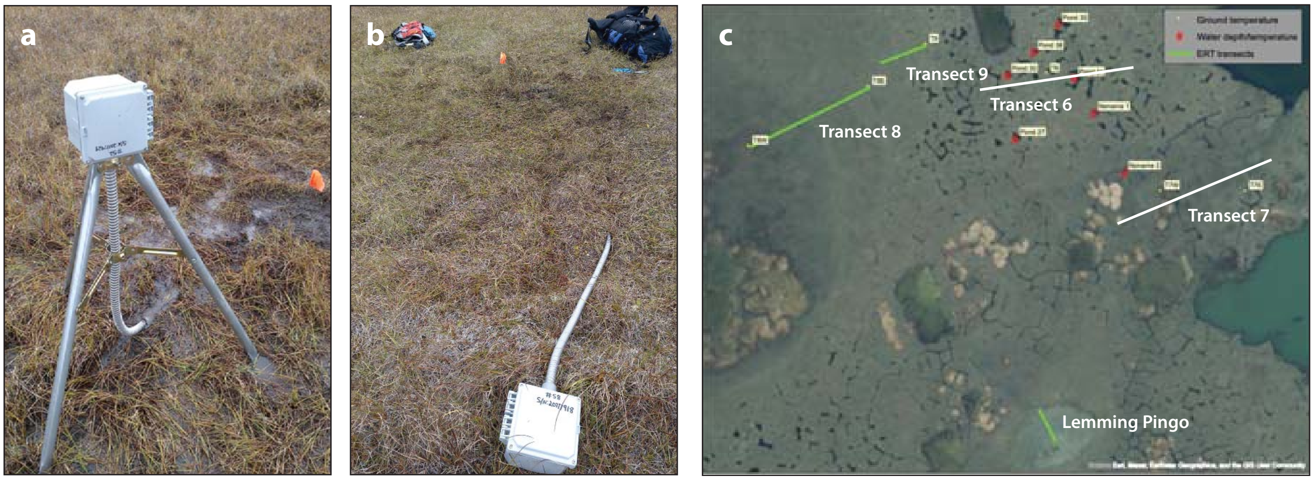

Figure 19. *Ground-temperature loggers, water depth/temperature sensors and ERT transects.* ***a.*** *Typical set up of a ground-temperature monitoring station in a flood prone wet/aquatic-tundra location where the logger is elevated on a tripod.* ***b.*** *Station located in moist-tundra site, where the logger case is located on the ground. (Credits: Nicholas Hasson).* ***c.*** *Map of ground-temperature logger locations (yellow dots, T6, T7E, T7W, T8E, T8W, and T9), water depth/temperature sensors (red markers) in seven ponds (Pond 24, 27, 30, 34, 35, Noname 1, Noname 2), and three ERT transects (green lines) at transects T8, T9, and Lemming Pingo. (Credit Sergei Rybakov. Basemap: North Slope Borough, Maxar / ESRI)*

- **T8W:** West end of transect T8. No visible troughs or polygons, aquatic tundra. Vegetation type: M4. Maximum depth: 1.5 m (gravel at 1.2 m). Temperature at the bottom: -2.7 ˚C. Coordinates: -148.461380, 70.230996.
- **T8E:** East end of transect T8. Flat-centered polygon, wet tundra. Vegetation type: M2. Maximum depth: 2.06 m. Temperature at the bottom: -3.6 ˚C. Coordinates: -148.457094, 70.231716.
- **T9:** Transect T9. High-centered polygon, moist tundra. Vegetation type: U4. Maximum depth: 2.45 m. Temperature at the bottom: -4.4 ˚C. Coordinates: -148.455061, 70.232227.

Colleen site

- **T1:** Colleen site transect T1. Roadside, northeast side of the road, heavily impacted by road dust. Maximum depth: 2.34 m. Temperature at the bottom: -3.3 ˚C. Coordinates: -148.471324, 70.223152.
- **T2:** Colleen site transect T2. Roadside, southwest side of the road, heavily impacted by road dust and flooding. Maximum depth: 2.29 m. Temperature at the bottom: -2.8 ˚C. Coordinates: -148.471669, 70.222962.

2.6.2.3 Preliminary results

- Mean annual ground temperature (MAGT) profiles (Figure 20) show patterns related to the site conditions and disturbance of different landscapes.
- In 2021–2022, the coldest mean annual temperatures at the surface and at 2-m depth occurred on

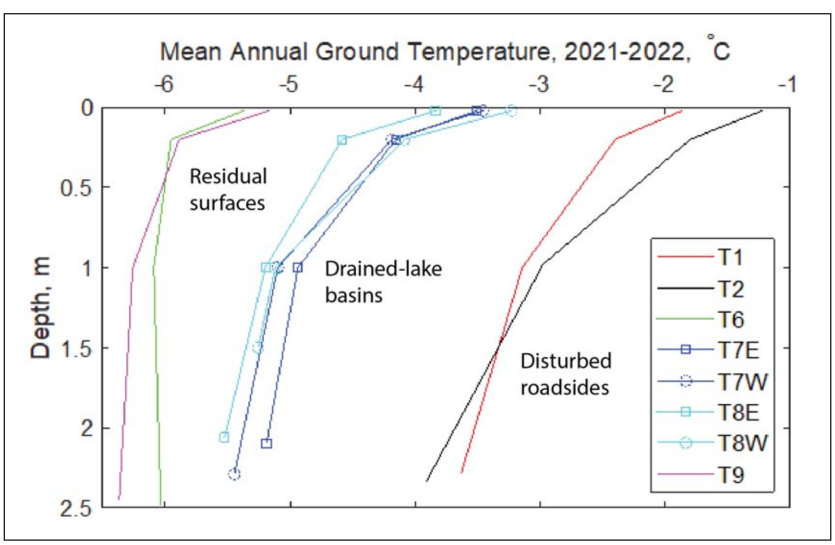

Figure 20. *Ground-temperature profiles for the eight boreholes at the NIRPO (T6–T9) and Colleen (T1 and T2) sites based on one year of monitoring. (Credit: D.N. Nicolsky)*

the residual surfaces at T6 and T9 (e.g., MAGT T6 at -0.02 m = -5.27 ˚C and at -2 m = -6.05 ˚C).

- The warmest temperatures were at the highly disturbed Colleen site (e.g., MAGT of T2 at -0.02 m = -1.23 ˚C and at -2 m = -3.68 ˚C).
- Intermediate temperatures were in the wet drained thaw-lake basins (e.g., MAGT of T7E at -0.02 m = -3.51 ˚C and at -2 m = -5.17 ˚C).
- The largest differences between the temperature at -2 m and -0.02 m (ΔT) occurred in the highly distrubed site (e.g., ΔT at T2 = 2.45 ˚C). The least ΔT occurred on the residual surfaces (e.g., ΔT at T6 = 0.78). The wet drained thaw lake transects showed intermediate differences (e.g., ΔT at T7E = 1.66 ˚C).

2.6.3 Electrical Resistivity Tomography (ERT) transects

Sergei Rybakov

2.6.3.1 Background for electrical resistivity of rocks and soils

Electrical resistivity ρ, measured in ohm meters (Ω m), is the most well-known electromagnetic property and varies for geologic materials over a wide range: from 10^{-5} to 10^{15} Ω m.

Electrical conductivity (1/ρ) of most rocks is ionic. The resistivity of ion-conducting rocks is influenced by many factors. The general formula for the dependence of ρ on the main influencing factors is given by Dakhnov's formula:

$$\rho \sim P_p \cdot P_m \cdot P_c \cdot P_t \cdot P_e \cdot \rho_w$$

where: P_p - porosity parameter, P_m - moisture content parameter, P_c - clay content parameter, P_t - temperature parameter, P_p - electric conductor presence, ρ_w - water resistivity. The resistivity of rocks increases abruptly when it freezes since free water becomes an insulator, and electrical conductivity is determined only by bound water, which freezes at very low temperatures (< -50 °C).

The increase in resistivity during the freezing of different rocks is differential: it increases several times for clays, up to 10 times for rocks, up to 100 times for loams and sandy loams, and up to 1,000 times or more for sands and coarse-grained rocks.

Despite the dependence of ρ on many factors and a wide range of changes in different rocks and soils, the main resistivity patterns have been established. Igneous and metamorphic rocks are characterized by very high resistivities (500 to 10,000 Ω m). Among sedimentary rocks, rock salt, gypsum, limestone, sandstone, and some others have somewhat lower resistivity (100 to 1,000 Ω m). Clastic sedimentary rocks, as a rule, have greater resistivity the larger the size of the grains that make up the rock (i.e., depend primarily on clay content). When moving from clays to loams, sandy loams, and sands, the resistivity changes first from fractions to a few Ω m, then to tens and hundreds of Ω m.

2.6.3.2 Electrical resistivity tomography (ERT)

The electrical resistivity tomography method for subsurface investigation is widely used to study various properties of rocks and soil. Electrical resistivity studies in geophysics may be understood in the context of current flow through a subsurface medium consisting of layers of materials with different resistivities.

A typical ERT study involves the measurement of the apparent resistivity of subsurface materials by injecting electric current into the subsurface through current electrodes and measuring the potential difference between the electrodes. The ERT method includes several steps:

- Electrodes (steel rods) are grounded along the investigated transect with a certain linear interval. The resolution of the method directly depends on this interval and should be considered when choosing a survey methodology.
- All electrodes (72 pieces and more) are connected to a multi-core cable, which is connected to an ERT station.
- The station, in turn, according to principles described in the protocol instructions, injects direct low-frequency current with the known value (I) through the current electrodes (A, B) and simultaneously measures the potential difference (ΔU) between receiver electrodes (M, N). The number of measurements for a transect can reach several thousand. The apparent resistivity (ρ_app) relates the current, voltage, and coefficient K (contained in the protocol):

$$\rho_{app} = K \cdot \frac{\Delta U_{MN}}{I_{AB}}$$

- The coefficient carries information about the position of the electrodes involved in the measurement and characterizes a certain media area that is being measured. When changing the length between the electrodes AB, the depth of penetration of the current will change and carry informa-

Table 4. *Protocols and measurements along ERT transects, NNA-IRPS sites, 24-30 August 2022.*

Site	ERT transect number	Spacing	Length	Array type	Topography	ALT
T8	1	1 m	251 m	Schlumberger, Dipole-Dipole	+-	+
T9	1	1 m	125 m		+-	+
T1	2	1 x 1 m and 2 x 2-m spacing	71 m, 2 x 142 m		-	-
Pingo	2	2 x 2 m spacing	2 x 142 m		-	-

tion about deeper structures. Thus, by changing the relative position of the electrodes and carrying out many measurements, apparent resistivity sections are revealed. Sections carry information about the changes in electrical properties laterally and at various depths. Apparent resistivity is not the true resistivity of the medium. To obtain true values, several approaches are used based on modeling or automatic data inversion (automatic inversion program Res2dInv). At this stage, it is possible to consider a priori information, introduce topography, etc.

- The last step is the interpretation of geoelectrical sections based on the a priori information, including borehole data, active layer probes, temperature data, and known dependences of rock resistivity on many factors.

2.6.3.3 ERT methods at NNA-IRPS sites

Geophysical work using the method of electrical tomography was carried out from 24 to 30 August 2022 using the protocols in Table 4. Processing included rejection of apparent resistivity measurements associated with large error (>4%).

During the data inversion process for the section, the boundary of the active layer was fixed, and resistivity was estimated using one-dimensional modeling of local apparent resistivity curves. The resistivity of the upper layer of fine-grained silty sediment, for example, taking into account its water saturation as well as considering the depth of thawing, is about 25–35 Ω m.

2.6.3.4 Example of results from transect T9

Figure 21 shows the resistivity section for NIRPO transect T9 obtained from automatic data inversion in the Res2Dinv program. The irregular shape of the picture at depth is related to the specifics of the processing and reflects the actual measurement points with depth. The depth of investigation is about 8–10 m based on the one-dimensional comparison and the results of automatic inversion.

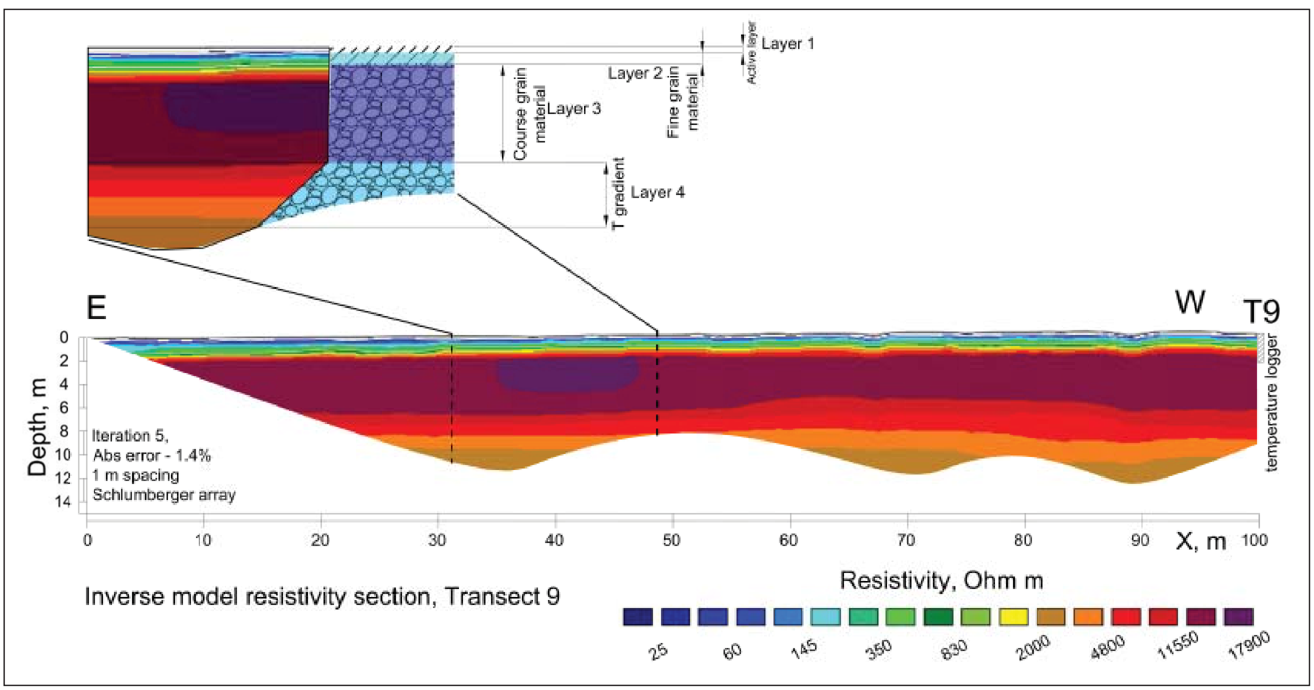

Figure 21. *Resistivity section and interpretation results for transect T9.*

Based on the data interpretation results, considering topography and active layer depth correction, it is possible to distinguish 3-4 layers:

- The top layer is an active layer with a resistivity of about 25-35 Ω m, represented by fine-grained silty material.
- The second layer is likely a transition from fine-grained to coarse-grained material and reflects the temperature gradient. This gradient layer has a resistivity varying from 150 to >3,000 Ω m.
- The third layer has a high resistance and, according to the interpretation of results, is coarse clastic rocks with low temperatures. The layer resistivity is up to 19,000 Ω m.
- At a depth of ~ 6–8 meters, according to the results of automatic data inversion, a gradient structure is traced, which can be caused by a temperature gradient in the presence of coarse clastic material.

A comparison of the MAGT data and the results of one-dimensional resistivity models based on the results of automatic inversion, shows the correspondence in temperature measured in the borehole and ERT-model-derived results (Figure 22). It is possible to trace the relation between resistivity and temperatures obtained at the different sites. For example, the maximum MAGTs among the boreholes are for transect T1 (Figure 22: T1 MAGT, at < 2m; ~ -3.9 ˚C), which corresponds to ~ 550 Ω m in the T1 resistivity model, at >2m). The minimum MAGTs are for transect T9 (MAGT at < 2m; ~ -6.3 ˚C), which corresponds to the maximum resistivity of ~ 19,000 Ω m.

2.6.3.5 Preliminary conclusions

- The ERT method is a useful and relatively fast method of geophysics that allows researchers to study large areas and obtain preliminary information about the geological structure and temperature regime of the area.
- Comparing the results of the resistivity study, it is possible to distinguish sections with different temperatures based on the data in summer 2022.
- It is possible to trace the behavior of the boundary of deep clastic material with very low temperatures (T9, T8). In conditions of relatively high temperatures (e.g., along transect T1), it is also possible to determine the temperature gradient in the upper part of the section for fine and coarse grain sediments (T1).
- In the future, it is recommended to refine the areas of interest using a finer measurement step of 0.5 m together with a 1 or 2 m step. It is also recommended to accompany the measurements with measurements of the active layer and the topography near each electrode for further consideration of a priori information.

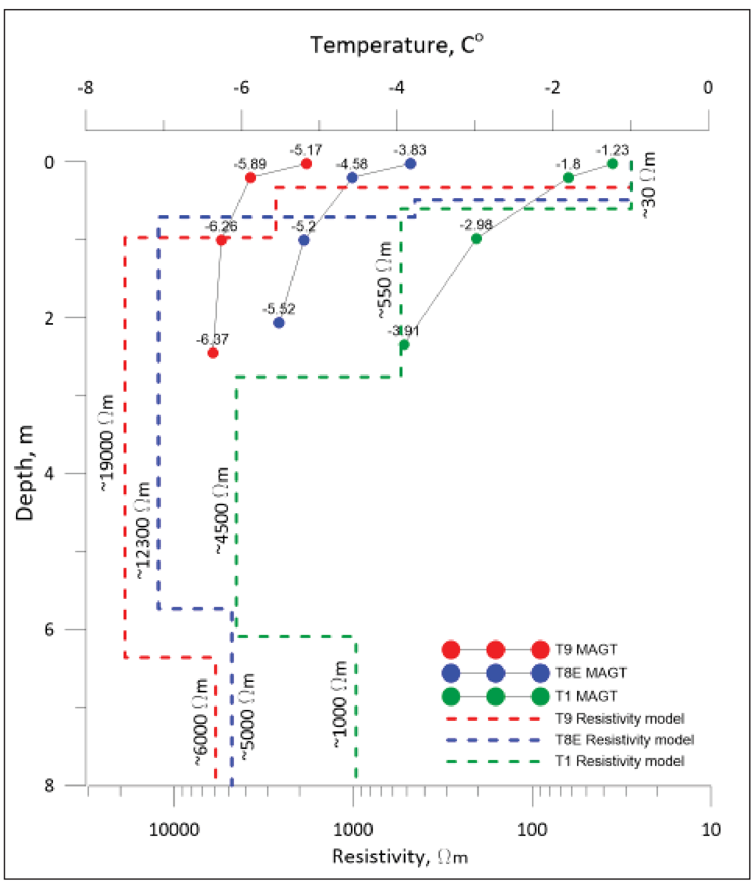

Figure 22. *MAGT and resistivity comparison for transects T9, T8, and T1.*

2.6.4 2022 borehole studies of ice-wedge degradation

Mikhail Kanevskiy and Yuri Shur

2.6.4.1 Introduction

A total of 31 permafrost boreholes were drilled during 26–30 August 2022 to examine the status of permafrost and protective layers above ice wedges in:

- NIRPO thermokarst ponds along transect T6
- Jorgenson transect thermokarst ponds
- ice-wedge troughs along NIRPO Transect T7
- road-related disturbed sites along Colleen site transect T2.

2.6.4.2 NIRPO site thermokarst ponds

Ten boreholes were drilled at the NIRPO site in thermokarst ponds where the vegetation was sampled by Emily Watson-Cook in 2021 (Watson-Cook 2022) (Figure 23 and Appendix 14, Table A14.1).

Of the 17 observed ice wedges in NIRPO thermokarst ponds, 16 were stable at the time of drilling, which was indicated by occurrence of frozen protective layers above the ice wedges up to 21 cm thick (Table A14.1). The protective layer (PL2) is the sum of the thickness of the transient layer (TL), which is a frozen layer that can be subject to thawing in abnormally warm or wet summers with deep seasonal thaw, and the intermediate layer (IL), which is an exceptionally ice-rich zone immediately above the ice wedge that has likely not thawed for at least several consecutive years.

Only one of 17 wedges drilled at the NIRPO site had no TL or IL and was actively degrading at the time of drilling; however, seven wedges had PL2s <10 cm thick and were considered vulnerable to thaw in the future.

2.6.4.3 Jorgenson site thermokarst ponds

Nine boreholes were drilled at the Jorgenson site in thermokarst ponds where the vegetation was sampled by Emily Watson-Cook in 2021 (Watson-Cook 2022). Shown here are all boreholes drilled in 2019, 2021, and 2022 in ponds sampled by Emily Watson-Cook at the Jorgenson site in 2021 (Figure 24 and Appendix14, Table A14.2).

The Jorgenson site ice wedges have been observed since 2011. Of 13 ice wedges drilled in September 2021 and late August 2022 (Table A14.2), all had pro-

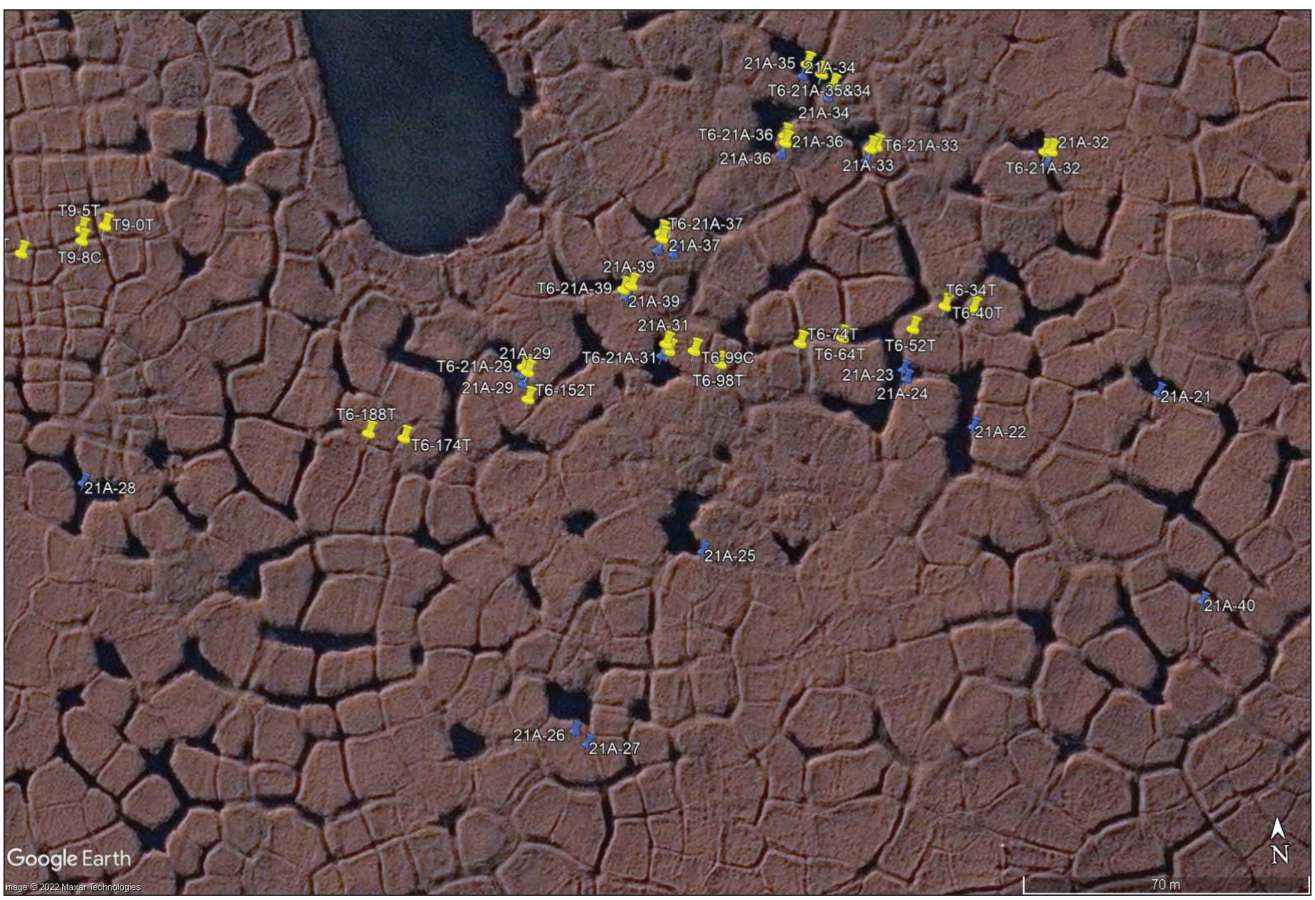

Figure 23. *Permafrost boreholes along NIRPO transects T6 and T9 in 2021 and 2022. Yellow markers are boreholes drilled by Kanevskiy in 2021 and 2022. Blue markers are ponds sampled by Watson-Cook in 2021 and by Kanevskiy in 2022.*

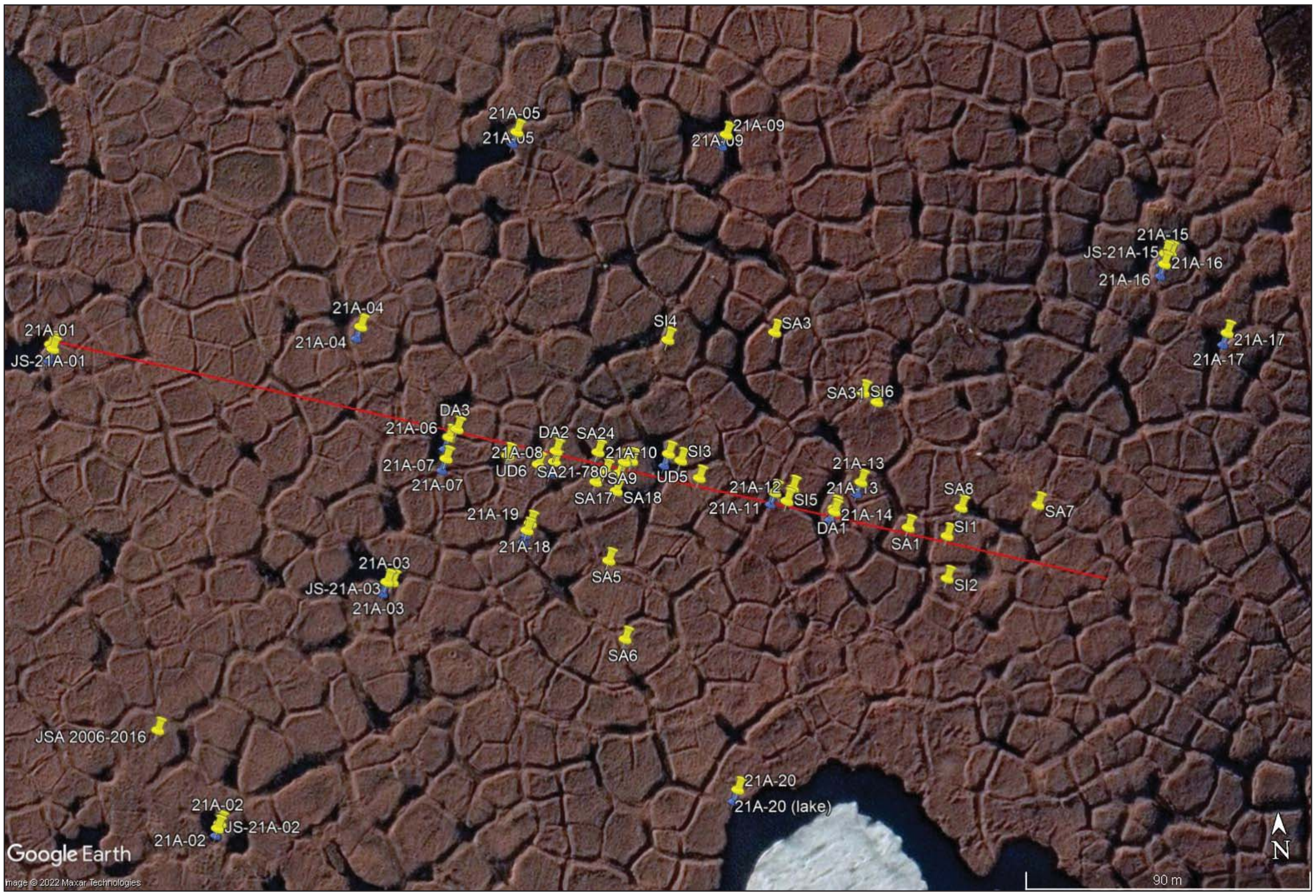

Figure 24. *Permafrost boreholes along the Jorgenson transect (red line). Yellow markers are boreholes drilled by Kanevskiy in 2011, 2012, 2019, 2021 and 2022. Blue markers are ponds sampled by Watson-Cook in 2021.*

tective layers up to 29 cm thick; eight of these had PL2s <10 cm thick and were considered vulnerable to thaw in the future.

2.6.4.4 Ice-wedge troughs near transect T7

Three boreholes were drilled near NIRPO permanent vegetation plots 21-35, 21-32, and 21-31, which were in ice-wedge troughs that appeared to be stabilizing after undergoing degradation (Table 5 and Figure 25).

All three ice-wedges in polygon troughs at NIRPO transect T7 site were stable with PL2s averaging 9 cm thick; one of these had a PL <10 cm thick (Table 5).

2.6.4.5 Colleen site, transect T2

Nine ice wedges that were sampled in 2014 on transect T2 at the road-disturbed Colleen site were re-drilled to assess the status of ice-wedge degradation/stabilization (Table A14.3). All nine were stable at the time of drilling. Protective layers averaged 14.3 cm thick. Four of 9 wedges had PL2s <10 cm thick and were considered vulnerable to degradation in 2014, but all nine were protected by PL2 >10 cm in 2022.

2.6.4.6 Preliminary interpretation

- The data obtained to date show that degradation and stabilization of ice wedges may occur within the same areas simultaneously.
- While many ice wedges have not experienced significant changes over the period of study, some formerly stable ice wedges have shown degradation with the formation of new ponds. However, most of the ice wedges that were actively degrading in 2011–2015 have experienced recent stabilization detected by thicker intermediate and transient layers.
- The most significant stabilization has occurred in deep thermokarst ponds, where rapid development of aquatic vegetation has resulted in a decrease in active-layer thickness and formation of a thick intermediate layer above the partially degraded ice wedges in these ponds.
- In areas near roads at the Airport site where degradation has been most evident, seven of 13 ice wedges, which were originally drilled in 2014, had been degrading in September 2015, but only one

Table 5. *Results of coring at T7-21-35, 32, and 31, Water depth and thaw depth were measured at the borehole location. Transient Layer (TL), Intermediate Layer (IL), depth to massive ice, and Protective Layer (PL=TL+IL, total thickness of frozen soil layer above wedge ice) were measured on the core samples.*

Borehole	Date	Borehole depth (cm)	Water depth (cm)	Thaw depth (cm)	Transient layer (TL) (cm)	Intemediate layer (IL, PL3) (cm)	Depth to massive ice (cm)	TL+IL (PL2) (cm)	Notes
T7-21-35	8/27/2022	58	28	39	1	4	44	5	1.2 m N of 21-35, belt at 40
T7-21-32	8/27/2022	71	20	36	6	6	48	12	1.2 m N of 21-32, belt at 42
T7-21-31	8/27/2022	55	22	38	8	2	48	10	1.2 m NW of 21-31, belt at 46
Average T7 2022, n=3		**61.3**	**23.3**	**37.7**	**5**	**4**	**46.7**	**9**	**No degrading ice wedges**

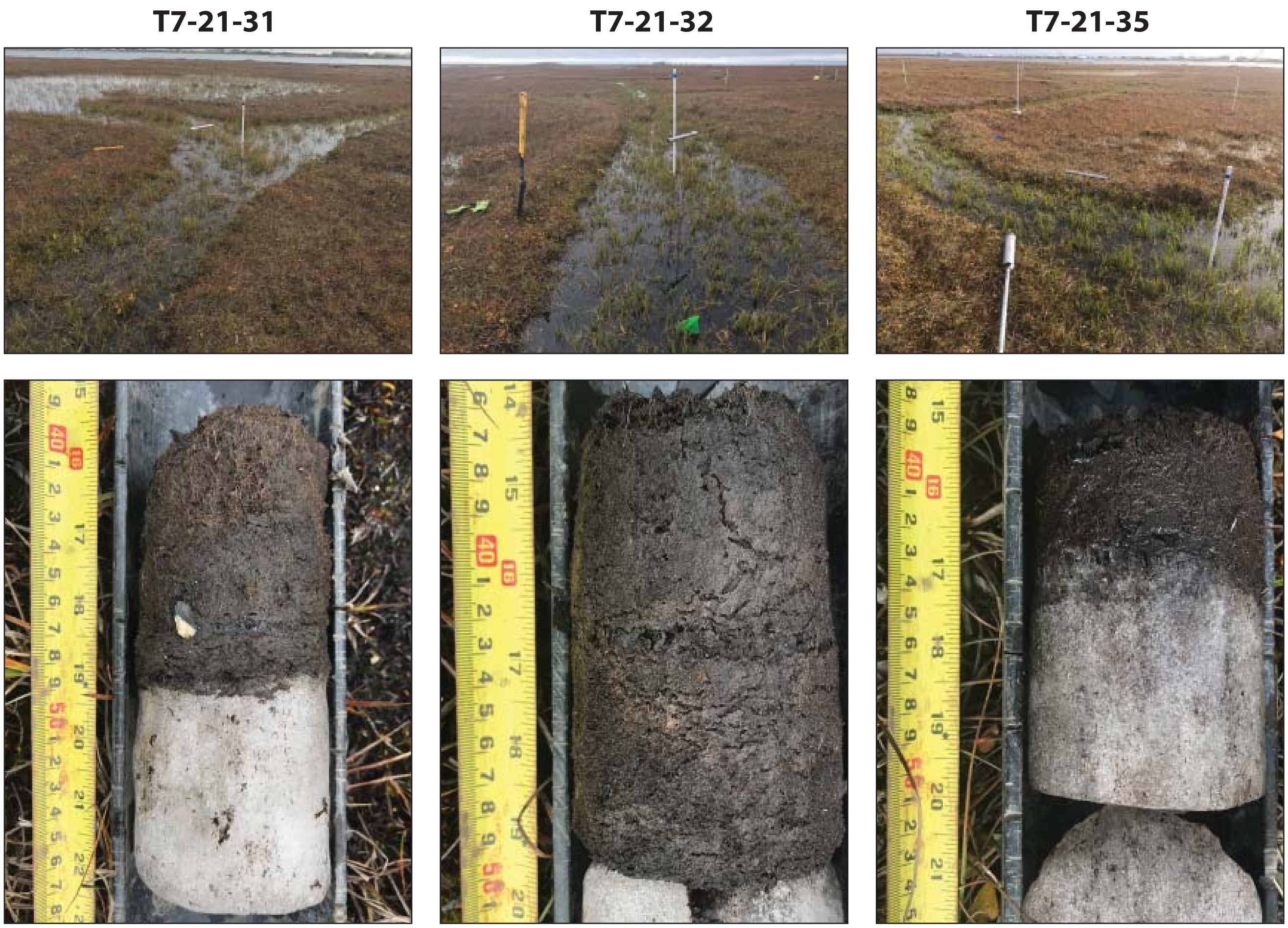

Figure 25. *Permanent vegetation plots with* Carex aquatilis *plant communities and frozen cores showing the interface between the ice wedge and protective layers of frozen soils. Vegetation plots (marked by white stakes in the upper photos) were sampled in 2021 (AGC 22-01, Walker et al. 2022b). Borehole locations are marked with the permafrost probe (upper photos).*

of the 13 was degrading in September 2021 when boreholes were redrilled (see Table A7.1 in AGC 22-01, Walker et al. 2022b).

- Some of the observed stabilization may be due to relatively cold summers at Prudhoe Bay in 2021 and 2022, which resulted in relatively thin active-layers (Romanovsky et al. 2017) (Figure 18).

2.6.5 Basal-peat dating

Helena Bergstedt and Ben Jones

2.6.5.1 Results from 2021 basal peat samples

- Basal-peat dates are needed to determine the ages of the various thaw-lake basins and areas apparently unaffected by thaw lakes at the NIRPO site.

Figure 26. *Helena Bergstedt and Skip Walker examining soil plug from a vegetation plot for C14 dating. (Photo: J.L. Peirce, IMG 4452)*

- Nine peat samples obtained for basal-peat dating in 2020 (Figure 26) yielded uncalibrated accelerator-mass spectrometry (AMS) Carbon-14 dates between modern and 1640 y BP (Table 6).
- Four dates from the residual surface (145 y BP – 445 y BP) are likely not from basal peat. The other dates are also very young (modern, 620 y BP, 690 y BP, 890 y BP and 1640 y BP) but do align with perceived sequence of lake drainage events. The young dates could be indicative of very recent stabilization and colonization of alluvial gravel sediments very close to the Sagavanirktok River.

2.6.5.1.1 Samples collected in 2021

Another 10 basal peat samples were collected for AMS Carbon-14 dating at the NIRPO site on 19 July 2021. Samples were collected adjacent to 10 terrestrial vegetation plots along transects T6, T7, T8, and T9 and will be used to examine trends in surface age along the terrain-age and soil-moisture gradients. NIRPO transects are on surfaces believed to represent three different thaw-lake drainage events and one residual surface that has no surface indications of prior thaw-lake activity. Four samples were obtained from T6 and T9 (the oldest residual surface); three from T7 (a relatively old drained-thaw-lake basin), and three from T8 (a recently drained thaw lake with two stages of drainage). See Table A6.1 in AGC 22-01 (Walker et al. 2022b) for descriptions and locations of basal peat samples obtained in 2021.

The chosen locations also represent the main vegetation types along the NIRPO soil-moisture gradient (three relatively well-drained moist tundra plots (U3 and U4), three wet tundra types without summer-long standing water (M2), and three wet/aquatic tundra types with persistant standing water (M4).

Each soil plug was described, including thaw depth, water depth, organic thickness, dominant texture, dominant mineral, state of the organic horizon (hemic, fibric, sapric), and depth of the sample.

A small amount of material was removed from the base of lowest organic horizon and frozen for later pretreatment at UAF where small intact macrofossils of organic material (e.g., bits of woody stems, sedge leaves or stems, moss) will be removed for dating.

2.7 Remote-sensing studies

2.7.1 Helicopter-based LiDAR snow mapping

Ronald Daanen

2.7.1.1 Introduction

A helicopter-based LiDAR survey of the snow-covered NNA-IRPS areas was made on 10 May 2022. The goal was to make a snow depth map of the eastern portion of the Prudhoe Bay Oilfield.

Table 6. *AMS C14 dates of material from basal peat samples collected on 17 August 2020 at the NIRPO reconnaissance area. See Figure 7 and Table A2.1 in AGC 22-01 for locations and descriptions of 2020 samples (Walker et al. 2022b).*

Sample basin ID	Depth (cm)	Age (y BP, uncalibrated)	Error	Lower Bound (y BP)	Upper Bound (y BP)	Surficial geology
BP-NIRPO-W-grass	13	145	15	8	278	Residual surface with thermokarst ponds
BP-NIRPO-W-moss	13	300	15	305	429	Residual surface with thermokarst ponds
BP-NIRPO-W-grass	17	250	15	156	309	Residual surface with thermokarst ponds
BP-NIRPO-W-moss	17	445	15	494	516	Residual surface with thermokarst ponds
BP1-grass, 24-26, 24-26	24	620	15	555	649	Recent drained lake basin surface
BP1-moss, 24-26, 24-26	24	890	15	735	897	Older portion of recent drained lake basin
BP2, 23-25	23	690	15	572	671	More recent portion of drained lake basin surface
BP3, 14-15	14	> Modern				Drained lake margin around current small oriented lake
BP4, 44-45	44	1,640	15	1418	1546	Small older drained lake basin

2.7.1.2 Methods

The flights lines covered the area between the Putuligayuk River and the Sagavanirktok River including the NNA-IRPS intensive research area and the Airport site (Figure 27).

A snow-depth map was made by subtracting the LiDAR-derived ground-surface elevations obtained August 2021 (see Section 3.2.1, p. 12-14, in AGC 22-01, Walker et al. 2022b) from the snow-surface elevations.

2.7.1.3 Results

- A portion of the LiDAR-derived snow-depth map that covers the NNA-IRPS intensive research area is shown in Figure 28a.
- Versions of the snow map in the vicinity of the 4-m tall Lemming Pingo indicate up to approximately 1.5 m of snow in the drift surrounding the pingo, and portions of its south-facing slopes have < 25 cm of snow. (Figure 28b, c).
- Snow depths along transect T6, have up to 65 cm of snow in the polygon troughs, and shallow snow < 25 cm deep in most polygon centers (Figure 28d).

2.7.1.4 Discussion

Early analyses in the vicinity of Lemming Pingo and Transect 6 indicate that the map can be used to determine snow depths at very fine (cm-scale) resolution. Future analyses will (1) compare the 2022 ground-based snow measurements at all the permanent plots, which were sampled 10 days prior to the LiDAR surveys, and (2) examine the depth and volume of snow drifts on pingos, lake and river margins, and near various forms of infrastructure, including buildings, gravel pads, and roads and pipelines at different angles to the prevailing winds and with different traffic regimes.

Figure 27. *Helicopter flight lines for the May 2022 snow survey.*

2.7.2 Remote sensing of dust impacts to snow

Helena Bergstedt, Ben Jones, Skip Walker

2.7.2.1 Introduction

A World View 2 image taken on 15 May 2022 (Figure 29) shows the snow conditions in the eastern portion of the Prudhoe Bay Oilfield during the spring melt season. Areas distant from heavily traveled gravel roads have nearly pure white surfaces. Nearly all areas within the boundaries of the road network have a subtle brownish color due to the presence of wind-blown dust; snow within 25–50 meters of heavily traveled roads has completely melted. The image shows a large contrast between the snow conditions at the NIRPO site which is only lightly impacted by road dust and the Colleen site, which is heavily impacted. This difference was also apparent two weeks earlier in ground-based photos of both sites taken on 2 May (Figure 11).

Sentinel 1 and 2 satellite data from April–May 2021 were used to examine the differences in the timing of snowmelt across the region due to the presence of road dust (Figure 30) (Bergsted et al. 2022). Areas near gravel roads with heavy traffic became snow free at least 1–2 weeks earlier than areas remote from roads. This study highlights the impact of infrastructure on a large area beyond the direct human footprint and the interconnectedness between snow-off timing, vegetation, surface hydrology, and near-surface ground temperatures.

A 24 May 2009 World View satellite image (Figure 31) illustrates typical large contrasts in snow cover near the end of the period of maximum snow melt in the vicinity of the NIRPO and Colleen sites. Much more of the landscape near roads is snow free compared to the images taken at the beginning of snowmelt (e.g., Figure 29). Many of these areas are covered with ponded water due to flooding caused by the elevated road surfaces. Remote infrequently traveled roads, elevated pipelines, elevated gravel pads, and lake bluffs have late-lying snowdrifts along their margins. The grid of snow trails in the center portion of the photo is caused by late-lying compressed snow in tracks from seismic vehicles. Areas more remote from the oilfield, such as in the lower left of the image, are still largely snow covered.

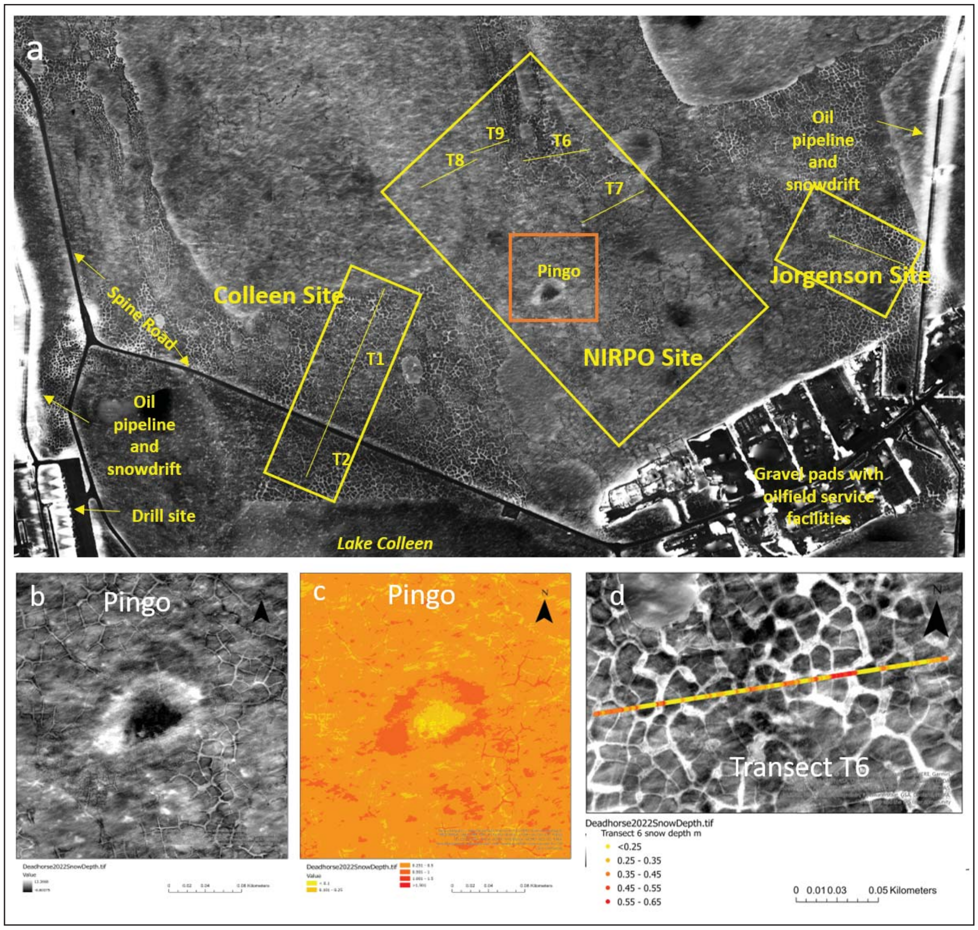

Figure 28. *LIDAR-derived snow map of NNA-IRPS intensive research area.* ***a.*** *Section covering the NNA-IRPS Colleen, NIRPO, and Jorgenson intensive research sites.* ***b.*** *Detail of the black and white snow map in the vicinity of Lemming Pingo.* ***c.*** *Colored version of the Lemming Pingo snow map with six snow-depth classes.* ***d.*** *Snow depths along transect T6. White areas indicate deeper snow in drifts and depressions; the darkest areas are very shallow snow.*

Figure 29. *World View 2 image of the Prudhoe Bay region, 15 May 2022, illustrating the contrast in snow conditions at the NIRPO and Colleen sites approximately two weeks after the 2022 ground survey of snow conditions at the the sites and five days after the LiDAR snow survey. Snow had melted along heavily traveled gravel roads, such as the Spine Road, while snow along infrequently traveled corridors such as the TAPS pipeline access road and the paved Dalton Highway remained white. Snow over much of the oilfield including the NIRPO site had discolored snow due to road dust. See Figure 11 showing ground views of snow conditions at the NIRPO site and near the road at the Colleen site on May 2, 2022. (World View 2 browse image.)*

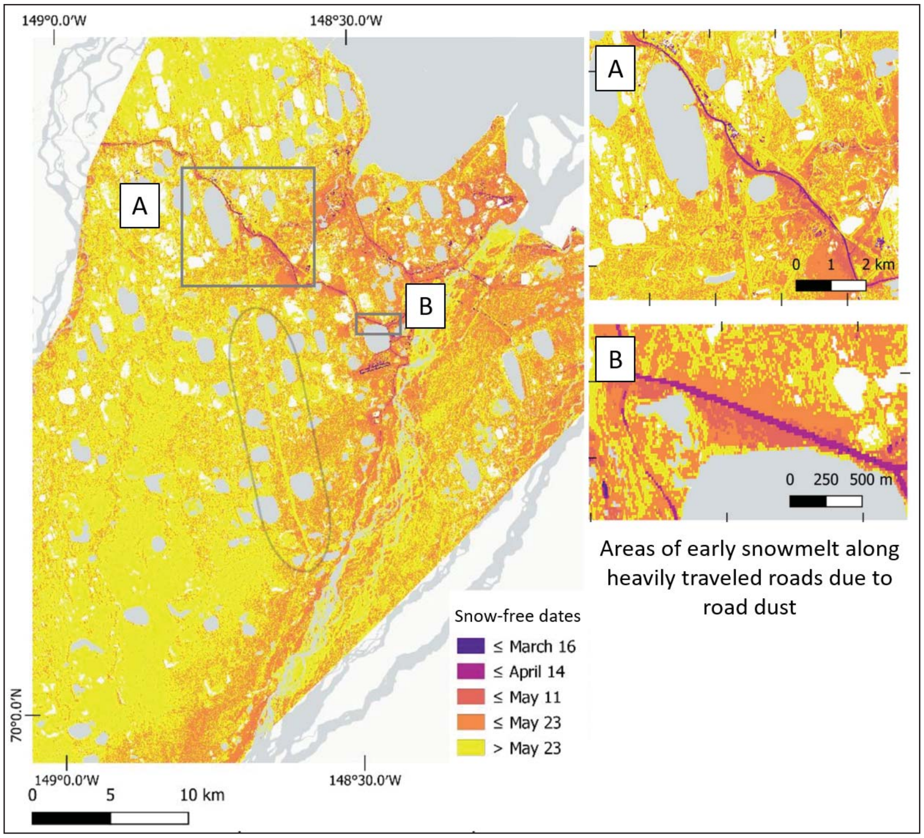

Figure 30. *Analysis of snow-free dates in 2021 using Sentinel 1 and 2 data. Areas shown in orange shades near roads and areas downwind from the Sagavanirktok and Kuparuk Rivers were generally snow free 1–2 weeks earlier than areas farther from roads and rivers. Area A is in the vicinity of the Hilcorp operations center, Pump Station 1, and the road to the regional landfill. Area B contains the Colleen site. Both areas show the earliest snowmelt on the southwest (leeward) side of the road where road dust is heaviest. Areas with late snow-free dates included the colder coastal area (northwest corner of the map), areas remote from roads and rivers south of the oilfield, and the large snowdrift that develops along the elevated portion of Trans-Alaska Pipeline System (yellow line within the grey oval). (Modified from Bergstedt et al. 2022)*

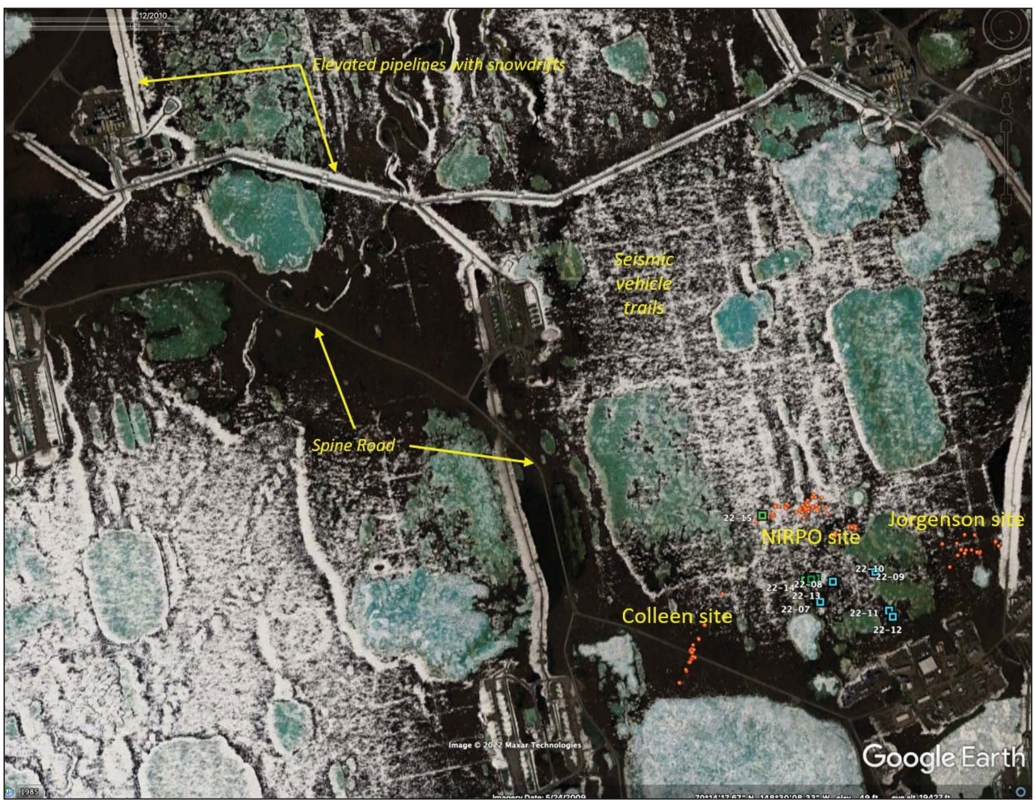

Figure 31. *Google Earth image of the vicinity of the NNA-IRPS intensive research area on 24 May 2009. Orange and blue squares are current locations of plots established at the NIRPO, Jorgenson, and Colleen sites. Large snowdrifts occur along elevated pipelines and lake bluffs. Large areas near heavily traveled gravel roads such as the Spine Road are snow free, and large parts of these areas are flooded due to damming effects of elevated roads. The grid of snow trails at center right was caused by a seismic survey during the winter. Spacing between the trails is about 230 m N-S and 400 m E-W. Areas more remote from the oilfield, such as that in the lower left, still have nearly continuous snow cover of snow. (Base image: Maxar Technologies)*

2.7.3 Automated recognition of ice-wedge polygons, waterbodies, and infrastructure from Maxar imagery in the PBO

Chandi Witharana, Elias Manos, Anna Liljedahl

2.7.3.1 Introduction

Data from the NNA-IRPS project is helping the Permafrost Discovery Gateway project develop pan-Arctic products at sub-meter resolution using machine and deep-learning models. These products include maps of ice-wedge polygons (Witharana et al. 2020, 2021), waterbodies (based on methods of Kaiser et al. 2021), and human-built infrastructure (Manos et al. 2022).

2.7.3.2 Methods

Artificial intelligence software developed at the University of Connecticut (Witharana et al. 2020) uses deep-learning convolutional neural nets (DLCNNs), fusion of multispectral and very high spatial resolution panchromatic satellite imagery, image-derived digital elevation models (DEMs), LiDAR-based DEMs, and large super computers to identify and map a variety Arctic features for the whole circumpolar Arctic. The software is being utilized by the Permafrost Discovery Gateway, hosted by the Arctic Data Center to make this information available through the internet (*arcticdata.io/catalog/portals/permafrost*, Anna Liljedahl, PI. NNA Award #1927723).

Figure 32. *Preliminary maps of ice-wedge polygons in NNA-IRPS Study Areas A, B, and C, the NNA-IRPS intensive research area, and NIRPO site using high-resolution Maxar imagery (Courtesy of Chandi Witharana).*

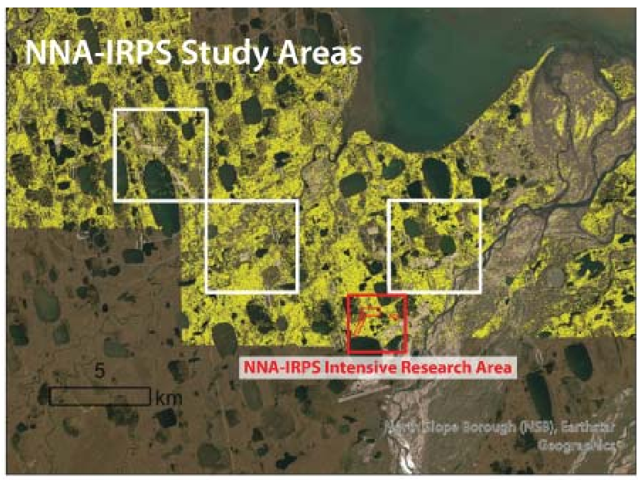

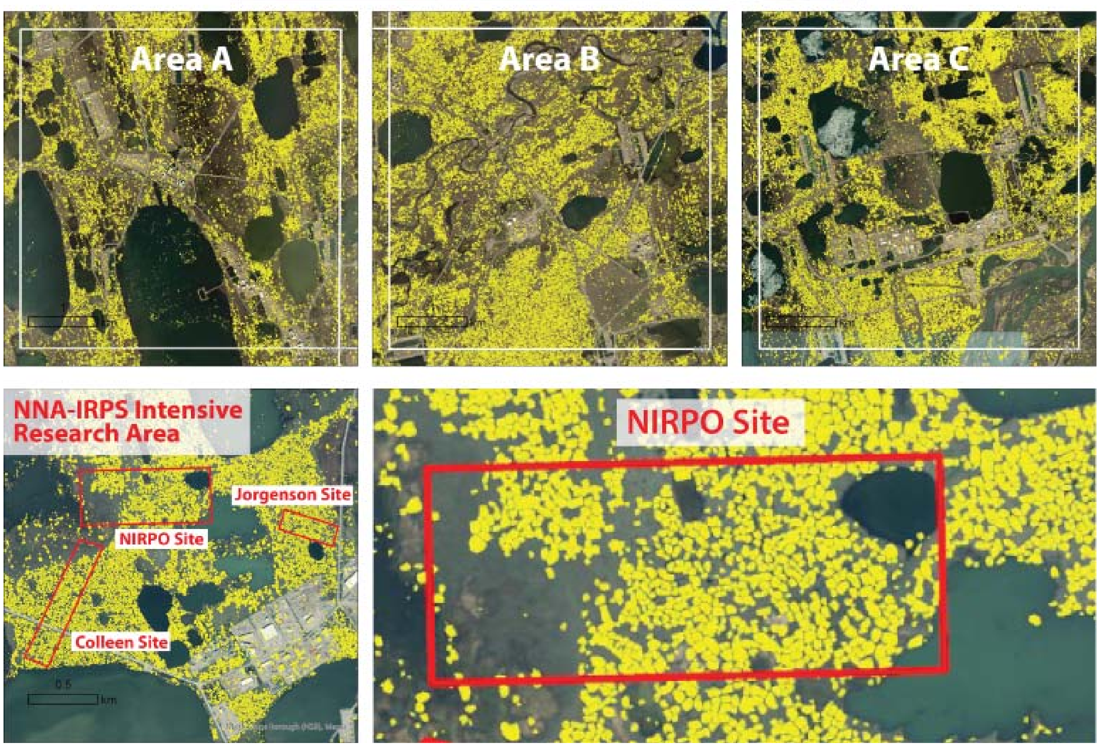

The time series of integrated geoecological historical disturbance maps (IGHDMs, Raynolds et al. 2014) of Areas A, B, and C and the NNA-IRPS intensive research area provide manually identified datasets of terrain and infrastructure to help train automated recognition of climate- and infrastructure-related changes in Arctic oilfields and the terrain conditions typical of the Central Arctic Coastal Plain, Alaska. A first step is to use high-resolution Maxar imagery to help the AI software recognize ice-wedge polygons (Figure 32), waterbodies (Figure 33), and the variety of infrastructure features specifically in the PBO (Figure 34).

2.7.3.3 Preliminary interpretation

- Early results indicate that the PDG software can detect most ice-wedge polygons in landscapes of the PBO where polygons and ice-wedges are relatively easy to identify on available high-resolution satellite images and aerial photographs. An analysis of the accuracy of prediction is needed across the various landscape units with differing concentrations and types of ice-wedge polygons.
- The early waterbody map of the NIRPO vicinity indicates that the current software, which has not been specifically trained to detect the variety of waterbodies in the rather unique conditions of PBO, is able to detect the larger lakes, but has trouble with three categories of smaller lakes: marl-bottomed ponds, small ice-wedge thermokarst ponds, and ponds with dark-colored aquatic vegetation. These are relatively distinct features that should be identifiable with more training of the software.
- The current version of the PDG software, again untrained to the conditions of a complex Arctic oilfield, is able to identify the larger roads and buildings but has not yet been trained to identify gravel pads, pipelines, and fine-scale disturbances such as off-road vehicle trails, and powerlines. Some of these features, particularly gravel pads and pipelines should be relatively easy to distinguish.

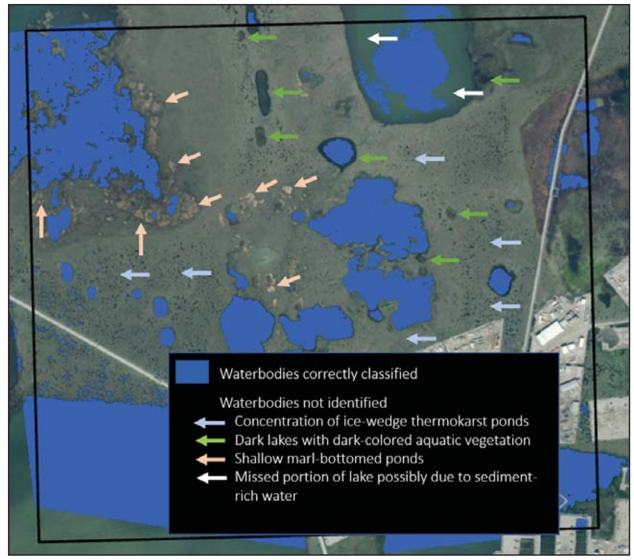

Figure 33. *Draft AI-assisted map of waterbodies in the NNA-IRPS intensive research area showing correct and missed water body identification. (Base image: Chandi Witharana)*

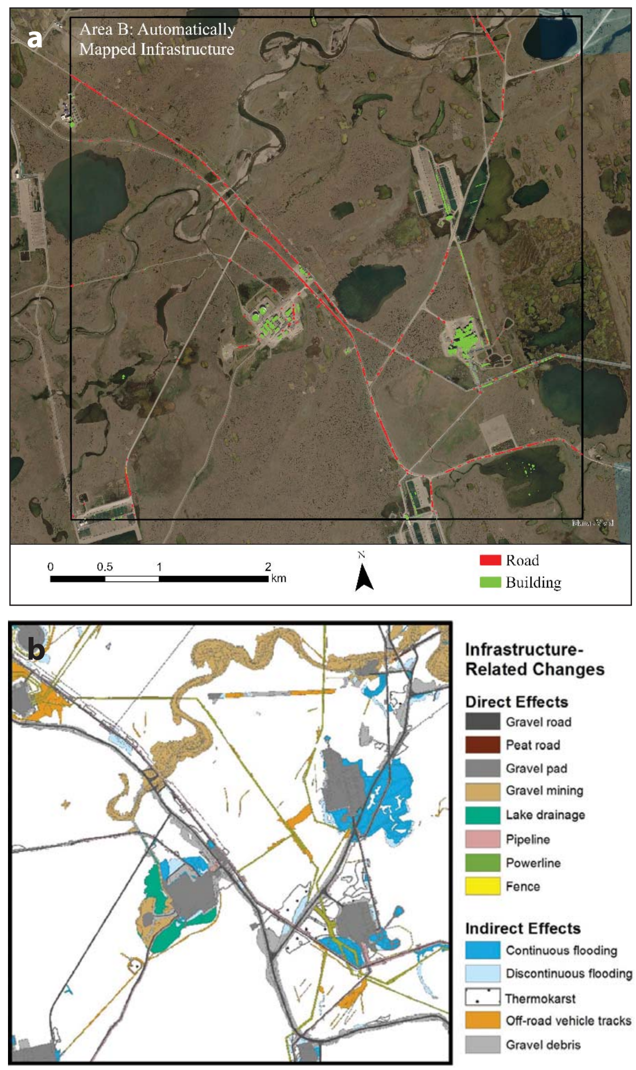

Figure 34. ***a.*** *Draft AI-assisted map of infrastructure in Area B prepared by Elias Manos, and comparison with* ***b.*** *manually mapped infrastructure by Raynolds et al. (2014).*

3 Summary of accomplishments and observations of the 2022 studies and future directions

3.1 The NIRPO research site

- Research at the NIRPO site is examining an ice-rich Arctic coastal-plain landscape, where thaw-lake and ice-wedge-polygon development occurs on gravelly, carbonate-rich, alluvial deposits of the Sagavanirktok River. The landscapes have windblown loess, nonacidic-tundra, and shallow marl-bottomed lakes. These conditions contribute to the rich basiphilous vascular-plant and bryophyte floras and abundant wildlife populations of the Prudhoe Bay region.
- Recent Arctic warming and disturbances associated with oilfield infrastructure have melted the tops of ice wedges, modifying the microtopography of ice-wedge polygons, creating an exponential increase in the number and size of thermokarst ponds that have altered hydrological patterns in the region.
- The NIRPO site was developed to better understand how these changes are affecting the permafrost and local ecosystems. Studies at the NIRPO site and the adjacent Jorgenson site are relatively distant from infrastructure and complement studies at the heavily impacted Colleen and Airport research sites.

3.2 Vegetation studies

3.2.1 New plots

- In 2022, the NIRPO boundaries were expanded to include a small pingo and two adjacent partially drained thaw-lake basins.
- Fifteen new vegetation plots were surveyed in the vicinity of a small pingo and nearby ponds and lakes, focusing on the vegetation of the dry and aquatic ends of the soil-moisture gradient. The new plots complement the 79 plots surveyed at the NIRPO and Jorgenson sites in 2021 and the 59 road-disturbed plots surveyed at the Colleen and Airport sites in 2014–2015, bringing the total number of NNA-IRPS permanent vegetation plots to 138.
- The pingo plots provided insights to vegetation and soil response along meso-topographic hillslope gradients and the zoogenic soils and vegetation on pingo summits and south-facing slopes.
- The samples from marl-bottomed lakes and ponds are the first to focus on this habitat type, which is likely a major contributor to the high biodiversity in the region's ecosystems. Much more work is needed on a variety of related topics including the composition of the marl deposits, methods of formation, paleo-significance of marl bands found in local soils, and the biological diversity of the marl and its contributions to local food webs.

3.2.2 Aboveground biomass

- Aboveground biomass on the 75 plots sampled in 2021 and 2022 ranged from a mean of 25 g/m^2 in marl-bottomed-lake plots with sparse sedge (*Carex aquatilis*) vegetation to 3617 g/m^2 in the aquatic moss communities (*Calliergon richardsonii*) in ice-wedge thermokarst ponds.
- Moss biomass made up a large portion of the total biomass in most vegetation types. Such extraordinarily high biomass in thermokarst ponds is not found anywhere else in local plant communities. Future studies should examine the reasons for this and determine if these aquatic moss communities are likely to persist or are temporary phenomena.

3.2.3 Bryophyte life-form classification

- A total of 77 bryophyte taxa were identified in 19 plots that spanned nine vegetation types along the moisture gradient at the NIRPO site.
- A trend of decreasing species richness occurred between moist U3 tundra, with means of 24-26 species/plot, and the very wet aquatic plots (M4, M4/E1, E1, and E2), with 0–4.5 species/plot.
- A life-form categorization of bryophytes could simplify characterization of moss mats in different habitats and possibly help in modeling the insulative properties of the moss layer.

- The most common life forms were short turfs, followed by short solitaires, and rough mat species.
- Further examination of the rich bryophyte flora of the Prudhoe Bay region should focus on additional habitat types and the influence of bryophyte life forms on the insulative capacity of the moss layer. Other approaches to dividing bryophytes into functional units should also be explored.

3.2.4 Soil-temperature loggers

- Soil-temperature loggers were installed at three depths in 35 plots across the NIRPO soil-moisture gradient. The loggers will be retrieved in August 2023 to contribute to an analysis of the effect of different types of vegetation on soil temperatures.

3.2.5 Snow and active-layer studies

- Snow depth, snow density and snow water equivalent were measured on 125 permanent vegetation plots in spring 2022. Water depth and thaw depth were measured on all 138 plots in August 2022. These data along with the soil temperature data will be used in Olivia Hobgood's MS thesis research, which will include a multivariate analysis of vegetation/environmental relationships along a soil-moisture gradient at the NIRPO site.
- Snow was generally much deeper in polygon troughs and thermokarst pits, compared to polygon centers and featureless areas with no patterned ground. Deep snow also occurred in drifts adjacent to roads and other forms of infrastructure.
- The snow measurements were made at the beginning of the snow-melt season, when road dust covered the snow at the Colleen site while the NIRPO plots were relatively clean. The dust has a large effect on the timing of snowmelt (Bergstedt et al. 2022). Future surveys should quantify the amount of dust in the snow at varying distances from the roads in relation to the prevailing winds.

3.2.6 Greenhouse gas monitoring

- Ecosystem respiration was low in all plots sampled along the NIRPO soil-moisture gradient in late winter/early spring 2022 as expected due to cold soils and snow cover. However, small but relatively high winter CO_2 flux (approximately 0.055 µmol m^{-2} s^{-1}) did occur in wet/aquatic troughs, where thick ice and moderately deep snow also occurred. Summer 2021 net ecosystem exchange (NEE) was also highest in trough plots.
- Midsummer 2022 net ecosystem exchange was approximately 2–5 times greater in wet and aquatic trough plots along the Colleen transects than on the well-drained polygon centers.

3.3 Permafrost

3.3.1 Climate and active-layer thickness

- The 2022 maximum snowpack at the Deadhorse site was anomalously deep, approximately 80 cm compared to 40–60 cm in the previous four years.
- The 2022 mean annual air temperature was the coldest in the past 22 years (-11.6 ˚C), but the ground-surface and permafrost-surface temperatures rebounded after three years of declining temperatures and were approximately 1 ˚C warmer than in 2021, probably due to the deep snowpack.
- The mean active layer thickness (ALT) in 2021 and 2022 was 65 cm, near the long-term (1996–2022) mean but thinner than in any year of the last warm decade.

3.3.2 NIRPO and Colleen ground-surface and near-surface permafrost-temperatures

- The mean annual ground temperature (MAGT) profiles from eight stations established in 2021 showed patterns related to a complex gradient involving surface age, site moisture, and snow cover. Mean annual ground-surface temperatures were coldest on the oldest, driest, least snowy residual surfaces at T6 and T9, and warmest at the wettest, snowiest, disturbed roadside sites at T1 and T2.
- The smallest temperature declines with depth were on the residual surfaces, and the largest declines were at the highly disturbed Colleen sites.

3.3.3 Electromagnetic Resistivity Tomography (ERT) transects

- The ERT results indicate that it was possible to distinguish sections with different temperatures based on the data in summer 2022. A comparison of the MAGT data and the results of one-dimensional resistivity models based on the results of automatic inversion shows the maximum resistivity of ~ 19,000 Ω m corresponded with the coldest MAGT along Transect T9 at -2 m depth (approximately -6.3 ˚C) and the minimum resistivity of ~ 550 Ω m along Transect T1 corresponded to the warmest temperatures at -2 m depth (approximately -3.9 ˚C).

3.3.4 Borehole studies of ice-wedge degradation

- Thirty-one permafrost boreholes were drilled in late August 2022 to examine the status of permafrost and protective layers above ice wedges (10 boreholes in thermokarst ponds at the NIRPO site along transect T6; nine in thermokarst ponds at the Jorgenson transect; three in ice-wedge troughs along transect T7 at the NIRPO site, and nine in road-related disturbed sites along Colleen site transect T2).
- Most ice wedges that were actively degrading in 2011–2015 have shown recent stabilization as detected by thicker intermediate and transient layers.
- Some of the recently observed stabilization is likely due to relatively cold summers in 2021 and 2022.
- The most significant stabilization occurred in deep thermokarst ponds, where rapid growth of aquatic vegetation has resulted in a decrease in active-layer thickness and formation of a thick ice-rich protective layer above partially degraded ice wedges.
- Degradation was previously most evident in areas near roads. For example, seven ice wedges of 13 at the Airport site (T3 and T5) were degrading in September 2015, but only one was degrading in September 2021. Similarly, ice wedges at the Colleen site (T1 and T2) that were vulnerable in 2014 had experienced some stabilization by 2021-2022.

3.3.5 Basal peat dating

- Nine basal peat samples obtained for C14 dating in 2020 yielded young dates that could be indicative of recent stabilization and colonization of alluvial gravel sediments close to the Sagavanirktok River.
- Ten samples collected in 2021 adjacent to terrestrial vegetation plots along transects T6–T9 will be used to examine trends in vegetation and permafrost properties along the surface-age gradient.

3.4 Remote sensing

3.4.1 Helicopter-based LIDAR snow mapping

- A helicopter-based LiDAR snow-surface-topography survey covered the area between the Putuligayuk River and the Sagavanirktok River, including the NNA-IRPS intensive research area and the Airport site. A snow-depth map was made by subtracting the ground-surface elevations obtained from the 2021 LiDAR survey from the 2022 snow-surface elevations.
- Early analyses in the vicinity of Lemming Pingo and transect T6 indicate that the map can be used to determine snow depths at very fine (cm-scale) resolution.
- Future analyses will (1) compare the 2022 LiDAR snow depth with 2022 ground-based snow measurements at all permanent plots, (2) examine the depth and volume of snow drifts near infrastructure including roads and pipelines at different angles to the prevailing winds and with different traffic regimes, and (3) analyze snow gradients on different aspects of pingos within the mapped area.

3.4.2 Remote sensing of dust impacts to snow

- Satellite images and ground-based photos obtained near the beginning of the snowmelt season illustrate the contrasts between the snow conditions at the relatively dust-free NIRPO site and the heavily dusted Colleen site.
- Sentinel 1 and 2 satellite data were used to analyze differences in the timing of snowmelt across the PBO region due to presence of road dust in April–May 2021 (Bergstedt et al. 2022). Areas near gravel roads with heavy traffic were snow free at least 1-2 weeks earlier than areas remote from roads.

3.4.3 Automated recognition of ice-wedge polygons, waterbodies, and infrastructure from Maxar imagery in the PBO

- Data from the NNA-IRPS project is helping the Permafrost Discovery Gateway develop pan-Arctic products at sub-meter resolution. These products include maps of ice-wedge polygons, waterbodies, and human-built infrastructure.
- Early results indicate that the PDG software can detect most ice-wedge polygons in this landscape where polygons and ice-wedges are relatively close to the surface. An analysis of the accuracy of prediction is needed across the various landscape units with differing concentrations and types of ice-wedge polygons.
- An early waterbody map of the NIRPO vicinity indicates that the AI software, in its current state of training, has trouble with three categories of smaller water bodies: marl bottomed ponds, small ice-wedge thermokarst ponds, and ponds with dark-colored aquatic vegetation.
- The current version the PDG software can identify the larger roads and building but has not yet been trained to identify gravel pads, pipelines, and fine-

scale disturbances such as off-road vehicle trails and powerlines. The gravel pads and pipelines should be relatively easy to distinguish.

3.5 Future directions and synthesis

3.5.1 Vegetation

- Complete analysis of vegetation along the NIRPO site-moisture gradient and compare with information from the 1970s for Olivia Hobgood’s MS thesis.
- Collect iButton temperature loggers at permanent vegetation plots and analyze soil temperature data from 2021 and 2022.
- Develop a vegetation map of the NIRPO-Jorgenson-Colleen (NJC) Area using the most recent high-resolution satellite imaging.
- Complete a manuscript describing the use of the LiDAR snow map to quantify snow in relation to patterned-ground microtopography and vegetation and in relation to infrastructure features.

3.5.2 Trace-gas fluxes

- Complete analysis and publish a paper on the seasonal variation in greenhouse gas fluxes across the site-moisture gradient at the NIRPO site and roadside disturbance gradients at the Colleen site.

3.5.3 Permafrost

- Continue collection of borehole ground-temperature data.
- Examine 2022–2023 pond water-depth and temperature data from thermokarst ponds.
- Continue development of a permafrost-temperature model using integrated terrain maps.
- Expand ERT data collection to other transects at the NIRPO, Jorgenson, and Airport sites.
- Synthesis of thermokarst-pond, ice-wedge borehole, and vegetation data.

3.5.4 Remote sensing

- Obtain 1949 and nearly annual 1970–2022 industry aerial photographs of the NIRPO area. Use the photos to determine the age of all the studied NIRPO and Jorgenson thermokarst ponds, original surface forms, and vegetation at all NIRPO permanent vegetation plots.
- Use Maxar Google Earth imagery to determine how many vegetation plots sampled in the 1970s have been covered by roads, gravel pads, and other forms of infrastructure or eliminated by natural disturbances.
- Continue to work with the Permafrost Discovery Gateway scientists to develop automated high-resolution maps of ice-wedge polygons, waterbodies, and infrastructure.

3.5.5 Synthesis

- The synthesis will focus on the past and future evolution of the landscapes, soils, vegetation, and permafrost at the NIRPO site under the influence of climate- and infrastructure-related changes with a focus on the influence of surficial geology.
- A focus will be describing the unique ecosystems that have developed on the carbonate-rich alluvial deposits of the Sagavanirktok alluvial, eolian, and lacustrine deposits, and their influence on ice-rich permafrost.
- The data collected to date will be used for developing several manuscripts including:
    - Landscape evolution in the Prudhoe Bay Oilfield caused by climate-change and infrastructure-related impacts
    - Snow conditions in the PBO in relation to terrain, vegetation, infrastructure, and road dust.
    - Trace-gas fluxes in disturbed and undisturbed ice-wedge polygon landscapes
    - Spatial models of ice-wedge degradation sensitivity
    - Spatial models of permafrost temperature change due to climate and infrastructure
    - Publication(s) from Olivia Hobgood's MS thesis describing the present-day vegetation and landscapes of the NIRPO site and comparisons with those of the 1970s

4 References

Bates J. W. 1998. Is 'life-form' a useful concept in bryophyte ecology? Oikos, 82:223–237.

Bergstedt, H., B. M. Jones, D. A. Walker, J. L. Peirce, A. Bartsch, G. Pointner, M. Z. Kanevskiy, M. K. Raynolds, and M. Buchhorn. 2022. The spatial and temporal influence of infrastructure and road dust on seasonal snowmelt, vegetation productivity, and early season surface water cover in the Prudhoe Bay Oilfield. Arctic Science, e-First. DOI:10.1139/as-2022-0013

Brown. 1975. Ecological investigations of the tundra biome in the Prudhoe Bay region, Alaska. Biological Papers of the University of Alaska Nr. 2, 2:240. www.arlis.org/docs/vol1/B/3035866.pdf.

Everett, K. R., and R. J. Parkinson. 1977. Soil and landform associations, Prudhoe Bay area, Alaska. Arctic and Alpine Research, 9:1–19.

Fahnestock, J. T., M. H. Jones, P. D. Brooks, D. A. Walker, and J. M. Welker. 1998. Winter and early spring CO_2 efflux from tundra communities of northern Alaska. Journal of Geophysical Research, 103:29023–29027. DOI:10.1029/98JD00805

Grace M. 1995. A key to the growth forms of mosses and liverworts and guide to their educational value. Journal of Biological Education, 29:272–278.

Guillet, G. R., 1969. Marl in Ontario. Ontario Department of Mines, Industrial Mineral Report 28.

Hill, M. O., C. D. Preston, S. D. S. Bosanquet, and D. B. Roy. 2007, updated 2017. BRYOATT: Attributes of British and Irish mosses, liverworts and hornworts. NERC Centre for Ecology and Hydrology, UK.

Jorgenson, M. 2011. Coastal region of northern Alaska: guidebook to permafrost and related features. Guidebook 10. State of Alaska Division of Geological and Geophysical Surveys. https://dggs.alaska.gov/webpubs/dggs/gb/text/gb010.pdf

Jorgenson, M. T., M. Kanevskiy, Y. Shur, N. Moskalenko, D. R. N. Brown, K. Wickland, R. Striegl, and J. Koch. 2015. Role of ground ice dynamics and ecological feedbacks in recent ice wedge degradation and stabilization. Journal of Geophysical Research: Earth Surface, 120:2280–2297.

Kaiser, S., G. Grosse, J. Boike, and M. Langer. 2021. Monitoring the transformation of arctic landscapes: automated shoreline change detection of lakes using very high resolution imagery. Remote Sensing, 13:2802. DOI:10.3390/rs13142802

Kanevskiy, M., Y. Shur, T. Jorgenson, D. R. N. Brown, N. Moskalenko, J. Brown, D. A. Walker, M. K. Raynolds, and M. Buchhorn. 2017. Degradation and stabilization of ice wedges: implications for assessing risk of thermokarst in northern Alaska. Geomorphology, 297:20–42. DOI: 10.1016/j.geomorph.2017.09.001

Kanevskiy, M., Y. Shur, D. A. Walker, T. Jorgenson, M. K. Raynolds, J. L. Peirce, B. M. Jones, and M. Buchhorn. 2022. The shifting mosaic of ice-wedge degradation and stabilization in response to infrastructure and climate change, Prudhoe Bay Oilfield, Alaska, USA. Arctic Science, 8:498–530. DOI:10.1139/as-2021-0024

Koch, J. C., M. T. Jorgenson, K. P. Wickland, M. Kanevskiy, and R. Striegl. 2018. Ice wedge degradation and stabilization impact water budgets and nutrient cycling in Arctic trough ponds. Journal of Geophysical Research: Biogeosciences, 123:2604–2616. DOI:10.1029/2018JG004528

Lett S., I. Jónsdóttir, A. Becker-Scarpitta, C. Christiansen, H. During, F. Ekelund, G. Henry, S. Lang, A. Michelsen, K. Rousk, J. Alatalo, K. Betway, S. Busca, T. Callaghan, M. Carbognani, E. Cooper, J. Cornelissen, E. Dorrepaal, D. Egelkraut, and K. van Zuijlen K. 2022. Can bryophyte groups increase functional resolution in tundra ecosystems? Arctic Science, 8: 609–637. DOI:10.1139/as-2020-0057

Longton R. E. 1988. Adaptations and strategies of polar bryophytes. Botanical Journal of the Linnean Society, 98:253–268. DOI:10.1111/j.1095-8339.1988.tb02429.x

Mägdefrau, K. 1982. Life-forms of bryophytes. Pages 45–48 *in* A. J. E. Smith, editor. Bryophyte Ecology. 1st edition. Chapman and Hall, NY, USA.

Manos, E., C. Witharana, M. Udawalpola, A. Jasam, and A. Liljedahl. 2022. Convolutional neural networks for automated built infrastructure detection in the Arctic using sub-meter spatial resolution satellite imagery. Remote Sensing, 14:2719. DOI:10.3390/rs14112719

May J. L., T. Parker, S. Unger, and S. F. Oberbauer. 2018. Short term changes in moisture content drive strong changes in Normalized Difference Vegetation Index and gross prima productivity in four Arctic moss communities. Remote Sensing of Environment, 212:114–120.

Moxham, R. M., and R. A. Eckhart. 1956. Marl Deposits in the Knik Arm area, Alaska, Geological Survey Bulletin 1039-A. Department of the Interior, Washington, DC, USA. DOI:10.3133/b1039A

Munsell Color. 1975. Munsell soil color charts. Kollmorgen Corporation, Baltimore, MD, USA.

Musselman, R. C., W. J. Massman, J. M. Frank, and J. L. Korfmacher. 2005. The temporal dynamics of carbon dioxide under snow in a high elevation Rocky Mountain subalpine forest and meadow. Arctic, Antarctic, and Alpine Research, 37:527–538. DOI: 10.1657/1523-0430(2005)037[0527:TTDOCD]2.0.CO;2

Nakatsubo, T. 1994. The effect of growth form on the evaporation in some subalpine mosses. Ecological Research, 9:245–250.

National Research Council. 2003. Cumulative environmental effects of oil and gas activities on Alaska's North Slope. National Academies Press, Washington, DC, USA. DOI: 10.17226/10639

Porada, P., A. Ekici, and C. Beer. 2016. Effects of bryophyte and lichen cover on permafrost soil temperature at large scale. The Cryosphere, 10:2291–2315. DOI:10.5194/tc-10-2291-2016

Proctor M. C. F., J. O. Melvin, A. J. Wood, P. Alpert, L. R. Stark, N. L. Cleavitt, and B. D. Mishler. 2007. Desiccation tolerance in bryophytes: a review. The Bryologist, 110:595–621.

Raynolds, M. K., A. L. Breen, D. A. Walker, R. Elven, R. Belland, N. Konstantinova, H. Kristinsson, and S. Hennekens. 2013. The pan-arctic species list (PASL). Pages 92–95 *in* D. A. Walker, A. L. Breen, M. K. Raynolds, and M. D. Walker, editors. Arctic Vegetation Archive Workshop: Krakow, Poland, 14–16 April 2013. CAFF Proceedings Series Report Nr. 10. Conservation of Arctic Flora and Fauna, Akureyri, Iceland. https://www.caff.is/proceedings-series/252-arctic-vegetation-archive-ava-workshop-krakow-poland-april-14-16-2013; updated list at: www.caff.is/flora-cfg/ava/pan-arctic-species-list.

Rawlinson, S. E. 1993. Surficial geology and morphology of the Alaskan central Arctic coastal plain. Alaska Division of Geology and Geophysical Surveys, Report of Investigations, 93–1.

Raynolds, M. K., D. A. Walker, K. J. Ambrosius, J. Brown, K. R. Everett, M. Kanevskiy, G. P. Kofinas, V. E. Romanovsky, Y. Shur, and P. J. Webber. 2014. Cumulative geoecological effects of 62 years of infrastructure and climate change in ice-rich permafrost landscapes, Prudhoe Bay Oilfield, Alaska. Global Change Biology, 20:1211–1224. DOI:10.1111/gcb.12500.

Romanovsky, V., K. Isaksen, D. Drozdov, O. Anisimov, A. Instanes, M. Leibman, A. D. McGuire, N. Shiklomanov, S. Smith, and D. Walker. 2017. Changing permafrost and its impacts. Pages 66–102 *in* Snow, Water, Ice and Permafrost in the Arctic (SWIPA) 2017. Arctic Monitoring and Assessment Programme (AMAP), Oslo, Norway.

Romanovsky, V. E., and T. E. Osterkamp. 1995. Interannual variations of the thermal regime of the active layer and near-surface permafrost in Northern Alaska. Permafrost and Periglacial Processes, 6:313–335.

Schindlbacher, A., S. Zechmeister-Boltenstern, G. Glatzel, and R. Jandl. 2007. Winter soil respiration from an Austrian mountain forest. Journal of Agricultural and Forest Meteorology, 146:205–215. DOI: 10.1016/j.agrformet.2007.06.001

Smith, T., H. Shugart, and F. Woodward, editors. 1997. Plant Functional Types. Cambridge University Press, Cambridge, UK.

Sullivan, P. F. (2010), Snow distribution, soil temperature and late winter CO_2 efflux from soils near the arctic treeline in northwest Alaska. Biogeochemistry, 99:65–77. DOI:10.1007/s10533-009-9390-0

Schwert, D. P., T. W. Anderson, A. Morgan, A. V. Morgan, and P. F. Karrow. 1985. Changes in late Quaternary vegetation and insect communities in southwestern Ontario. Quaternary Research, 23:205–226.

Truett, J. E., and S. R. Johnson, editors. 2000. The natural history of an arctic oilfield development and biota. Academic Press, San Diego, CA.

Turetsky, M. R., B. Bond-Lamberty, E. Euskirchen, J. Talbot, S. Frolking, A. D. McGuire, and E.-S. Tuittila. 2012. The resilience and functional role of moss in boreal and arctic ecosystems. New Phytologist, 196:49–67. DOI:10.1111/j.1469-8137.2012.04254.x

Victoria F., Costa D. & Pereira A. 2009. Life-forms of moss species in defrosting areas of King George Island, South Shetland Islands, Antarctica. Bioscience Journal, 25:151–160.

Vreeken, W. J., 1981. Distribution and chronology of freshwater marls between Kingston and Belleville, Ontario. Canadian Journal of Earth Sciences, 18:1228.1239

Walker, D. A. 1985. Vegetation and environmental gradients of the Prudhoe Bay region, Alaska. CRREL Report 85–14. US Army Cold Regions Research and Engineering Laboratory, Hanover, NH, USA. http://hdl.handle.net/11681/9420

Walker, D. A., M. Buchhorn, M. Kanevskiy, G. V. Matyshak, M. K. Raynolds, Y. L. Shur, and J. L. Peirce. 2015. Infrastructure-thermokarst-soil-vegetation interactions at Lake Colleen Site A, Prudhoe Bay, Alaska. AGC Data Report 15-01. Alaska Geobotany Center, Fairbanks, AK, USA. DOI: 10.18739/A2M61BQ8M

Walker, D. A., M. Buchhorn, M. Kanevskiy, M. K. Raynolds, Y. L. Shur, and L. M. Wirth. 2016. Road effects at Airport study site, Prudhoe Bay, Alaska, summer 2015. AGC Data Report 16-01. Alaska Geobotany Center, Fairbanks, AK, USA. DOI: 10.18739/A2VM42Z20

Walker, D.A., and K. R. Everett. 1991. Loess ecosystems of northern Alaska: regional gradient and toposequence at Prudhoe Bay. Ecological Monographs, 61:437-464. DOI:10.2307/2937050.

Walker, D. A., K. R. Everett, P. J. Webber, and J. Brown. 1980. Geobotanical atlas of the Prudhoe Bay region, Alaska. CRREL Report 80–14. US Army Cold Regions Research and Engineering Laboratory, Hanover, NH, USA. http://hdl.handle.net/11681/9008

Walker, D. A., M. Kanevskiy, M. K. Raynolds, and J. L. Peirce. 2018. 2016 ArcSEES data report: snow, thaw, temperature and permafrost borehole data from the Colleen and Airport sites, Prudhoe Bay, Alaska, and Quintillion fiber optic cable impacts, North Slope, Alaska. AGC Data Report 18-01. Alaska Geobotany Center, Fairbanks, AK, USA. DOI: 10.18739/A28K74X6T

Walker, D. A., M. Kanevskiy, A. L. Breen, A. Kade, R. P. Daanen, B. M. Jones, D. J. Nicolsky, H. Bergstedt, E. Watson-Cook, and J. L. Peirce. 2022b. Observations in ice-rich permafrost systems, Prudhoe Bay, Alaska, 2020–2021. AGC Data Report 22-01. Alaska Geobotany Center, Fairbanks, AK, USA.

Walker, D. A., M. K. Raynolds, M. Buchhorn, and L. M. Wirth. 2014. Landscape and permafrost changes in the Prudhoe Bay Oilfield, Alaska. AGC 14-01. Alaska Geobotany Center, Fairbanks, AK, USA. DOI: 10.18739/A24X54H5D

Walker, D. A., M. K. Raynolds, M. Z. Kanevskiy, Y. S. Shur, V. E. Romanovsky, B. M. Jones, M. Buchhorn, M. T. Jorgenson, J. Šibík, A. L. Breen, A. Kade, E. Watson-Cook, H. Bergstedt, A. K. Liljedahl, R. P. Daanen, B. Connor, D. Nicolsky, and J. L. Peirce. 2022a. Cumulative impacts of a gravel road and climate change in an ice-wedge polygon landscape, Prudhoe Bay, Alaska. Arctic Science, 8:1040-1066. DOI: 10.1139/as-2021-0014.

Walker, D. A., P. J. Webber, E. F. Binnian, K. R. Everett, N. D. Lederer, E. A. Nordstrand, and M. D. Walker. 1987. Cumulative impacts of oil fields on northern Alaskan landscapes. Science, 238:757–761. DOI: 10.1126/science.238.4828.757

Wang, Z., X. Liu, and W. Bao. 2016. Higher photosynthetic capacity and different functional trait scaling relationships in erect bryophytes compared with prostrate species. Oecologia, 180:359–369. DOI: 10.1007/s00442-015-3484-2

Watson-Cook, E. 2022. Thermokarst-pond plant community characteristics and effects on ice-wedge degradation in the Prudhoe Bay region, Alaska. MS thesis, University of Alaska Fairbanks.

Wickland, K. P., M. T. Jorgenson, J. C. Koch, M. Kanevskiy, and R. G. Striegl. 2020. Carbon dioxide and methane flux in a dynamic Arctic tundra landscape: decadal-scale impacts of ice wedge degradation and stabilization. Geophysical Research Letters, 47, e2020GL089894. DOI:10.1029/2020GL089894

Witharana, C., M. A. E. Bhuiyan, A. K. Liljedahl, M. Kanevskiy, H. E. Epstein, B. M. Jones, R. Daanen, C. G. Griffin, K. Kent, and M. K. W. Jones. 2020. Understanding the synergies of deep learning and data fusion of multispectral and panchromatic high resolution commercial satellite imagery for automated ice-wedge polygon detection. ISPRS Journal of Photogrammetry and Remote Sensing, 170:174–191. DOI:10.1016/j.isprsjprs.2020.10.010

Witharana, C., M. A. E. Bhuiyan, A. K. Liljedahl, M. Kanevskiy, T. Jorgenson, B. M. Jones, R. Daanen, H. E. Epstein, C. G. Griffin, K. Kent, and M. K. W. Jones. 2021. An object-based approach for mapping tundra ice-wedge polygon troughs from very high spatial resolution optical satellite imagery. Remote Sensing, 13:558. DOI:10.3390/rs13040558

Yang, J., P. F. Karrow, and G. L. Mackie. 2001. Paleoecological analysis of molluscan assemblages in two marl deposits in the Waterloo region, Southwestern Ontario, Canada. Journal of Paleolimnology, 25:313-328.

LIST OF APPENDICES

1 Field data sheets for vegetation plot surveys

Table A1.1 *Site descriptions* ... 44
Table A1.2 *Species cover-abundances* ... 46
Table A1.3 *Soil descriptions* ... 47

2 Site variable, vegetation type, and habitat type codes

Table A2.1 *Codes for categorical and scalar environmental site variables* ... 48
Table A2.2 *Vegetation type codes and categorical descriptors* ... 50
Table A2.3 *Habitat type codes and categorical descriptors* ... 51

3 Soil characteristics

Table A3.1 *Abbreviated descriptions of soil horizons at 2022 NIRPO vegetation plots* ... 53
Table A3.2 *Soil characteristics of 2022 NIRPO vegetation plots* ... 55

4 Vegetation plot photographs

Table A4.1 *Photographs of 2022 NIRPO vegetation plot lanscapes* ... 56
Table A4.2 *Photographs of 2022 NIRPO plot vegetation* ... 57
Table A4.3 *Photographs of 2022 NIRPO plot soils* ... 58

5 Environmental variables and plant growth forms

Table A5.1 *Environmental variables and growth-form cover for 2022 NIRPO plots* ... 60

6 Plant species list

Table A6.1 *Plant species list, 2021–2022 NIRPO vegetation plots* ... 62

7 Plant species cover

Table A7.1 *Percent species cover-abundance, 2022 NIRPO vegetation plots* ... 65

8 Aboveground biomass

Table A8.1 *Aboveground biomass of 2021–2022 NIRPO vegetation plots* ... 68

9 Bryophyte species cover and life forms

Table A9.1 *Bryophyte life-form analysis and species cover* ... 70

10 Snow survey

Table 10.1 *Snow depth, snow density, and SWE at NJC vegetation plots* ... 73

11 Ground temperature loggers

Table 11.1 *Placement of ground temperature loggers at NIRPO and Jorgenson sites* ... 76

12 Thaw and water depths

Table A12.1 *Thaw depth and water depth at NJC and Airport site vegetation plots* ... 77

13 Trace gas fluxes

Table A13.1 *Dates of 2021-2022 trace-gas flux sampling at NIRPO and Colleen sites* ... 79

14 Permafrost boreholes

Table 14.1 *Frozen protective layers above massive ice in T6 NIRPO site ponds, 2021–2022* ... 80
Table 14.2 *Frozen protective layers above massive ice in Jorgenson site ponds, 2019–2022* ... 81
Table 14.3 *Frozen protective layers above massive ice in T2 Colleen site ponds, 2014 & 2022* ... 82

APPENDIX 1 Field data sheets for vegetation plot surveys

Table A1.1. *Site description data sheet (reproduced at 85%).*

2022 NIRPO vegetation plot surveys: *Site descriptions* *pg. 1 of 3*

Location:				**Date:**			
Site:				**Observer(s):**			
Vegetation Type (code or dominant species):		**Plot number**					**Notes**
Photo No.	**Landscape** (from S. Side w/ plot #))						camera owner:
	Closeup (vertical w/ alum. cap #)						
	Soil (soil plug w/ plot # & scale)						
Slope	**Slope** (est. degrees, or inclinometer)						
	Aspect (N, NE, E, SE, S, SW, W, NW)						
Site factors (see 2022 site description codes)	**Landform**						
	Surficial geology (parent material)						
	Surficial geomorphology						
	Microsite						
	Site moisture						
	Soil moisture						
	Soil texture of top mineral horizon						
	Glacial geology						
	Topographic position						
	Habitat type						
	Estimated snow duration						
	Disturbance degree						
	Disturbance type						
	Physical stability						
	Exposure						
	Soil sample taken (Y, N)						
Live / standing dead cover %	**Low shrubs** (40-200 cm)	/	/	/	/	/	
	Erect dwarf shrubs (15-40 cm)	/	/	/	/	/	
	Prostrate dwarf shrubs (<15 cm)	/	/	/	/	/	
	Evergreen shrubs	/	/	/	/	/	
	Deciduous shrubs	/	/	/	/	/	
	Erect forbs	/	/	/	/	/	
	Mat & cushion forbs	/	/	/	/	/	
	Non-tussock graminoids	/	/	/	/	/	
	Tussock graminoids	/	/	/	/	/	
	Horsetails	/	/	/	/	/	
	Fruticose lichen	/	/	/	/	/	
	Foliose lichen	/	/	/	/	/	
	Crustose lichen	/	/	/	/	/	
	Pleurocarpous bryophytes	/	/	/	/	/	
	Acrocarpous bryophytes	/	/	/	/	/	
	Liverworts	/	/	/	/	/	
	Biological soil crust	/	/	/	/	/	
	Algae	/	/	/	/	/	
Other cover %	**Rock**						
	Bare soil						
	Litter						
	Water						

Table A1.1 *(continued)*

2022 NIRPO vegetation plots surveys: *Site descriptions*

pg. 2 of 3

Vegetation Type (code):		**Plot number**				
Vertical plant-canopy stucture, microrelief, thaw and water depths	**Mean top-of-plant-canopy height** (cm, 5 measurements)					
	Erect-dwarf-shrub-layer height (cm, 5 measurements)					
	Herb-layer height (inculdes prostrate dwarf shrubs) (cm, 5 measurements)					
	Live green moss thickness (cm, 5 measurements)					
	Live moss-layer thickness (lichens & mosses) (cm, 5 measurements)					
	Organic-soil horizons total thickness (cm, 1 measurement from soil plug)					
	Microrelief height (cm, 5 measurements)					
	Thaw depth (cm, 5 measurements; 4 plot corners and center)					
	Water depth (cm, 5 measurements; ; 4 plot corners and center)					

Plot Nr.	**Plant community name** (dominant species in each layer or plant community code (Walker 1985))

Plot Nr.	**GPS Elevation** (m)/**Accuracy** (m)	**GPS North** (decimal degrees, WGS 84)	**GPS West** (decimal degrees, WGS84)
	/		
	/		
	/		
	/		
	/		

Notes:

Table A1.2. *Species cover-abundance data sheet (reproduced at 90%).*

2022 NIRPO vegetation plots: *Species cover abundances*

pg. 3 of 3

Location:	**Date:**
Site:	**Observer(s):**

Vegetation Type(code	**Layer**	**Total cover** (live + stnd. dead) **(Br.-Bl. Cover abundance code)**				
		Plot Number				
Species						
Shrubs:						
Forbs & seedless vascular plants:						
Graminoids:						

Note if used back of datasheet	**Layer**	**Total cover** (live + stnd. dead) **(Br.-Bl. Cover abundance code)**				
		Plot Number				
Species						
Bryopyhtes:						
Lichens:						

Br.-Bl. Cover abundance codes: **r** = rare, **+** = common but < 1%, **1** = 1-5%, **2** = 6-25% (2a = 6-12%; 2b = 13-25%), **3** = 26-50%, **4** = 51-75%, **5** = 76-100%

Layers: **LS** = Low shrub layer (0.4 m–2 m), **DS** = Erect dwarf-shrub layer (0.15-0.4 m), **H** = Herb layer (prostrate dwarf shrubs, graminoids, forbs, horsetails; **M** = Moss layer (Mosses, lichens, biological soil crusts)

Table A1.3. *Soil description data sheet (reproduced at 90%).*

2022 NIRPO Vegetation Plots **Soil Description**

Soil Description Location____

Site No. ________________________________ Date:__________________ Soil Classification: _________________________________

Microsite (A,B, or C)_____________________

Parent Material(s) ____ Described By: ___________________________

Depth (cm)	Horizon	Color moist/dry	Structure Type Str Sz	Gravel %	Consistency Wet	Consistency Moist	Dry	Texture	pH	Clay Films Fr Th Dis	Boundaries	Roots Ab Sz	Collect Notes
			gr m vf	0 50	so po	lo	lo	S SiCL		v1 n pf	a s	1 vf	
			pl sg f	<10 75	ss ps	vfr	so	LS SiL		1 mk po	c w	2 f	
			pr 1 m	10 >75	s p	fr	sh	SL Si		2 k br	g i	3 m	
			cpr 2 c	25	vs vp	fi	h	SCL SiC		3 co	d b	c	
			abk 3 vc			vfi	vh	L C		4 cobr			
			sbk			efi	eh	CL SC					
			gr m vf	0 50	so po	lo	lo	S SiCL		v1 n pf	a s	1 vf	
			pl sg f	<10 75	ss ps	vfr	so	LS SiL		1 mk po	c w	2 f	
			pr 1 m	10 >75	s p	fr	sh	SL Si		2 k br	g i	3 m	
			cpr 2 c	25	vs vp	fi	h	SCL SiC		3 co	d b	c	
			abk 3 vc			vfi	vh	L C		4 cobr			
			sbk			efi	eh	CL SC					
			gr m vf	0 50	so po	lo	lo	S SiCL		v1 n pf	a s	1 vf	
			pl sg f	<10 75	ss ps	vfr	so	LS SiL		1 mk po	c w	2 f	
			pr 1 m	10 >75	s p	fr	sh	SL Si		2 k br	g i	3 m	
			cpr 2 c	25	vs vp	fi	h	SCL SiC		3 co	d b	c	
			abk 3 vc			vfi	vh	L C		4 cobr			
			sbk			efi	eh	CL SC					
			gr m vf	0 50	so po	lo	lo	S SiCL		v1 n pf	a s	1 vf	
			pl sg f	<10 75	ss ps	vfr	so	LS SiL		1 mk po	c w	2 f	
			pr 1 m	10 >75	s p	fr	sh	SL Si		2 k br	g i	3 m	
			cpr 2 c	25	vs vp	fi	h	SCL SiC		3 co	d b	c	
			abk 3 vc			vfi	vh	L C		4 cobr			
			sbk			efi	eh	CL SC					
			gr m vf	0 50	so po	lo	lo	S SiCL		v1 n pf	a s	1 vf	
			pl sg f	<10 75	ss ps	vfr	so	LS SiL		1 mk po	c w	2 f	
			pr 1 m	10 >75	s p	fr	sh	SL Si		2 k br	g i	3 m	
			cpr 2 c	25	vs vp	fi	h	SCL SiC		3 co	d b	c	
			abk 3 vc			vfi	vh	L C		4 cobr			
			sbk			efi	eh	CL SC					
			gr m vf	0 50	so po	lo	lo	S SiCL		v1 n pf	a s	1 vf	
			pl sg f	<10 75	ss ps	vfr	so	LS SiL		1 mk po	c w	2 f	
			pr 1 m	10 >75	s p	fr	sh	SL Si		2 k br	g i	3 m	
			cpr 2 c	25	vs vp	fi	h	SCL SiC		3 co	d b	c	
			abk 3 vc			vfi	vh	L C		4 cobr			
			sbk			efi	eh	CL SC					

Notes:

Texture Type: gr - granular, pl - platey, pr - prismatic, cpr - columnar, abk - angular blocky, sbk - subangular blocky
Texture Strength: m - massive, sg - single grain, 1 - weak, 2 - moderate, 3 - strong
Texture Size: vf - very fine, f - fine, m - medium, c - coarse, vc - very coarse
Wet Consistency Stickiness: so - not sticky, ss - slightly sticky, s - sticky, vs - very sticky
Wet Consistency Plasticity: po - not plastic, ps - slightly plastic, p - plastic, vp - very plastic
Moist Consistency: lo - loose, vfr - very friable, fr - friable, fi - firm, vfi - very firm, efi - extremely firm
Dry Consistency: lo - loose, so - soft, sh - slightly hard, h - hard, vh - very hard, eh - extremely hard
Texture: S - sand, Si - silt, C - clay, L - loam (SCL = silty clay-loam)
Clay Film Frequency: v1 - very few, 1 - few, 2 - common, 3 - many, 4 - continuous
Clay Film Thickness: n - thin, mk - moderately thick, k - thick
Clay Film Morphology: pf - on ped faces, po - on pores, br - bridges, co - staining mineral grains
Boundary Sharpness: a - abrubt, c - clear, g - gradual, d - diffuse
Boundary Shape: s - smooth, w - wavy, i - irregular, b - broken
Root Frequency: 1 - few, 2 - common, 3 - many; Root Size: vf - very fine, f - fine, m - medium, c - coarse

APPENDIX 2 Site variable, vegetation type, and habitat type codes

Table A2.1. *Codes for categorical and scalar site variables used in the description of environmental characteristics.*

Code	Categorical site variables
Surficial Geology (Parent Material)	
1	**Unconsolidated marine deposits**
1.1	Marine sands and gravels
1.2	Marine silts and clays
2	**Unconsolidated eolian deposits (deposited by wind)**
2.1	Eolian sands
2.2	Eolian silts (loess)
3	**Eluvial deposits (deposited by in situ weathering and gravity)**
3.1	Frost shattered bedrock
4	**Colluvial deposits (slope deposits, derived from a combination of gravity and alluvial processes)**
4.1	Hillslope colluvium
4.2	Talus
4.3	Solifluction deposits
4.4	Basin colluvium
5	**Lacustrine deposits (lake deposits)**
5.1	5 Organic lacustrine deposits
5.2	5 Mineral lacustrine deposits
6	**Alluvial deposits (deposited by rivers and streams)**
6.1	Alluvial sands and gravels
6.2	Alluvial silts
7	**Glacial deposits**
7.1	Glacial till
7.2	Glacio-marine sediments
7.3	Glacio-fluvial sediments
8	**Bedrock**
8.1	Sedimentary rocks and metamorphosed sedimentary rocks
8.1.2	Sedimentary and metamorphic rocks derived from course grained sediments of mixed mineralogy: conglomerates and breccias
8.1.3	Sedimentary and metamorphic rocks derived from quartz-rich sediments: sandstones, quartzites, cherts
8.1.4	Sedimentary and metamorphic rocks derived from fine grained silts and clays: siltstones, claystones, mudstones, shales
8.1.5	Sedimentary and metamorphic rocks derived from carbonate sediments: limestone, dolomite, marlstone, marble
8.2	Igneous and metamorphosed igneous rocks
8.2.1	Felsic igneous rocks (rich in Si, Al): obsidian pumice, rhyolite, granite, pegmatite, gneiss
8.2.2	Mafic igneous rocks (rich in Fe, Mg): basaltic glass, scoria, basalt, diabase, gabbro
8.2.3	Ultramafic igneous rocks (extremely rich in Fe, Mg and often other metaliferous minerals Co, Ni, Ch), peridotite, dunite, serpentine, olivine, hornblende, pyroxene
Landforms	
1	**Hills and mountains**
2	**Plateaus**
3	**Plains**
3.1	Coastal plain
3.1.1	Flat thaw-lake plain
3.1.1.1	Thaw lake
3.1.1.2	Drained thaw-lake basin
3.1.1.3	Primary (residual) surface unaffected by thaw-lake processes
3.1.2	Hilly coastal plain

Code	Categorical site variables
Topographic Position	
1	**Flat elevated plain** (includes plateaus, elevated river terraces)
2	**Hill crest**
3	**Shoulder**
4	**Backslope**
5	**Foot slope** (includes toeslopes)
6	**Flat plain**
7	**Riparian zone** (includes active floodplains, drainage channels, water tracks, avalanche tracks)
8	**Lake or pond**
Surficial Geomorphology	
1	**Lowland features**
1.1	Lake and pond
1.2	Drained lake basin
1.2	Thermokarst pits or ponds
1.3	Flat featureless wetland, < 20% frost scars or hummocks
1.4	Strangmoor or aligned hummocks or disjunct polygon rims
1.5	Wetland hummocks
1.6	Lowland frost boils, non-sorted polygons, often with rings
1.7	Lowland ice-wedge polygons
1.7.1	Low-centered polygons
1.7.2	High-centered, flat-centered, or transitional polygons
1.7.3	Mixed high- and low-centered polygons
1.8	Palsas
1.9	Pingos
2	**Upland features** (interfluves)
2.1	Featureless upland or slope, < 20% frost scars or hummocks
2.2	Turf hummocks (mainly snowbeds)
2.3	Upland frost scars, sometimes forming earth mounds
2.4	Gelifluction features (including solifluction terraces)
2.5	Sorted and non-sorted stripes or hummocks
2.6	Gently rolling or irregular microrelief
2.7	Stoney hill slope or crest
3	**Riparian, water-track, or stream features**
3.1	Stream or river active floodplain
3.2	Stream or river inactive or stabilized floodplain
3.3	Stream or river terrace or bluff
3.4	Well-developed hillslope water tracks, small streams > 50 cm deep
3.5	Poorly developed hillslope water tracks, channels < 50 cm deep
Animal and Human Disturbance (type)	
0	**No sign**
1	**Ptarmigan scat**
2	**Caribou tracks**
3	**Caribou scat**
4	**Goose tracks, scat, feathers, and/or grazing**
5	**Squirrel mounds**
6	**Vole tracks & scat**
7	**Vehicle tracks**
8	**Wind erosion**
9	**Swan grazing**
10	**Owl pellets**

Table A2.1 *(continued)*

Code	Categorical site variables
Microsite	
1	**Frost-scar element**
2	**Inter-frost scar element**
3	**Strang, disjunct polygon rims (S)**
4	**Flat featureless or interhummock area (F)**
5	**Polygon center (C)**
5.1	Low-centered-polygon basin (LC)
5.2	High-centered, flat-centered, or transitional polygon center (HC)
6	**Polygon trough (T)**
7	**Low-centered-polygon rim (R)**
8	**Stripe element**
9	**Inter-stripe element**
10	**Point bar** (raised element)
11	**Slough** (wet element)
12	**Non-sorted polygon ring of tussocks**
13	**Lake or pond (P)**
14	**Bird mound (B)**
15	**Hummock (H)**
16	**Reticulate pattern (RP)**

Code	Scalar site variables
Estimated relative surface age (applies only to NIRPO site)	
1	**Youngest** (flat with few disjunct polygon rims or hummocks)
2	**Young** (flat with disjunct polygon rims or hummocks)
3	**Intermediate** (low-centered ice-wedge polygons with no or little thermokarst in polygon troughs)
4	**Old** (low-centered ice-wedge polygons with thermokarst in polygon troughs
5	**Oldest** (high-, flat-, or transitional ice-wedge polygons with extensive thermokarst in polygon troughs)
Site Moisture (modified from Komárková 1983)	
1	**Extremely xeric** - almost no moisture; no plant growth
2	**Very xeric** - very little moisture; dry sand dunes
3	**Xeric** - little moisture; stabilized sand dunes, dry ridge tops
4	**Subxeric** - noticeable moisture; well-drained slopes, ridges
5	**Subxeric to mesic** - slightly moist site, flat to gently sloping
6	**Mesic** - moderate moisture; flat or shallow depressions
7	**Mesic to subhygric** - considerable late season moisture; saturated soils, depressions
8	**Subhygric** - very considerable moisture; saturated but with< 5% standing water < 10 cm deep
9	**Hygric** - much moisture; up to 100% of surface under water 10 to 50 cm deep; lake margins, shallow ponds, streams
10	**Hydric** - very much moisture; 100% of surface under water 50 to 150 cm deep; lakes, streams

Code	Scalar site variables
Soil Moisture (from Komárková 1983)	
1	**Very dry** - very little moisture; soil does not stick together
2	**Dry** - little moisture; soil somewhat sticks together
3	**Damp** - noticeable moisture; soil sticks together but crumbles
4	**Damp to moist** - very noticeable moisture; soil clumps
5	**Moist** - moderate moisture; soil binds but can be broken apart
6	**Moist to wet** - considerable moisture; soil binds and sticks to fingers
7	**Wet** - considerable moisture; water drops can be squeezed from soil
8	**Very wet** - much moisture can be squeezed out of soil
9	**Saturated** - very much moisture; water drips out of soil
10	**Very saturated** - extreme moisture; soil is more liquid than solid
Estimated Snow Duration	
1	**Snow free all year**
2	**Snow free most of winter; some snow cover persists after storm but is blown free soon afterward**
3	**Snow free prior to melt out but with snow**
4	**Snow free immediately after melt out**
5	**Snow bank persists 1-2 weeks after melt out**
6	**Snow bank persists 3-4 weeks after melt out**
7	**Snow bank persists 4-8 weeks after melt out**
8	**Snow bank persists 8-12 weeks after melt out**
9	**Very short snow free period**
10	**Deep snow all year**
Animal and Human Disturbance (degree)	
0	**No sign present**
1	**Some sign present; no disturbance**
2	**Minor disturbance or extensive sign**
3	**Moderate disturbance; small dens or light grazing**
4	**Major disturbance; multiple dens or noticeable trampling**
5	**Very major disturbance; very extensive tunneling or large pit**
Site Stability	
1	**Stable**
2	**Subject to occasional disturbance** (e.g. ice-wedge thermokarst in polygon troughs)
3	**Subject to prolonged but slow disturbance such as solifluction**
4	**Annually disturbed** (e.g. annual flooding, grazing by geese in polygon troughs)
5	**Disturbed more than once annually**
Exposure to wind	
1	**Protected from winds**
2	**Somewhat protected from winds**
3	**Moderate exposure to winds**
4	**Exposed to winds**
5	**Very exposed to winds**

Table A2.2. *Vegetation type codes and categorical descriptors based on site moisture, dominant plant species, growth forms, and physiognomy for Prudhoe Bay, Alaska. (Modified from Walker 1985; Watson-Cook 2022).*

Code	Vegetation type description
DRY TUNDRA (B)	
B1	Dry *Dryas integrifolia, Carex rupestris, Oxytropis nigrescens, Lecanora epibryon* dwarf shrub, crustose lichen tundra
B2	Dry *Dryas integrifolia, Saxifraga oppositifolia, Lecanora epibryon* dwarf-shrub, crustose-lichen tundra
B3	Dry *Saxifraga oppositifolia, Juncus biglumis* forb, biological soil crust barren
B16	Dry *Puccinellia angustata, P. andersonii, Salix ovalifolia, S. lanata* graminoid, dwarf-shrub barren (dry saline disturbed areas near roads)
B17	Dry *Dryas integrifolia, Saxifraga oppositifolia, Hulteniella integrifolia, Carex capillaris* prostrate-shrub, herb tundra (dry dust-disturbed tundra)
MOIST TUNDRA (U)	
U2	Moist *Eriophorum vaginatum, Dryas integrifolia, Tomentypnum nitens, Thamnolia subuliformis* tussock-graminoid, prostrate dwarf-shrub, moss, lichen tundra
U3	Moist *Eriophorum angustifolium, Dryas integrifolia, Tomentypnum nitens, Thamnolia subuliformis* graminoid, prostrate dwarf-shrub, moss, lichen tundra
U3d	Disturbed version of type U3
U4	Moist *Eriophorum angustifolium, Dryas integrifolia, Tomentypnum nitens* graminoid, dwarf-shrub, moss tundra
U4d	Disturbed version of type U4
U6	Moist/dry *Dryas integrifolia,Cassiope tetragona, Masonhalea richardsonii,* dwarf-shrub, moss, lichen tundra (snowbeds)
U10	Moist *Festuca baffinensis, Papaver macounii, Ranunculus pedatifidus* forb, grass tundra (zoogenic vegetation)
U17	Moist version of B17 (*Carex scirpidea, Dryas integrifolia, Oxytropis borealis, Chrysanthemum integrifolium)*
WET TUNDRA (M)	
M2	Wet *Carex aquatilis, Drepanocladus brevifolius* sedge, moss tundra
M2d	Disturbed version of type M2
M4	Wet *Carex aquatilis, Scorpidium scropioides* sedge, moss tundra
M10	Wet *Carex aquatilis, Eriophorum angustifolium, Dupontia fisheri* graminoid tundra (coastal wet saline graminoid tundra)
M10d	Disturbed version of type M10
AQUATIC VEGETATION (E, W)	
M4/E1	Transitional wet to aquatic *Carex aquatilis, Scorpidium scorpioides* graminoid, moss tundra
E1	Aquatic *Carex aquatilis* sedge marsh (CARAQU)
E1d	Disturbed version of type E1
E2	Aquatic *Arctophila fulva* grass marsh
E3	Aquatic *Scorpidium scorpioides* marsh tundra (SCOSCO)
E5	Aquatic *Calliergon richardsonii* marsh tundra (CALGIG)
E6	Aquatic *Hippurus vulgaris* forb, marsh tundra (HIPVUL)
Es	Sparse aquatic vegetation
Em	Aquatic moss vegetation (includes E3 and/or E4)
Ef	Aquatic forb vegetation (includes E6)
W	Unvegetated water

Table A2.3. *Habitat type codes and categorical descriptors, after Mucina et al. 2014.*

Code	Habitat type description
1	*ARCTIC ZONAL TUNDRA*
1.01	Polar desert vegetation, subzone A
1.01.1	Polar deserts of the Arctic zone of the Arctic Ocean archipelagos – North America
1.02	Dry and mesic dwarf-shrub and graminoid zonal vegetation on non-acidic base-rich soils
1.02.1	Dry zonal habitats of graminoid tundra and dwarf-shrub heath vegetation of Scotland, Scandinavia, Iceland and the Arctic Ocean islands on base-rich soils, subzones B and C
1.02.2	Mesic zonal habitats of graminoid tundra and dwarf-shrub heath vegetation of Arctic, Western Russia and Siberia on base-rich soils, subzones B, C & D
1.02.3	Graminoid tundra and dwarf-shrub heath vegetation of Greenland and the Arctic North America, subzones B, C & D, (includes for now early-melting base-rich *Cassiope-Tomentypnum* snowbeds)
1.03	Dry to mesic dwarf-shrub heath on acidic substrates, subzones D and E
1.03.1	Wind-swept dry habitats with prostrate-dwarf-shrub tundra acidic soils, subzones D and E
1.03.2	Zonal habitats with erect-dwarf-shrub tundra acidic soils, subzones D and E (includes for now early-melting acidic *Cassiope-Hylocomium* snowbeds)
1.03.3	Low-shrub tundra, acidic soils, warmest parts of subzone E
1.03.4	Amphiberingian chionophytic heath communities
1.03.5	Achionophytic heath communities (a vicariant alliance to the *Loiseleurio-Arctostaphyllion* that occurs in Northern Europe, Greenland as well as the Eastern part of North America)
2	*BOREAL MARITIME TUNDRA*
2.01	Mesic tall-herb vegetation, boreal maritime tundra
2.01.1	Mesic tall-herb vegetation, boreal maritime tundra
3	*INTRAZONAL VEGETATION OF THE ARCTIC ZONE*
3.01	Cryoxerophytic steppe and associated shrub on base-rich and (sub)saline substrates in continental Greenland and North America
3.01.1	Cryoxerophytic steppe and associated shrub on base-rich soils
3.01.2	Mesic forb-rich, turfy low Arctic (sub)saline steppe vegetation on base-rich soils
3.02	Arctic rush swards on acidic substrates in arctic region
3.02.1	Wind-swept, chionophobous habitats on acidic soils dominated by rushes
3.03	Grass- & rush-rich, zoogenic habitats, subzones A, B & C
3.03.1	Zoogenic, disturbed habitats, subzones, all sub- zones
4	*EXTRAZONAL BOREAL VEGETATION OCCURRING IN THE ARCTIC ZONE*
4.01	Boreal coniferous forest enclaves within the tundra zone
4.02	Subalpine and subarctic herb-rich alder and willow scrub and krummholz
4.02.1	Moist to dry alder (*Alnus viridis*) communities and alder savannas
4.02.2	Willow shrublands along streams, rivers, and water tracks on hill slopes
4.02.3	Herb-rich willow scrub and krummholz, subzones D and E
5	*AZONAL ARCTIC HABITATS*
5.01	SALT MARSHES, SAND DUNES, SEA CLIFFS
5.01.1	Wet saline coastal marshes
5.01.1.1	Coastal salt-marshes
5.01.2	Tall-grass swards, sand dunes
5.01.2.1	Tall-grass swards, sand dunes (*Leymus arenarius*), and for now other undescribed saline coastal embryonic communities
5.02	***Talus, screes, and boulder fields*** *(see also habitat codes 5.08.1 to 5.08.4 for epilithic moss- and lichen-dominated communities)*
5.02.1	Rock-crevices, ledges, faces of rocky cliffs & walls
5.02.1.1	Siliceous rock crevices, ledges, faces and walls
5.02.2	Scree habitats and course alluvium
5.02.2.1	Base-rich and neutral screes and moraines
5.02.2.2	Herb-rich snow-beds, stabilized course calcareous soils
5.02.2.3	Herb-rich vegetation, damp coarse gravels, siliceous substrates of Iceland
5.02.2.4	Ruderal riparian floodplain and terrace vegetation (*Epilobium latifolium*)
5.03	***Snowbeds and wet cold frost-active soils***
5.03.1	Late-melting snowbeds and wet cold frost active soils
5.03.1.1	Prostrate dwarf-shrub snowbeds on acidic siliceous substrates
5.03.1.2	Wet late-melting snowbeds and frost boils, cold acidic fine-grained soils
5.03.1.3	Amphiberingian late-melting snowbed communities
5.03.1.4	Early melting snowbed communities of the Alasko-Yukonian phytogeographical sector
5.04	***Springs***
5.04.1	Cold oligotrophic springs in the boreal and arctic zones of northern Europe
5.05	***Fresh water bodies***
5.05.1	Aquatic rooted floating or submerged macrophyte vegetation of meso-eutrophic water
5.05.1.1	Aquatic forb marshes
5.05.2	Pond and lake margins with aquatic grasses
5.05.2.1	Aquatic grass marshes

Table A2.3 *(continued)*

Code	Habitat type description
5.06	***Mires (wetlands)***
5.06.1	Fens, base-rich wetlands
5.06.1.1	Sedge fens on calcareous mineral substrates
5.06.1.2	Sedge-brown-moss fens on peats and peaty mineral soils
5.06.1.3	Moist to wet coastal sedge-grass tundra calcareous slightly saline soils (*Carex stans-Saxifraga cernua, Dupontia fisheri*)
5.06.1.4	Poor fens, slightly acidic organic soils (sedge-dwarf-shrub-*Sphagnum*)
5.06.1.5	Wet acidic sedge forb mires of Aleutian Islands
5.06.1.6	Moist to wet grassy meadows (*Calamagrostis canadensis, Polemonium acutiflorum, Potentilla palustris*)
5.06.2	Bogs, wetlands on acidic ombrotrophic soils
5.06.2.1	Tussock tundra (*Eriophorum vaginatum*)
5.06.2.2	Dwarf-shrub and peat-moss raised bog vegetation in the boreal and Arctic zones
5.07	***Riparian shrublands and gallery forests***
5.07.1	Riparian habitats, willow (*Salix*) shrublands and poplar (*Populus*) forests
5.07.1.1	Floodplains, springs, aufeis deposits and warm south facing slopes with balsam poplar (*Populus balsamifera*)
5.08	***Bryophyte and lichen vegetation***
5.08.1	Bryophyte communities on sunny exposed siliceous rocks, boulders and screes
5.08.2	Bryophyte communities on exposed limestone rocks and screes
5.08.3	Ombryophilous lichen communities of siliceous rock surfaces
5.08.4	Mainly crustose lichen communities on moderately to highly nutrient-rich limestone substrates
5.08.5	Bryophyte and lichen vegetation on dry acid to subneutral, silty-sand and gravelly soils
5.08.6	Bryophyte and lichen vegetation on subneutral and
5.09	***Anthropogenic and ruderal vegetation***
5.09.1	Human-disturbed habitats in the subarctic and Arctic zones of Russia, Siberia and North America
5.09.1.1	Ruderal vegetation of natural disturbances (e.g., lake bluff erosion)

APPENDIX 3 Soil characteristics

Table A3.1 *Abbreviated descriptions of soil horizons at 2022 NIRPO vegetation plots, Prudhoe Bay, August 2022.* ***Horizon:*** *Soil layer.* ***Depth:*** *Distance below soil surface.* ***Field color:*** *Munsell 1975 Soil Color Charts.* ***Structure type:*** *granular (gr), platey (pl), prismatic (pr), columnar (cpr), angular blocky (abk), subangular blocky (sbk).* ***Structure strength:*** *massive (m), single grain (sg), weak (1), moderate (2), strong (3).* ***Structure size:*** *very fine (vf), fine (f), medium (m), coarse (c), very coarse (vc).* ***Gravel:*** *Percentage of particles >2mm.* ***Consistence stickiness:*** *not sticky (so), slightly sticky (ss), sticky (s), very sticky (vs).* ***Consistence plasticity:*** *not plastic (po), slightly plastic (ps), plastic (p), very plastic (vp).* ***Field texture:*** *sand (S), silt (Si), clay (C), loam (L), silt loam (SiL).* ***Boundary sharpness:*** *abrupt (a), clear (c), gradual (g), diffuse (d).* ***Boundary shape:*** *smooth (s), wavy (w), irregular (i), broken (b).* ***Root, Frequency:*** *none (0), few (1), common (2), many (3).* ***Root size:*** *very fine (vf), fine (f), medium (m), coarse (c).* ***Preliminary soil classification:*** *Using old classification Everett and Parkinson (1977).*

Plot ID	Hori-zon	Depth (cm)	Field color	Structure			Gravel %	Consistence		Field texture	Boundary		Root		Notes	Preliminary soil classification
				Type	Strength	Size		Sticki-ness	Plas-ticity		Sharp-ness	Shape	Fre-quencey	Size		
22-01	IA	0-17	10YR 3/1	sbk	2	c	10	ss	po	SiL	c	i	3	vf	Well developed A horizon with some gravel. Carbonate crust on rock fragments, many fine roots	Pergelic Cryoboroll
	IIC	17-46+	10YR 4/1	sg	2	m	30	so	po	S	-	-	1	vf	Sandy gravel, few roots, permafrost 120 cm	
22-02	IA	0-22	10YR 3/1	sbk	2	c	10	ss	po	SiL	c	i	2	vf	Well developed A horizon with some gravel, common roots	Pergelic Cryoboroll
	IIC	22-34+	10YR 4/1	sg	2	m	30	so	po	S	-	-	1	vf	Sandy gravel, few roots, permafrost 120 cm	
22-03	IA/B	0-43	10YR 2/2	sbk	2	c	<10	so	po	SiL	c	i	2	vf, f	Well developed A horizon	Pergelic Cryoboroll
	IIC	43-55+	10YR 3/2	sg	-	-	>75	so	po	S	-	-	0	-	Sandy gravel, few roots, permafrost 97 cm	
22-04	IA	0-14	10YR 3/1	sbk	1	f	<10	ss	ps	SiL	c	i	3	f	Well developed A horizaon,	Pergelic Cryaquoll
	IIB	14-53+	10YR 4.5/2	sg	1	m	<10	so	po	SL	-	-	1	vf	Very wet silty loamy gravel. Water at 46 cm., permafrost 80 cm	
22-05	IA	0-28	7.5YR 2.5/2	sbk	2	-	10	ss	-	L	c	i	2	f	Well developed A, breaks to weak fine granular structure	Pergelic Cryaquoll
	IIB	28-37+	2.5YR 4/2	sg	-	-	75	ps	-	S	-	-	1	vf	Very wet silty loamy gravel. Water level at 37m, permafrost 102 cm	
22-06	IA	0-28	7.5YR 2.5/1	sbk	m	m	<10	ss	-	L	c	w	2	f	Well developed A, Breaks to fine granular structure	Pergelic Cryaquoll
	IIB	28-38+	2.5Y 4/4	sbk	1	m	25	ps	-	S	-	-	1	vf	Very wet silty loamy gravel. Water level at 30 cm, perma-frost, 90 cm	
22-07	O1	0–18	10YR 2.5/2	-	-	-	0	so	po	Si	d	s	3	vf	Marl organic layer filleds with fine and med roots	Pergelic Cryofibrist
	O2	18–32+	10YR 2/1	m	-	-	<10	so	po	Si	-	-	1	vf	Few roots, could be highly organic mineral horizon with abundant marl, permafrost 56 cm	
22-08	O1	0–20	10YR 2/2	m	-	-	0	so	po	Si	d	s	3	vf, f	Contains marl. mostly hemic organic material with many fine and very fine roots	Pergelic Cryohemist
	O2	20–38+	10YR 2/1	m	-	-	0	so	po	Si	-	-	1	vf	Similar to O1 but more compact and fewer roots, abun-dant marl, permafrost 40 cm	
22-09	O1	0–13	10YR 2/2	m	-	-	0	so	po	LS	c	w	1, 3	vf	Fibric O1, with many fine to medium Caraqu roots. Clear boundary with silty marl lake sediments	Pergelic Cryohemist
	O2	13–28	10YR 2/1	m	-	-	0	so	po	LS	-	-	3	vf	Highly organic marl lakle sediments with common very fine roots	
22-10	O1	0–14	5YR 3/1	m		-	0	ss	ps	SiL(?)	d	s	1, 3	m, vf	Marly high organic, few medium Caraqu rhizomes, many very fine roots	Pergelic Cryohemist
	O2	14–34	10YR 3/1	m		-	0	ss	ps	SiL(?)	-	-	3	vf	Marly high organic, many very fine roots, permafrost 45 cm	

Table A3.1 *(continued)*

Plot ID	Hori-zon	Depth (cm)	Field color	Structure			Gravel %	Consistence		Field texture	Boundary		Root		Notes	Preliminary soil classification
				Type	Strength	Size		Sticki-ness	Plas-ticity		Sharp-ness	Shape	Fre-quencey	Size		
22-11	Oi	0–8	10YR 2/1	-	-	-	0	ss	ps	-	c	w	3	vf, f	Fibric organic; many Arcfiul roots & SCOSCO	Histic Pergelic Cryaquept
	Oa	8–18	10YR 2/2	-	-	-	0	ss	ps	Si	a	s	1	vf	Sapric organic, many fine and very fine roots	
	IIB	18–32+	10YR 3/2	m	-	-	0	ss	ps	SiL	-	-	1	vf	Mineral lake sediment, permafrost 44 cm	
22-12	Oi	0–8	10YR 2/1	-	-	-	0	-	-	Si	c	s	3	f, m	Loose fibric horizon composed of roots, stems, & minerals	Histic Pergelic Cryaquept
	B	36–45+	10YR 3/2	-	m	-	0	ss	ps	SiL	-	-	2	vf	Organic-rich silt, difficult to describe because of shallow depth of the core, permafrost 38 cm	
22-13	A	0–36	5YR 2.5/1.5	sbk	2	-	0	ss	ps	SiL	a	w	3	vf, f	Well developed A horizon, 0-20 cm, dk rbr, moderately hard, breaks to fine granular structure, many fine, vf roots, many animal bones inclulding lemmings, birds, and other mammals! 20-35 cm, looser and more gravelly.	Pergelic Cryoboroll
	IIC	36–45+	10YR 3.5/1	-	sg	-	50	so	po	S	-	-	0	-	Gray sandy gravel, permafrost 73 cm	
22-14	A	0–18	10YR 2/2	sbk	2	m	0	ss	ps	SiL	a	i	3	vf, f	Well developed A horizon	Pergelic Cryoboroll
	IIB	18–35+	10YR 4/1	-	sg	-	>75	-	-	S	-	-	0	-	Dark brown gravelly B horizon, permafrost 102 cm	
22-15	Oa1	0–9	7.5YR 2.5/1.5	gr	1	f	0	so	po	SiL	c	i	3	f	Well decomposed, loose v. dk brn organic horizon, with many small animal bones	Pergelic Cryosaprist
	Oa2	9–14	7.5YR 2.5/2.5	gr	1	f	0	so	po	SiL	c	i	3	f	More reddish sapric organic horizon, possibly due to different moss origind, many small animal bones, probably from owl and jaeger pellets.	
	Oa3	14–24	7.5YR 2.5/1	sbk	1	f	0	so	po	SiL	-	-	3	f	Firmer dark organic, breaks to fine granular structure, permafrost 37 cm	

Table A3.2. *Soil characteristics of 2022 NIRPO terrestrial vegetation plots, Prudhoe Bay, 23-30 August 2022.* ***Horizon****: Soil layer.* ***Depth:*** *Distance below soil surface.* ***Gravimetric soil moisture****: Mass of water lost by oven drying divided by the mass of the dried sample.* ***Volumetric soil moisture****: Mass of water lost by oven drying divided by the volume of the soil can (180cm^3).* ***Soil texture: Gravel****: Percentage of particles >2mm;* ***Sand, Silt, and Clay****: Hydrometer method (Klute 1986);* ***Texture:*** *USDA textural triangle.* ***Organic Matter****: Mass loss on ignition.* ***Bulk density****: Mass of the oven-dried sample divided by the volume of the can it was sampled in (180 cm^3).* ***Soil pH: Saturated paste method****: Moistened as much as possible without pooling;* ***1:2.5 volume method:*** *Soil-to-water ratio.*

		Horizon		Soil moisture		Soil texture and organic matter							Soil pH	
Plot ID	Date sampled	Horizon	Depth (cm)	Gravimetric soil moisture (%)	Volumetric soil moisture (%)	Gravel (%)	Sand (%)	Silt (%)	Clay (%)	Texture	Organic matter (%)	Bulk density (g/cm^3)	Saturated paste method	1:2.5 volume method
22-01	8/23/2022	A	10-15	30.99	32.02	21.21	49.05	47.39	3.55	Sandy loam	8.74	1.03	6.91	7.05
22-02	8/23/2022	A	4-9	41.47	32.37	13.85	38.34	58.17	3.49	Silt loam	11.85	0.78	6.92	7.05
22-03	8/26/2022	A	5-10	53.12	40.39	2.17	42.81	53.61	3.57	Silt loam	14.87	0.76	6.9	7.09
22-04	8/23/2022	A	13-18	30.27	36.49	3.18	66.63	28.80	4.57	Sandy loam	13.41	1.21	6.73	7.02
22-05	8/26/2022	A	5-10	73.82	55.11	1.09	32.35	64.15	3.50	Silt loam	13.65	0.75	6.94	7.3
22-06	8/26/2022	A	5-10	73.16	62.05	0.60	34.59	59.86	5.55	Silt loam	16.18	0.85	6.56	6.75
22-07	8/30/2022	O2	18-23	66.93	59.48	0.00	53.18	43.42	3.40	Sandy loam	14.87	0.89	7.0	7.06
22-08	8/24/2022	O1	5-10	149.30	69.72	0.00	37.06	59.40	3.54	Silt loam	20.34	0.47	7.26	7.31
22-09	8/24/2022	O2	11-16	107.24	56.81	0.00	44.41	49.99	5.60	Sandy loam	17.11	0.53	7.33	7.32
22-10	8/30/2022	O2	14-19	127.08	63.82	0.00	35.43	57.09	7.48	Silt loam	29.49	0.50	7.07	7.14
22-11	8/24/2022	B	18-23	42.72	45.01	0.00	49.80	43.65	6.55	Sandy loam	8.63	1.05	7.27	7.3
22-12	8/24/2022	B	8-13	186.46	69.14	0.00	50.85	42.74	6.41	Sandy loam	16.27	0.37	7.41	7.4
22-13	8/26/2022	A	5-10	76.52	43.77	0.00	40.45	54.96	4.60	Silt loam	23.69	0.57	6.89	6.94
22-14	8/25/2022	A	2-7	67.31	51.12	2.11	32.86	63.57	3.58	Silt loam	12.03	0.76	6.99	7.03
22-15	8/25/2022	Oa2	10-15	157.10	60.74	0.00	36.59	56.83	6.58	Silt loam	26.94	0.39	6.93	7.04

APPENDIX 4 Vegetation plot photographs

Table A4.1. *Photographs of 2022 NIRPO permanent vegetation plot landscapes. (Credits: A.L. Breen, O. Hobgood)*

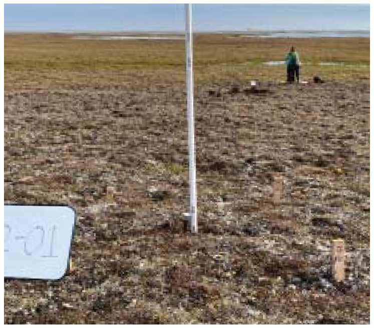

22-01 (IMG 9222.jpg)

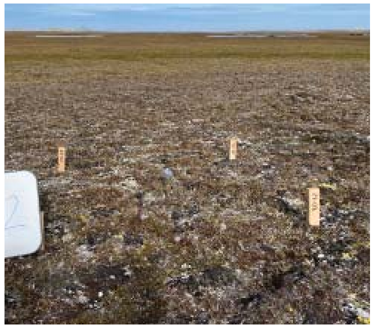

22-02 (IMG 9237.jpg)

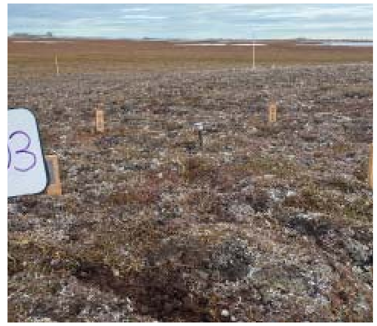

22-03 (IMG 9279.jpg)

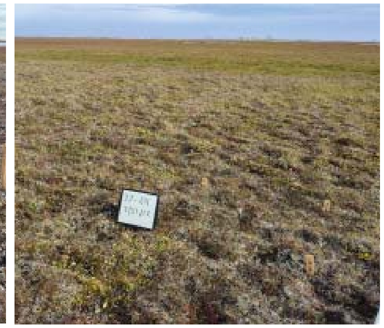

22-04 (IMG 101043.jpg)

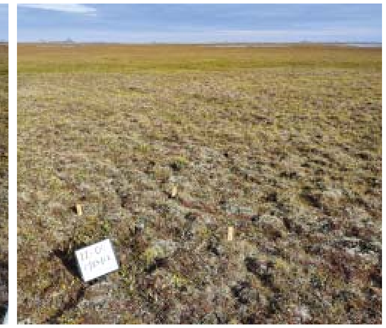

22-05 (IMG 131229.jpg)

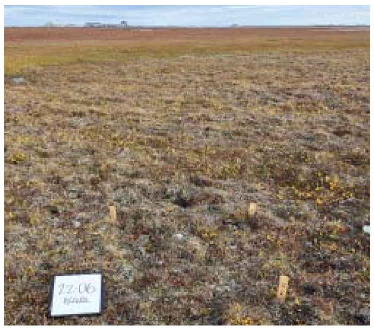

22-06 (IMG 110837.jpg)

22-07 (IMG 9374.jpg)

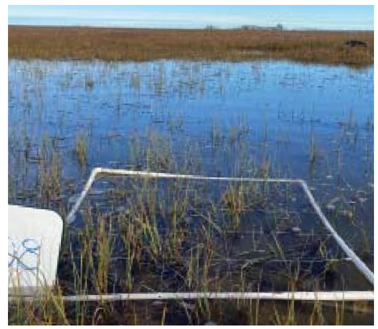

22-08 (IMG 9241.jpg)

22-09 (IMG 9244.jpg)

22-10 (IMG 9380.jpg)

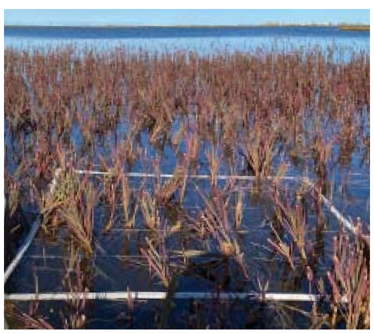

22-11 (IMG 9250.jpg)

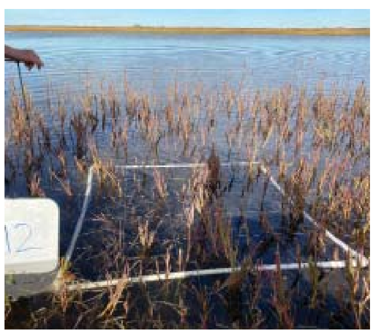

22-12 (IMG 9257.jpg)

22-13 (IMG 154146.jpg)

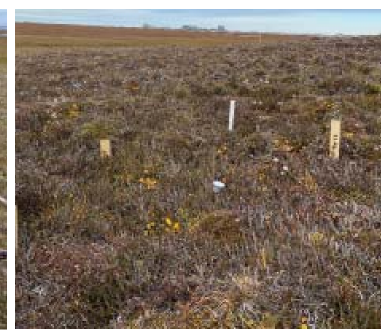

22-14 (IMG 9270.jpg)

22-15 (IMG 9264.jpg)

Table A4.2. *Photographs of 2022 NIRPO permanent plot vegetation. (Credits: A.L. Breen, O. Hobgood)*

22-01 (IMG 9223.jpg)

22-02 (IMG 9238.jpg)

22-3 (IMG 9280.jpg)

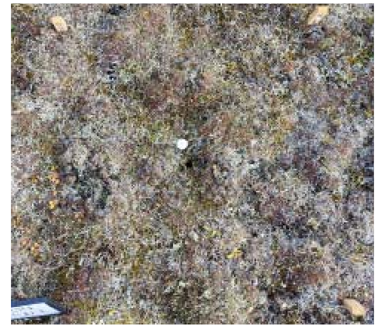

22-4 (IMG 101030.jpg)

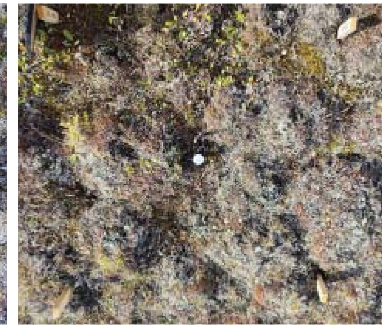

22-5 (IMG 131215.jpg)

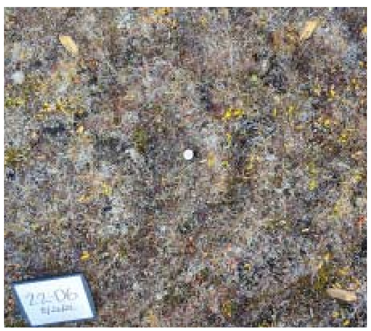

22-6 (IMG 110828.jpg)

22-7 (IMG 9376.jpg)

22-8 (IMG 9242.jpg)

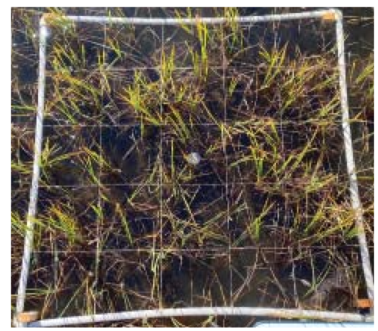

22-9 (IMG 9246.jpg)

22-10 (IMG 9379.jpg)

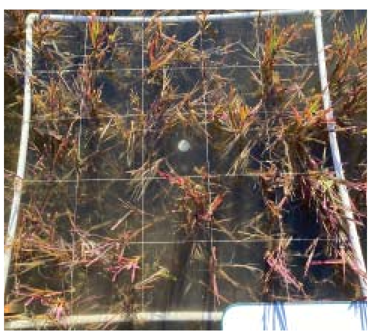

22-11 (IMG 9255.jpg)

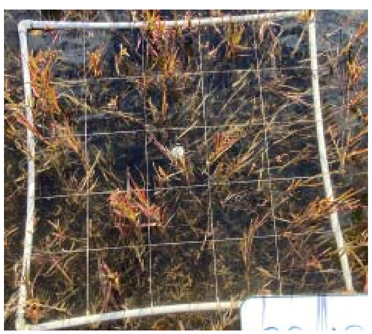

22-12 (IMG 9258.jpg)

22-13 (IMG 154139.jpg)

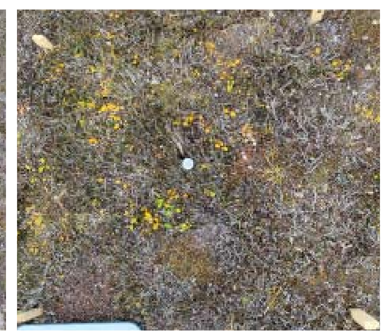

22-14 (IMG 9269.jpg)

22-15 (IMG 9265.jpg)

Table A4.3. *Photographs of 2022 NIRPO vegetation plot soils. (Credits: A.L. Breen, O. Hobgood)*

22-01 (IMG 9226.jpg)

22-02 (IMG 9239.jpg)

22-03 (IMG 9274.jpg)

22-04 (IMG 9235.jpg)

22-05 (IMG 160455.jpg)

22-06 (IMG 9284.jpg)

22-07 (IMG 9377.jpg)

22-08 (IMG 9243.jpg)

22-09 (IMG 9247.jpg)

22-10 (IMG 9381.jpg)

Table A.4.3 *(continued)*

22-11 (IMG 9256.jpg)

22-12 (IMG 9261.jpg)

22-13 (IMG 9282.jpg)

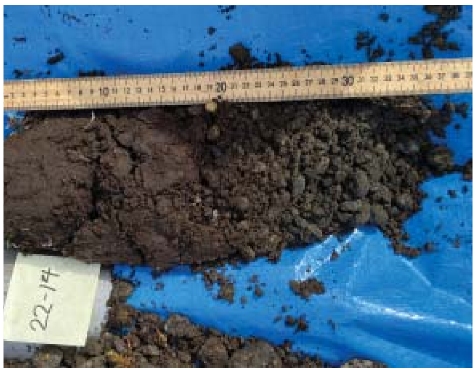

22-14 (IMG 9268.jpg)

22-15 (IMG 9266.jpg)

APPENDIX 5 Environmental variables and plant growth forms

Table A5.1. *Environmental characteristics and plant growth-form cover values for NIRPO vegetation plots, Prudhoe Bay, 23-30 August 2022.* ***Site factors:*** *Codes for environmental variables are in Appendix 2, Table A2.1.* ***Vegetation categorical descriptors:*** *See Table A2.2 for vegetation type and Table A2.3 for habitat type codes.*

Plot ID	22-01	22-02	22-03	22-04	22-05	22-06	22-07	22-08	22-09	22-10	22-11	22-12	22-13	22-14	22-15
SITE FACTORS: CATEGORICAL VARIABLES (SEE TABLE A2.1)															
Landform	3.1.1	3.1.1	3.1.1	3.1.1	3.1.1	3.1.1	3.1.1/2	3.1.1/2	3.1.1/2	3.1.1.1	3.1.1.1	3.1.1.1	3.1.1	3.1.1	3.1.1.2
Surficial geology / parent material	6.1	6.1	6.1	6.1	6.1	6.1	5.1	5.1	5.1	5.2	5.2	5.2	6.1	6.1	5.2
Surficial geomorphology	1.9	1.9	1.9	1.9	1.9	1.9	1.1	1.1	1.1	1.1	1.1	1.1	1.9	1.9	1.1
Microsite	16	16	16	15	15	15	13	13	13	13	13	13	15	15	14
Topographic position	3	3	3	5	5	5	8	8	8	8	8	8	2	4	0
Disturbance type	1, 8	1, 8	1, 8, 3	1	1	1	4	4	4	9	4, 9	9	5, 6, 10	1, 3, 22	1, 4, 5, 6, 10
SITE FACTORS: SCALAR VARIABLES (SEE TABLE A2.1)															
Estimated relative surface age (scalar, 1–5)	3	3	3	3	3	3	1	1	1	1	1	1	3	3	1
Site moisture (scalar, 1–10)	3	3	3	5	5	6	10	10	10	10	10	10	5	4	5
Soil moisture (scalar, 1–10)	4	4	4	6	6	6	10	10	10	10	10	10	5	3	5
Estimated snow duration (scalar, 1–10)	2	2	2	3	3	3	4	4	4	4	4	4	3	6	3
Animal and human disturbance degree (scalar, 0–5)	3	2	2	2	2	2	1	1	3	3	3	3	4	1	4
Site stability (scalar, 1–5)	2	2	1	2	2	2	2	2	2	4	4	4	4	1	4
Exposure to wind (scalar, 1-5)	5	5	4	3	3	3	3	3	3	3	3	3	5	2	4
SITE FACTORS: CONTINUOUS VARIABLES															
Latitude (decimal degrees)	70.227468	70.227523	70.227428	70.227595	70.227634	70.227594	70.2262	70.227386	70.227972	70.22789	70.225637	70.225318	70.227324	70.227469	70.231243
Longitude (decimal degrees)	-148.450157	-148.450488	-148.450674	-148.449703	-148.450626	-148.450928	-148.4489	-148.446718	-148.439121	-148.43928	148.436729	-148.43614	-148.450464	-148.451530	-148.459054
Elevation (m)	17	15	11	14	12	8	3	3	3	12	12	12	15	10	11
GPS accuracy (m)	2	2	3	2	2	1	6	6	10	4	2	4	2	15	2
Slope (degrees)	10	7	4	8	7	2	0	0	0	0	0	0	0	5	13
Aspect (cardinal)	N	NW	W	N	NNE	W	NA	NA	NA	NA	NA	NA	NA	SW	SW
Microrelief height (cm)	4	2	1.8	7	9.2	9.5	2.8	2.4	3	-	-	-	10	7	52
Thaw depth (cm, mean of 5 measurements), Aug. 23-30, 2022	120	120	98.67	72.8	94.2	87.4	55.6	37.4	43.8	45.2	42	37.2	58	99	33.6
Water depth (cm, mean of 5 measurements), Aug. 23–30, 2022	0	0	0	0	0	0	9.2	17.4	22.4	47.8	33.6	33.8	0	0	0
Herbaceous layer height, including erect dwarf shrubs <10 CM (cm above water or soil)	1	1.8	1.4	3.3	2.7	9	23.2	34.6	35.2	56.6	48.4	16.4	8	6.8	6.8
Live moss thickness (cm)	0.5	0.5	0.4	0.7	9.6	9.5	0	0	0	0	10	16.4	1.6	1.4	2
Total organic (+ a horizon) thickness (cm)	16.5	22	43	14	28	28	32+	38+	28+	34+	19	8	36	18	24+

Table A5.1 *(continued)*

Plot ID	22-01	22-02	22-03	22-04	22-05	22-06	22-07	22-08	22-09	22-10	22-11	22-12	22-13	22-14	22-15
COVER OF PLANT GROWTH FORMS AND OTHER VARIABLES (% COVER)															
Erect dwarf shrubs (15-40 cm tall) (live + attached dead)	0/0	0/0	0/0	0/0	0/0	0/0	0/0	0/0	0/0	0/0	0/0	0/0	0/0	0/0	0/0
Prostrate dwarf shrubs (<15 cm tall) (live + attached dead)	40/10	50/10	60/10	82/4	68/2	60/5	0/0	0/0	0/0	0/0	0/0	0/0	5/0	80/10	17/5
Evergreen shrubs (live + attached dead)	40/10	50/10	60/10	80/4	62/2	56/4	0/0	0/0	0/0	0/0	0/0	0/0	5/0	65/5	10/5
Deciduous shrubs (live + attached dead)	0/0	0/0	0/0	2/0	6/0	4/1	0/0	0/0	0/0	0/0	0/0	0/0	0/0	10/0	7/0
Erect forbs (live + attached dead)	0/0	0/0	0.1/0	3/0	10/0	1/0	0/0	0/0	4/0	3/0	5/0	7/0	15/3	1/0	5/0
Mat and cushion forbs (live + attached dead)	7/0	1/0	2/0	3/0	4/0	4/0	0/0	0/0	0/0	0/0	0/0	0/0	6/1	0/0	1/0
Non-tussock graminoids (live + attached dead)	1/1	3/1	1/1	4/2	7/2	5/1	15/25	20/5	30/30	20/10	30/30	40/20	65/20	2/0	30/10
Tussock graminoids (live + attached dead)	0/0	0/0	0/0	0/0	0/0	0/0	0/0	0/0	0/0	0/0	0/0	0/0	0/0	0/0	0/0
Horsetails (live + attached dead)	0/0	0/0	0/0	1/0	1/0	1/0	0/0	0/0	0/0	0/0	0/0	0/0	0/0	0.1/0	0.1/0
Foliose lichens	0.1/0	0/0	0/0	0/0	1/0	1/0	0/0	0/0	0/0	0/0	0/0	0/0	0/0	0.1/0	0.1/0
Fruticose lichens	5/0	5/0	10/0	22/0	30/0	23/0	0/0	0/0	0/0	0/0	0/0	0/0	0.5/0	2/0	0.1/0
Crustose lichens	5/0	5/0	5/0	6/0	2/0	5/0	0/0	0/0	0/0	0/0	0/0	0/0	0/0	0.1/0	0/0
Pleurocarpous bryophytes + leafy liverworts	0.1/0	0.1/0	5/0	12/0	7/0	19/0	0/0	0/0	0/0	10/0	60/0	90/0	20/0	15/0	50.1/0
Acrocarpous bryophytes	1/0	1/0	2/0	8/0	8/0	10/0	0/0	0/0	0/0	0/0	0/0	0/0	13/0	5/0	20
Total bryophytes (mosses + leafy liverworts)	1.1/0	1.1/0	7/0	20/0	15/0	29/0	0/0	0/0	0/0	10/0	60/0	90/0	23/0	20/0	70.1/0
Biological soil crusts	5/0	5/0	5/0	2/0	2/0	3/0	0/0	0/0	0/0	0/0	0/0	0/0	0/0	0.1/0	0.1/0
Algae	0/0	0/0	0/0	0/0	0/0	0/0	4/0	0.1/0	0/0	0/0	0/0	0/0	0/0	0/0	0/0
Rocks	1	0.1	0.1	0	0	0	0	0	0	0	0	0	0	0	0
Bare soil or marl	20	0.1	1	1	2	0	50	75	20	60	0	0	0	0.1	0.1
Water	0	0	0	0	0	0	100	100	100	100	100	100	0	0	0
Litter	0.1	0.5	1	2	2	2	5	5	5	5	10	5	3	2	10
VEGETATION CATEGORICAL DESCRIPTORS (SEE TABLES A2.2, A2.3)															
Vegetation type (after Walker 1985)	B1	B1	B1	B2	B2	B2	E1	E1	E1	E2	E2	E2	U10	U6	U10
Habitat type (after Mucina et al. 2014)	1.02.1	1.02.1	1.02.1	1.02.3	1.02.3	1.02.3	5.05.2.1	5.05.2.1	5.05.2.1	5.05.2.1	5.05.2.1	5.05.2.1	3.03.1	1.02.3	3.03.1

APPENDIX 6 Plant species list

Table A6.1. *Plant species list for NIRPO permanent vegetation plots, July 2021 and August 2022.* ***Field taxon:*** *Plant species name used in the field.* ***PASL taxon name:*** *Accepted taxon name following the nomenclature Panarctic Species List (PASL, v. 2019; Raynolds et al. 2016, and CAFF, www.caff.is/flora-cfg/ava/pan-arctic-species-list).* ***Taxon code:*** *6-letter code based on accepted name.* ***Growth form:*** *Plant growth form (PASL, ver. 2019).*

Field taxon	PASL taxon name	Taxon code	Growth form
Abietinella abietina	*Abietinella abietina* (Hedw.) Fleisch.	ABIABI	Pleurocarpous moss
Alectoria nigricans	*Gowardia nigricans* (Ach.) P.Halonen, L.Myllys, S. Velmala & H.Hyvarinen	GOWNIG	Fruticose lichen
Alectoria species	*Alectoria* species	ALECSP	Fruticose lichen
Androsace chamaejasme	*Androsace chamaejasme* Wulfen	ANDCHA	Cushion, mat, or rosette forb
Aneura pinguis	*Aneura pinguis* (L.) Dumort.	ANEPIN	Thalloid liverwort
Arctagrostis latifolia	*Arctagrostis latifolia* (R. Br.) Griseb.	ARCLAT	Grass
Arctophila fulva	*Arctophila fulva* (Trin.) Andersson	ARCFUL	Grass
Astragalus umbellatus	*Astragalus umbellatus* Bunge	ASTUMB	Low erect forb
Aulacomnium palustre	*Aulacomnium palustre* (Hedw.) Schwaegr.	AULPAL	Pleurocarpous moss
Aulacomnium turgidum	*Aulacomnium turgidum* (Wahlenb.) Schwaegr.	AULTUR	Pleurocarpous moss
Blepharostoma trichophyllum	*Blepharostoma trichophyllum* (Linn.) Dumortier	BLETRI	Leafy liverwort
Brachythecium species	*Brachythecium* species	BRACSP	Pleurocarpous moss
Bryum pallens	*Bryum pallens* Swartz	BRYPAL	Acrocarpous moss
Bryum pseudotriquetrum	*Bryum pseudotriquetrum* (Hedw.) P.G. Gaertn., B. Mey. & Scherb.	BRYPSE	Acrocarpous moss
Bryum species	*Bryum* species	BRYUSP	Acrocarpous moss
Calliergon giganteum	*Calliergon giganteum* (Schimp.) Kindb.	CALGIG	Pleurocarpous moss
Calliergon richardsonii	*Calliergon richardsonii* (Mitt.) Kindb.	CALRIC	Pleurocarpous moss
Calliergon species	*Calliergon* species	CALLSP	Pleurocarpous moss
Campylium species	*Campylium* species	CAMPSP	Pleurocarpous moss
Campylium stellatum	*Campylium stellatum* (Hedw.) C. Jens.	CAMSTE	Pleurocarpous moss
Cardamine digitata	*Cardamine digitata* Richardson	CARDIG	Low erect forb
Carex aquatilis	*Carex aquatilis* Wahlenb.	CARAQU	Wet to moist nontussock sedge
Carex atrofusca	*Carex atrofusca* Schkuhr	CARATR	Wet to moist nontussock sedge
Carex bigelowii	*Carex bigelowii* Torr.	CARBIG	Wet to moist nontussock sedge
Carex heleonastes	*Carex heleonastes* Ehrh. ex L. f.	CARHEL	Wet to moist nontussock sedge
Carex membranacea	*Carex membranacea* Hook.	CARMEM	Wet to moist nontussock sedge
Carex misandra	*Carex fuliginosa s. misandra* (R. Br.) Nyman	CARFUL	Wet to moist nontussock sedge
Carex rotundata	*Carex rotundata* Wahlenb.	CARROT	Wet to moist nontussock sedge
Carex rupestris	*Carex rupestris* All.	CARRUP	Dry nontussock sedge
Carex saxatilis s. laxa	*Carex saxatilis* L.	CARSAX	Wet to moist nontussock sedge
Carex scirpoidea	*Carex scirpoidea* Michx.	CARSCI	Wet to moist nontussock sedge
Carex species	*Carex* species	CARESP	Sedge
Cassiope tetragona	*Cassiope tetragona* (L.) D. Don	CASTET	Evergreen erect dwarf shrub
Catoscopium nigritum	*Catoscopium nigritum* (Hedw.) Brid.	CATNIG	Acrocarpous moss
Cephaloziella species	*Cephaloziella* species	CEPHSP	Leafy liverwort
Cerastium beeringianum	*Cerastium beeringianum* Cham. & Schltdl.	CERBEE	Cushion, mat, or rosette forb
Cerastium jenisejense	*Cerastium regelii* taxon jenisejense (Hulten)	CERREG	Cushion, mat, or rosette forb
Cetraria islandica	*Cetraria islandica* (L.) Ach.	CETISL	Fruticose lichen
Cetraria laevigata	*Cetraria laevigata* Rass.	CETLAE	Fruticose lichen
Cetraria tilesii	*Vulpicida tilesii* (Ach.) J.-E. Mattsson & M.J.Lai	VULTIL	Fruticose lichen
Chiloscyphus coadanutus	*Chiloscyphus* species *(not in PASL)*	CHIOSP	Liverwort
Chrysanthemum integrifolium	*Hulteniella integrifolia* (Richardson) Tzvelev	HULINT	Cushion, mat, or rosette forb
Cinclidium arcticum	*Cinclidium arcticum* Schimp.	CINARC	Acrocarpous moss
Cinclidium latifolium	*Cinclidium latifolium* Lindb.	CINLAT	Acrocarpous moss
Cinclidium species	*Cinclidium* species	CINCSP	Acrocarpous moss
Cinclidium stygium	*Cinclidium stygium* Swartz	CINSTY	Acrocarpous moss
Cirriphyllum cirrosum	*Cirriphyllum cirrosum* (Schwaegr.) Grout	CIRCIR	Pleurocarpous moss
Cladonia pyxidata	*Cladonia pyxidata* (L.) Hoffm.	CLAPYX	Fruticose lichen
Cladonia species	*Cladonia* species	CLADSP	Fruticose lichen
Cynodontium species	*Cynodontium* species	CYNOSP	Acrocarpous moss
Dactylina arctica	*Dactylina arctica* (Richardson) Nyl.	DACARC	Fruticose lichen

Table A6.1 *(continued)*

Field taxon	PASL taxon name	Taxon code	Growth form
Dactylina madreporiformis	*Allocetraria madreporiformis* (Ach.) Karnefelt & Thell	ALLMAD	Fruticose lichen
Dicranum elongatum	*Dicranum elongatum* Schleich. ex Schwaegr.	DICELO	Acrocarpous moss
Didymodon species	*Didymodon* species	DIDYSP	Acrocarpous moss
Distichium capillaceum	*Distichium capillaceum* (Hedw.) Bruch & Schimp.	DISCAP	Acrocarpous moss
Distichium inclinatum	*Distichium inclinatum* (Hedw.) B.S.G.	DISINC	Acrocarpous moss
Distichium species	*Distichium* species	DISTSP	Acrocarpous moss
Ditrichum flexicaule	*Ditrichum flexicaule* (Schwaegr.) Hampe	DITFLE	Acrocarpous moss
Draba species	*Draba* species	DRABSP	Cushion, mat, or rosette forb
Drepanocladus brevifolius	*Drepanocladus brevifolius* (Lindb.) Warnst.	DREBRE	Pleurocarpous moss
Drepanocladus species	*Drepanocladus* species	DREPSP	Pleurocarpous moss
Dryas integrifolia	*Dryas integrifolia* Vahl	DRYINT	Evergreen prostrate dwarf shrub
Dupontia fisheri	*Dupontia fisheri* R. Br.	DUPFIS	Grass
Encalypta rhabdocarpa	*Encalypta rhaptocarpa* Schwaegr.	ENCRHA	Acrocarpous moss
Encalypta species	*Encalypta* species	ENCASP	Acrocarpous moss
Equisetum scirpoides	*Equisetum scirpoides* Michx.	EQUSCI	Horsetail
Equisetum variegatum	*Equisetum variegatum* Schleich. ex Weber & Mohr	EQUVAR	Horsetail
Eriophorum angustifolium s. L.	*Eriophorum angustifolium* s.l. Honck.	ERIANG	Wet to moist nontussock sedge
Eriophorum scheuchzeri	*Eriophorum scheuchzeri* Hoppe	ERISCH	Wet to moist nontussock sedge
Eriophorum triste	*Eriophorum triste* (Th. Fr.) Hadac & A. Lîve	ERITRI	Wet to moist nontussock sedge
Eutrema edwardsii	*Eutrema edwardsii* R. Br.	EUTEDW	Low erect forb
Festuca baffinensis	*Festuca baffinensis* Polunin	FESBAF	Grass
Fissidens species	*Fissidens* species	FISSSP	Acrocarpous moss
Flavocetraria cucullata	*Flavocetraria cucullata* (Bell.) Karnefelt & Thell	FLACUC	Fruticose lichen
Flavocetraria nivalis	*Flavocetraria nivalis* (L.) Karnefelt & Thell	FLANIV	Fruticose lichen
Hamatocaulis vernicosus	*Hamatocaulis vernicosus* (Mitt.) Hedenas	HAMVER	Pleurocarpous moss
Hierochloe pauciflora	*Hierochloe pauciflora* R. Br.	HIEPAU	Grass
Hippurus vulgaris	*Hippuris vulgaris* L.	HIPVUL	Aquatic forb
Hypnum procerrimum	*Hypnum procerrimum* Molendo	HYPPRO	Pleurocarpous moss
Hypnum species	*Hypnum* species	HYPNSP	Pleurocarpous moss
Hypnum spp.	*Hypnum* spp.	HYPNSPP	Pleurocarpous moss
Hypogymnia subobscura	*Hypogymnia subobscura* (Vainio) Poelt	HYPSUB	Foliose lichen
Juncus triglumis	*Juncus triglumis* L.	JUNTRI	Rush
Lecanora epibryon	*Lecanora epibryon* (Ach.) Ach.	LECEPI	Crustose lichen
Lloydia serotina	*Lloydia serotina* (L.) Rchb.	LLOSER	Low erect forb
Lophozia species	*Lophozia* species	LOPHSP	Leafy liverwort
Masonhalea richardsonii	*Masonhalea richardsonii* (Hook.) Karnefelt	MASRIC	Foliose lichen
Meesia triquetra	*Meesia triquetra* (H. Richter) Aongstr.	MEETRI	Acrocarpous moss
Meesia uliginosa	*Meesia uliginosa* Hedw.	MEEULI	Acrocarpous moss
Minuartia arctica	*Minuartia arctica* (Steven ex Ser.) Graebn.	MINARC	Cushion, mat, or rosette forb
Mnium species	*Mnium* species	MNIUSP	Acrocarpous moss
Nostoc commune	*Nostoc* commune Vaucher ex Bornet & Flahault	NOSCOM	Alga
Nostoc species	*Nostoc* species	NOSTSP	Alga
Orthothecium chryseum	*Orthothecium chryseum* (Schwaegr.) B.S.G.	ORTCHR	Pleurocarpous moss
Oxytropis nigrescens	*Oxytropis nigrescens* (Pall.) Fisch.	OXYNIG	Cushion, mat, or rosette forb
Oxytropis species	*Oxytropis* species	OXYTSP	Cushion, mat, or rosette forb
Papaver macounii	*Papaver macounii* Greene	PAPMAC	Low erect forb
Parya nudicaulis	*Parrya nudicaulis* (L.) Regel	PARNUD	Low erect forb
Pedicularis albolabiata	*Pedicularis albolabiata* (Hultén) Kozhevn.	PEDALB	Low erect forb
Pedicularis capitata	*Pedicularis capitata* Adams	PEDCAP	Low erect forb
Pedicularis lanata	*Pedicularis lanata* Willd. ex Cham. & Schltdl.	PEDLAN	Low erect forb
Peltigera aphthosa	*Peltigera aphthosa* (L.) Willd.	PELAPH	Foliose lichen
Peltigera species	*Peltigera* species	PELTSP	Foliose lichen
Philonotis fontana	*Philonotis fontana* (Hedw.) Brid.	PHIFON	Acrocarpous moss
Philonotis species	*Philonotis* species	PHILSP	Acrocarpous moss
Physconia muscigena	*Physconia muscigena* (Ach.) Poelt	PHYMUS	Foliose lichen
Plagiothecium species	*Plagiothecium* species	PLAGSP	Pleurocarpous moss
Poa arctica	*Poa arctica* R. Br.	POAARC	Grass
Pohlia species	*Pohlia* species	POHLSP	Acrocarpous moss
Polemonium boreale	*Polemonium boreale* Adams	POLBOR	Cushion, mat, or rosette forb

Table A6.1 *(continued)*

Field taxon	PASL taxon name	Taxon code	Growth form
Polygonum viviparum	*Bistorta vivipara* (L.) Delarbre	BISVIP	Low erect forb
Potentilla hookerina	*Potentilla arenosa s. arenosa* (Turcz.) Juz.	POTARE	Cushion, mat, or rosette forb
Pyrola secunda	*Orthilia secunda* (L.) House	ORTSEC	Low erect forb
Radula species	*Radula* species	RADUSP	Leafy liverwort
Ranunculus gmelinii	*Ranunculus gmelinii* DC.	RANGME	Aquatic forb
Ranunculus species	*Ranunculus* species	RANUSP	Low erect forb
Rhytidium rugosum	*Rhytidium rugosum* (Ehrh. ex Hedw.) Kindb.	RHYRUG	Pleurocarpous moss
Salix arctica	*Salix arctica* Pall.	SALARC	Deciduous prostrate dwarf shrub
Salix lanata s. L.	*Salix lanata* L.	SALLAN	Deciduous erect dwarf shrub
Salix ovalifolia	*Salix ovalifolia* Trautv.	SALOVA	Deciduous prostrate dwarf shrub
Salix reticulata	*Salix reticulata* L.	SALRET	Deciduous prostrate dwarf shrub
Sanionia uncinata	*Sanionia uncinata* (Hedw.) Loeske	SANUNC	Pleurocarpous moss
Saxifraga hirculus	*Saxifraga hirculus* L.	SAXHIR	Cushion, mat and rosette forb
Saxifraga oppositifolia	*Saxifraga oppositifolia* L.	SAXOPP	Cushion, mat and rosette forb
Scapania simmonsii	*Scapania simmonsii* Bryhn & Kaal.	SCASIM	Leafy liverwort
Scapanium species	*Scapanium* species	SCAPSP	Leafy liverwort
Scorpidium scorpioides	*Scorpidium scorpioides* (Hedw.) Limpr.	SCOSCO	Pleurocarpous moss
Senecio atropurpureus s. frigidus	*Tephroseris frigida* (Richardson) Holub	TEPFRI	Low erect forb
Solorina species	*Solorina* species	SOLOSP	Foliose lichen
Stellaria laeta	*Stellaria longipes* taxon laeta	STELON	Low erect forb
Stereocaulon alpinum	*Stereocaulon alpinum* Laur.	STEALP	Fruticose lichen
Stereocaulon species	*Stereocaulon* species	STERSP	Fruticose lichen
Syntrichia ruralis	*Syntrichia ruralis* (Hedw.) Web. & D. Mohr	SYNRUR	Acrocarpous moss
Tetraplodon species	*Tetraplodon* species	TETRSP	Acrocarpous moss
Thamnolia subuliformis s. L.	*Thamnolia vermicularis s. subuliformis* (Sw.) Schaer.	THAVER	Fruticose lichen
Tomentypnum nitens	*Tomentypnum nitens* (Hedw.) Loeske	TOMNIT	Pleurocarpous moss
Unknown black crustose lichen	Unknown black crustose lichen	UNKLIC	Crustose lichen
Unknown bryophytes	Unknown bryophyte (including mosses and liverworts)	UNKBRY	Bryophyte
Unknown crustose lichen	Unknown crustose lichen	UNKLIC	Crustose lichen
Unknown dicot	Unknown/unidentified forb	UNKFOR	Forb
Unknown Dicranaceae	Unknown Dicranaceae	UNKBRY	Acrocarpous moss
Unknown *Encalypta* or *Bryum* species	Unknown *Encalypta* or *Bryum* species	UNKBRY	Acrocarpous moss
Unknown graminoid	Unknown graminoid	UNKGRA	Graminoid
Unknown leafy liverworts	Unknown leafy liverworts	UNKBRY	Aquatic forb
Unknown pleurocarpous moss	Unknown pleurocarpous moss	UNKBRY	Pleurocarpous moss
Unknown Pottiaceae	Unknown Pottiaceae	UNKBRY	Acrocarpous moss
Unknown white crustose lichen	Unknown white crustose lichen	UNKLIC	Crustose lichen
Utricularia vulgaris	*Utricularia vulgaris* L.	UTRVUL	Aquatic forb

APPENDIX 7 Plant species cover

Table A7.1. *Percent species cover-abundance, 2022 NIRPO vegetation plots, 23–25 July 2022. Values are Braun-Blanquet cover-abundance scores: r = rare; + = <1% cover; 1 = 1–5% cover; 2 = 6–25% cover; 3 = 26–50% cover; 4 = 51–75% cover; 5 = 76–100% cover.*

Taxon	21-01	21-02	21-03	21-04	21-05	21-06	21-07	21-08	21-09	21-10	21-11	21-12	21-13	21-14	21-15
Abietinella abietina	+	0	+	0	0	0	0	0	0	0	0	0	2	1	1
Alectoria species	+	+	+	0	0	0	0	0	0	0	0	0	0	0	0
Androsace chamaejasme	0	0	0	0	0	0	0	0	0	0	0	0	`1	0	0
Arctagrostis latifolia	0	0	0	0	0	0	0	0	0	0	0	0	0	0	2
Arctophila fulva	0	0	0	0	0	0	0	0	0	3	4	4	0	0	0
Astragalus umbellatus	0	0	0	0	1	0	0	0	0	0	0	0	0	0	0
Aulacomnium turgidum	0	0	0	0	0	0	0	0	0	0	0	0	0	0	1
Bistorta vivipara	+	0	0	r	r	+	0	0	0	0	0	0	0	+	+
Blepharostoma trichophyllum	0	0	0	+	+	1	0	0	0	0	0	0	0	+	0
Bryum pallens	0	0	0	+	1	0	0	0	0	0	0	0	0	0	0
Bryum species	0	0	0	+	+	0	0	0	0	0	0	0	+	1	1
Campylium species	0	0	0	0	0	0	0	0	0	0	0	0	0	+	0
Carex aquatilis	0	0	0	0	0	0	3	2	4	0	0	0	0	0	1
Carex fuliginosa	0	0	0	0	1	1	0	0	0	0	0	0	0	0	0
Carex membranacea	0	0	0	1	0	+	0	0	0	0	0	0	0	0	0
Carex rupestris	1	2	1	1	1	1	0	0	0	0	0	0	0	0	0
Carex scirpoidea	0	0	0	1	0	0	0	0	0	0	0	0	0	1	0
Cassiope tetragona	0	0	0	2	2	2	0	0	0	0	0	0	1	4	3
Cephaloziella species	0	0	0	0	0	0	0	0	0	0	0	0	0	0	+
Cerastium beeringianum	0	0	0	0	0	0	0	0	0	0	0	0	2	0	1
Cerastium regelii taxon jenisejense	0	0	0	0	0	0	0	0	0	0	0	0	0	0	+
Cetraria islandica	0	0	0	r	+	+	0	0	0	0	0	0	0	+	+
Chiloscyphus species	0	0	0	+	+	+	0	0	0	0	0	0	0	+	0
Cinclidium species	0	0	0	+	0	0	0	0	0	0	0	0	0	0	0
Cirriphyllum cirrosum	0	0	0	0	0	0	0	0	0	0	0	0	0	+	0
Cladonia pyxidata	0	0	0	+	+	+	0	0	0	0	0	0	0	r	0
Cladonia species	0	0	0	0	+	0	0	0	0	0	0	0	0	0	0
Cynodontium species	0	0	0	+	+	+	0	0	0	0	0	0	0	0	0
Dactylina arctica	+	+	1	r	0	+	0	0	0	0	0	0	+	+	+
Didymodon species	0	0	0	+	2	0	0	0	0	0	0	0	0	0	0
Distichium capillaceum	+	+	+	0	0	0	0	0	0	0	0	0	0	+	0
Distichium species	0	0	0	+	+	+	0	0	0	0	0	0	0	0	0
Ditrichum flexicaule	+	+	1	2	1	1	0	0	0	0	0	0	0	2	0
Draba species	0	0	0	0	0	0	0	0	0	0	0	0	1	0	+
Dryas integrifolia	3	4	4	4	3	3	0	0	0	0	0	0	0	3	0
Encalypta species	0	0	0	+	+	+	0	0	0	0	0	0	1	+	0

Table A7.1 *(continued)*

Taxon	21-01	21-02	21-03	21-04	21-05	21-06	21-07	21-08	21-09	21-10	21-11	21-12	21-13	21-14	21-15
Equisetum variegatum	0	0	0	1	1	r	0	0	0	0	0	0	0	+	+
Eriophorum triste	0	0	0	1	+	1	0	0	0	0	0	0	0	0	0
Festuca baffinensis	0	0	0	0	0	0	0	0	0	0	0	0	2	0	+
Flavocetraria cucullata	1	+	1	+	1	+	0	0	0	0	0	0	+	+	0
Flavocetraria nivalis	+	+	1	1	1	+	0	0	0	0	0	0	0	+	0
Gowardia nigricans	0	0	r	+	+	+	0	0	0	0	0	0	0	0	0
Hippuris vulgaris	0	0	0	0	0	0	0	0	0	+	+	+	0	0	0
Hulteniella integrifolia	+	+	r	+	+	+	0	0	0	0	0	0	0	+	0
Hypnum procerrimum	0	0	0	0	0	0	0	0	0	0	0	0	0	2	1
Hypnum species	0	0	0	1	1	+	0	0	0	0	0	0	0	1	0
Hypogymnia subobscura	+	+	0	0	0	0	0	0	0	0	0	0	0	0	0
Juncus triglumis	0	0	0	0	+	0	0	0	0	0	0	0	0	0	0
Lecanora epibryon	1	1	1	1	2	1	0	0	0	0	0	0	0	0	0
Lloydia serotina	0	0	0	0	0	0	0	0	0	0	0	0	1	0	0
Masonhalea richardsonii	0	0	0	0	0	+	0	0	0	0	0	0	+	1	0
Nostoc commune	0	0	0	0	0	0	1	r	0	0	0	0	0	0	0
Nostoc species	0	0	0	0	0	0	0	r	0	0	0	0	0	0	0
Orthothecium chryseum	0	0	0	+	0	+	0	0	0	0	0	0	0	0	0
Oxytropis nigrescens	1	+	+	0	0	0	0	0	0	0	0	0	+	0	0
Oxytropis species	+	+	+	0	1	+	0	0	0	0	0	0	0	r	0
Papaver macounii	0	0	0	+	+	+	0	0	0	0	0	0	0	+	+
Parrya nudicaulis	0	0	r	0	0	r	0	0	0	0	0	0	0	+	0
Pedicularis capitata	0	0	r	0	r	0	0	0	0	0	0	0	0	+	+
Pedicularis lanata	r	0	0	r	r	+	0	0	0	0	0	0	0	0	0
Peltigera species	0	0	0	0	0	0	0	0	0	0	0	0	0	r	0
Philonotis species	0	0	0	0	0	0	0	0	0	0	0	0	0	0	+
Physconia muscigena	+	0	0	0	0	0	0	0	0	0	0	0	0	0	0
Plagiothecium species	0	0	0	0	0	0	0	0	0	0	0	0	0	1.5	0
Poa arctica	0	0	0	0	0	0	0	0	0	0	0	0	3	0	0
Pohlia species	0	0	0	0	0	0	0	0	0	0	0	0	0	0	1
Polemonium boreale	0	0	0	0	0	0	0	0	0	0	0	0	1	0	1
Potentilla arenosa s. arenosa	0	0	0	0	0	0	0	0	0	0	0	0	1	0	0
Radula species	0	0	0	1	0	+	0	0	0	0	0	0	0	0	0
Ranunculus gmelinii	0	0	0	0	0	0	0	0	0	+	0	1	0	0	0
Ranunculus species	0	0	0	0	0	0	0	0	0	0	0	0	+	0	+
Rhytidium rugosum	+	0	1	0	0	0	0	0	0	0	0	0	0	0	0
Salix arctica	0	0	0	1	1	2	0	0	0	0	0	0	0	1	2
Salix reticulata	0	0	0	1	1	1	0	0	0	0	0	0	0	1	1
Sanionia uncinata	+	+	1	0	0	0	0	0	0	0	0	0	1	0	2
Saxifraga oppositifolia	+	+	+	1	1	1	0	0	0	0	0	0	0	0	0
Scapania simmonsii	0	0	0	+	0	0	0	0	0	0	0	0	0	0	0

Table A7.1 *(continued)*

Taxon	21-01	21-02	21-03	21-04	21-05	21-06	21-07	21-08	21-09	21-10	21-11	21-12	21-13	21-14	21-15
Scapanim species	0	0	0	+	0	0	0	0	0	0	0	0	0	0	0
Scorpidium scorpioides	0	+	+	0	0	0	0	0	0	2	4	5	0	0	0
Solorina species	r	r	0	0	+	+	0	0	0	0	0	0	0	+	0
Stellaria longipes	0	0	0	0	0	0	0	0	0	0	0	0	+	0	0
Syntrichia ruralis	0	0	0	0	0	0	0	0	0	0	0	0	2	1	1
Tephroseris frigida	0	0	0	1	+	+	0	0	0	0	0	0	0	+	+
Tetraplodon species	0	0	0	0	0	0	0	0	0	0	0	0	0	0	2
Thamnolia vermicularis	1	1	1	2	2	2	0	0	0	0	0	0	0	1	+
Tomentypnum nitens	0	0	0	1	1	2	0	0	0	0	0	0	0	2	1
Utricularia vulgaris	0	0	0	0	0	0	0	0	+	+	1	1	0	0	0
Vulpicida tilesii	+	1	+	0	0	0	0	0	0	0	0	0	0	0	0
Unknown black crustose lichen	2	1	2	1	1	1	0	0	0	0	0	0	0	0	0
Unknown bryophytes	0	0	0	1	+	0	0	0	0	0	0	0	0	0	1.5
Unknown Dicranaceae	0	0	0	0	0	0	0	0	0	0	0	0	0	+	0
Unknown *Encalypta* or *Bryum* species	0	0	0	0	0	0	0	0	0	0	0	0	0	+	+
Unknown leafy liverworts	+	0	0	+	0	1	0	0	0	0	0	0	0	1.5	0
Unknown pleurocarpous moss	0	r	0	0	0	0	0	0	0	0	0	0	0	0	0
Unknown Pottiaceae	0	0	0	0	0	0	0	0	0	0	0	0	0	+	+
Unknown white crustose lichen	1	+	1	0	0	0	0	0	0	0	0	0	0	+	0

APPENDIX 8 Aboveground biomass

Table A8.1. *Aboveground biomass of NIRPO vegetation plots, Prudhoe Bay, August 2021 and 2022. Data are dry weights in g/m² from a representative 50-cm x 20-cm sample of the plant communities at each plot sorted by growth form and life form.* ***Veg type:*** *See Table A2.2 for vegetation type codes.*

Plot ID	Veg type	Deciduous shrub (g/m²)	Evergreen shrub (g/m²)	Graminoid (live) (g/m²)	Graminoid (dead) (g/m²)	Forb (g/m²)	Horsetail (g/m²)	Lichen (g/m²)	Litter (g/m²)	Moss (g/m²)	Total (g/m²)
21-01	M2	33.8	69.9	44.3	41.3	0.0	32.0	5.8	134.7	295.8	657.6
21-02	M2	16.6	10.1	41.7	35.5	0.0	18.0	0.0	17.9	259.8	399.6
21-03	M4	0.0	0.0	30.2	75.6	0.0	0.0	0.0	25.0	28.5	159.3
21-04	M4	0.0	0.0	97.6	161.3	0.0	0.0	0.0	86.9	342.4	688.2
21-05	U3	29.0	160.0	53.9	52.4	0.0	7.4	64.8	291.1	265.3	923.9
21-06	U3	9.3	183.8	36.1	20.9	6.5	8.3	55.0	105.2	594.2	1019.3
21-07	U4	86.4	8.0	197.7	230.6	0.0	8.1	0.0	216.0	249.8	996.6
21-08	U4	311.2	24.8	58.0	157.6	0.0	10.0	0.0	183.2	130.6	875.4
21-09	U4	153.2	99.5	25.2	213.5	1.1	14.3	0.0	369.2	211.2	1087.2
21-10	U3	7.2	279.5	67.2	50.9	0.3	1.1	53.1	498.6	739.3	1697.2
21-11	M2	32.9	77.7	123.7	79.6	0.0	0.0	0.0	82.8	118.6	515.3
21-12	U4	26.5	0.0	139.4	165.7	0.0	6.7	0.0	149.0	129.0	616.3
21-13	U4	0.0	1.3	68.3	83.0	0.0	17.2	0.0	80.6	64.4	314.8
21-14	M2	15.6	0.0	106.5	92.9	0.0	8.4	0.0	51.3	613.6	888.3
21-15	U4	32.5	0.0	90.8	99.5	0.0	15.7	0.0	76.5	934.9	1249.9
21-16	M2	16.9	43.2	174.2	103.9	2.1	8.7	2.9	55.6	376.9	784.4
21-17	U4	29.7	149.7	31.4	122.7	2.7	23.9	37.6	186.6	411.4	995.7
21-18	U4	55.1	120.7	34.9	103.4	0.0	18.8	0.0	120.9	188.0	641.8
21-19	M2	0.0	0.0	61.6	124.4	0.0	39.0	0.0	24.9	269.7	519.6
21-20	U3	2.3	273.4	29.6	52.2	63.7	22.4	77.7	415.5	355.2	1292.0
21-21	U3	5.5	176.4	30.8	58.1	7.8	0.0	72.1	272.6	628.3	1251.6
21-22	U3	50.4	166.9	29.7	130.2	2.4	6.9	37.6	342.2	350.8	1117.1
21-23	M2	30.3	4.1	84.3	123.7	2.5	55.1	0.0	30.3	563.4	893.7
21-24	U3	1.4	230.2	33.4	109.6	0.0	19.3	43.9	114.3	531.4	1083.5
21-25	Marl	0.0	0.0	4.0	13.7	0.0	0.0	0.0	0.0	0.0	17.7
21-26	Marl	0.0	0.0	12.2	20.1	0.0	0.0	0.0	0.0	0.0	32.3
21-27	M2	0.0	0.0	82.4	126.4	0.0	1.6	0.0	0.0	1.1	211.5
21-28	M4	0.0	0.0	95.1	83.1	0.0	1.5	0.0	0.0	60.8	240.5
21-29	M2	0.0	0.0	85.1	93.4	1.9	32.0	0.0	22.9	413.2	648.5
21-30	U4	28.3	53.4	106.8	148.1	3.2	19.6	0.0	127.7	538.3	1025.4
21-31	M4/E1	0.0	0.0	271.4	65.5	0.0	0.0	0.0	0.0	142.4	479.3
21-32	M4	0.0	0.0	224.4	118.6	0.0	2.8	0.0	0.0	218.2	564.0
21-33	M4	0.0	0.0	130.1	98.2	0.0	0.6	0.0	0.0	56.8	285.7
21-34	U4	23.1	89.3	53.0	73.3	2.5	15.0	0.0	66.5	211.7	534.4
21-35	M4/E1	0.0	0.0	148.4	20.0	0.0	0.0	0.0	81.1	72.8	322.3
22-01	B1	0.0	504.2	4.1	3.8	29.8	0.0	83.5	120.0	170.4	915.8
22-02	B1	0.0	438.3	4.1	4.9	53.1	0.0	55.3	145.1	58.7	759.5
22-03	B1	0.0	402.7	5.7	8.6	74.6	0.0	41.0	177.2	102.5	812.3
22-04	B2	49.8	283.2	2.4	3.0	36.1	5.5	55.3	135.9	385.6	956.8
22-05	B2	18.4	433.9	12.0	12.2	63.3	8.6	72.7	103.3	573.6	1298.0
22-06	B2	8.3	254.4	14.0	19.6	3.9	9.4	46.7	109.8	119.4	585.5
22-07	E1	0.0	0.0	97.6	75.7	0.0	0.0	0.0	25.8	0.0	199.0
22-08	E1	0.0	0.0	82.8	41.1	0.0	0.0	0.0	16.4	0.0	140.3
22-09	E1	0.0	0.0	242.3	191.9	0.0	0.0	0.0	30.2	0.0	464.3
22-10	E2	0.0	0.0	104.7	25.2	0.0	0.0	0.0	13.7	14.3	157.9
22-11	E2	0.0	0.0	339.3	55.9	13.2	0.0	0.0	61.9	707.7	1178.1
22-12	E2	0.0	0.0	125.5	65.8	11.5	0.0	0.0	81.1	622.8	906.7
22-13	U10	0.0	195.8	89.2	104.9	53.5	0.0	0.0	212.7	168.7	824.8
22-14	U6	17.9	742.9	2.5	4.1	6.1	9.5	81.8	170.8	348.6	1384.2
22-15	U10	163.7	124.2	27.1	48.6	13.3	5.1	2.4	160.7	340.6	885.7
21A-21	Em	0.0	0.0	2.2	0.0	0.0	0.0	0.0	0.0	3547.5	3549.7

Table A8.1 *(continued)*

Plot ID	Veg type	Deciduous shrub (g/m²)	Evergreen shrub (g/m²)	Graminoid (live) (g/m²)	Graminoid (dead) (g/m²)	Forb (g/m²)	Horsetail (g/m²)	Lichen (g/m²)	Litter (g/m²)	Moss (g/m²)	Total (g/m²)
21A-22	Ef	0.0	0.0	0.0	0.0	166.1	0.0	0.0	0.0	1.1	167.2
21A-23	Em	0.0	0.0	3.3	0.0	0.0	0.0	0.0	0.0	3082.6	3085.9
21A-24	Es	39.5	0.0	48.8	0.0	0.0	0.0	0.0	261.0	188.6	537.8
21A-25	Ef	3.8	0.0	9.3	0.0	89.4	0.0	0.0	21.9	2.7	127.2
21A-26	Em	6.0	0.0	13.2	0.0	0.0	0.0	0.0	0.0	4702.0	4721.2
21A-27	Es	9.3	0.0	48.2	0.0	0.0	0.0	0.0	100.9	327.8	486.3
21A-28	Ef	1.6	0.0	0.0	0.0	390.9	0.0	0.0	0.0	3.3	395.8
21A-29	Em	0.0	0.0	36.7	0.0	0.0	0.0	0.0	0.0	6037.0	6073.7
21A-30	Es	13.7	0.0	42.2	0.0	8.2	0.0	0.0	225.3	100.9	390.3
21A-31	Ef	55.9	0.0	40.0	0.0	109.6	0.0	0.0	146.9	75.1	427.6
21A-32	Em	0.0	0.0	8.2	0.0	0.0	0.0	0.0	0.0	2712.0	2720.2
21A-33	Em	40.6	0.0	5.5	0.0	0.0	0.0	0.0	0.0	1491.7	1537.7
21A-34	Em	6.0	0.0	0.0	0.0	58.1	0.0	0.0	0.0	6346.7	6410.8
21A-35	Es	39.5	0.0	0.6	0.0	0.0	0.0	0.0	52.6	60.9	153.5
21A-36	Em	0.0	0.0	0.6	0.0	0.0	0.0	0.0	0.0	3733.9	3734.5
21A-37	Em	2.2	0.0	6.0	0.0	0.0	0.0	0.0	0.0	694.6	702.8
21A-38	Es	7.7	0.0	8.8	0.0	0.0	0.0	0.0	21.9	47.7	86.1
21A-39	Em	0.0	0.0	139.8	0.0	0.0	0.0	0.0	0.0	3498.2	3638.0
21A-40	Ef	0.0	0.0	19.7	0.0	36.2	0.0	0.0	0.0	28.5	84.4

APPENDIX 9 Bryophyte species cover and life forms

Table A9.1. *Bryophyte life-form analysis and species cover.* ***Life form:*** *Short turf (Ts), tall turf (Tt), rough mat (Mr), smooth mat (Ms), thallose mat (Mt), solitary creeping (Sc), solitary erect (Se); based on analysis by Anna Kučerová 2022.* ***Veg type:*** *See Table A2.2 for vegetation type codes.*

Taxon	Life form	22-01	22-02	22-04	22-05	21-05	21-21	21-09	21-34	21-01	21-16	21-29	21-03	21-28	21-31	21-35	22-11	22-12	Plot ID
		B1	B1	B2	B2	U3	U3	U4	U4	M2	M2	M2	M4	M4	E1,M4	E1,M4	E2	E2	Veg type
Abietinella abietina	Mr	+	.	.	.	.	.	.	.	.	.	.	.	.	.	.	.	.	
Amblystegium serpens cf.	Sc	.	r	.	.	.	.	.	.	.	.	.	.	.	.	.	.	.	
Anastrophyllum minutum	Sc	.	.	r	.	r	.	.	.	.	.	.	.	.	.	.	.	.	
Aneura pinguis	Mt	.	.	.	r	.	+	+	+	.	+	+	.	.	.	.	.	.	
Arnellia fennica	Sc	.	.	+	.	+	.	.	.	.	.	.	.	.	.	.	.	.	
Blepharostoma trichophyllum	Ms	.	.	+	+	+	.	.	1	.	.	.	.	.	.	.	.	.	
Brachythecium albicans	Ms	.	.	.	.	.	r	.	.	.	.	.	.	.	.	.	.	.	
Brachythecium cirrosum	Sc	r	.	r	.	r	+	.	.	.	.	.	.	.	.	.	.	.	
Brachythecium tauriscorum	Sc	.	.	.	r	.	.	.	.	.	.	.	.	.	.	.	.	.	
Bryum algovicum	Ts	.	.	.	.	.	.	.	1	.	.	.	.	.	.	.	.	.	
Bryum arcticum	Ts	.	.	.	.	.	.	.	.	.	.	1	.	.	.	.	.	.	
Bryum caespiticium	Ts	.	.	r	+	.	.	.	.	.	.	.	.	.	.	.	.	.	
Bryum calophyllum	Ts	.	.	.	.	.	.	.	+	.	+	.	.	.	.	.	.	.	
Bryum pallescens	Ts	.	.	+	.	+	r	+	r	.	+	.	.	.	.	.	.	.	
Bryum pseudotriquetrum	Tt	.	.	.	.	.	.	+	1	.	+	.	.	.	.	.	.	.	
Bryum species	Ts	r	.	.	r	+	+	.	.	.	.	r	.	.	.	.	.	.	
Buckia vaucheri	Mr	.	.	.	+	.	.	.	.	.	.	.	.	.	.	.	.	.	
Calliergon giganteum	Mr	.	.	.	.	.	.	.	r	.	1	+	.	+	2	3	.	.	
Calliergon richardsonii cf.	Sc	.	.	.	.	.	.	.	.	+	.	.	.	.	.	.	.	.	
Campyliadelphus chrysophyllus cf.	Sc	.	r	.	.	.	.	.	.	.	.	.	.	.	.	.	.	.	
Campylium stellatum	Mr	.	.	r	r	+	+	1	3	+	1	.	.	+	.	.	.	.	
Catoscopium nigritum	Ts	.	.	.	r	+	.	+	2	1	+	r	.	+	.	.	.	.	
Cephaloziella species	Sc	.	r	.	.	.	.	.	r	.	.	.	.	.	.	.	.	.	
Ceratodon purpureus	Ts	.	.	+	.	+	.	.	.	.	.	.	.	.	.	.	.	.	
Chiloscyphus polyanthos var. *polyanthos*	Sc	.	r	.	.	.	.	.	.	.	.	.	.	.	.	.	.	.	
Cinclidium arcticum	Ts	.	.	+	r	+	.	.	.	.	+	.	.	.	.	.	.	.	
Cinclidium latifolium	Ts	.	.	.	.	+	.	+	2	1	1	2	.	1	.	.	.	.	
Cinclidium stygium	Se	.	.	.	.	.	.	.	+	.	.	.	.	.	.	.	.	.	
Cinclidium subrotundum	Se	.	.	.	.	.	.	.	.	.	.	r	.	.	.	.	.	.	
Cratoneuron filicinum	Sc	.	.	.	.	.	.	.	.	.	.	+	.	.	.	.	.	.	
Ctenidium molluscum	Sc	.	.	r	.	+	.	.	.	.	.	.	.	.	.	.	.	.	
Cyrtomnium hymenophyllum	Se	.	.	.	.	.	.	.	.	+	.	+	.	+	.	.	.	.	
Dichodontium pellucidum	Ts	.	.	.	.	.	+	.	.	.	.	.	.	.	.	.	.	.	
Didymodon asperifolius	Tt	.	.	+	+	+	r	.	.	.	.	.	.	.	.	.	.	.	
Distichium capillaceum	Tt	+	+	+	+	+	+	+	2	1	+	.	.	.	.	.	.	.	

Table A9.1 *(continued)*

Taxon	Life form	22-01	22-02	22-04	22-05	21-05	21-21	21-09	21-34	21-01	21-16	21-29	21-03	21-28	21-31	21-35	22-11	22-12	Plot ID
		B1	B1	B2	B2	U3	U3	U4	U4	M2	M2	M2	M4	M4	E1,M4	E1,M4	E2	E2	Veg type
Distichium inclinatum	Tt	.	r	.	.	r	.	.	.	.	.	+	.	.	.	.	.	.	
Drepanocladus aduncus	Mr	.	.	.	.	.	.	.	.	.	.	.	.	.	1	1	.	.	
Drepanocladus polygamus	Mr	.	.	.	.	.	.	.	+	.	.	.	.	.	.	.	.	.	
Drepanocladus species	Mr	.	.	.	.	+	.	.	.	.	.	.	.	.	.	.	.	.	
Encalypta alpina	Ts	r	r	+	+	+	.	+	+	.	.	.	.	.	.	.	.	.	
Encalypta mutica	Ts	.	r	.	r	.	.	.	.	.	.	.	.	.	.	.	.	.	
Encalypta rhaptocarpa	Ts	.	.	r	.	.	+	+	.	.	.	.	.	.	.	.	.	.	
Entodon concinnus	Sc	.	.	r	.	.	.	.	.	.	.	.	.	.	.	.	.	.	
Fissidens adianthoides	Se	.	.	.	.	.	.	.	.	+	.	.	.	.	.	.	.	.	
Fissidens osmundoides	Se	.	.	r	.	.	.	.	.	.	.	.	.	.	.	.	.	.	
Flexitrichum flexicaule	Tt	+	+	2	1	1	2	2	1	+	1	.	.	.	.	.	.	.	
Flexitrichum gracile	Ts	.	.	.	.	.	+	.	.	.	.	.	.	.	.	.	.	.	
Gymnocolea inflata	Sc	r	.	.	.	r	.	.	+	.	.	.	.	.	.	.	.	.	
Hygrohypnum luridum cf.	Sc	.	.	.	.	.	.	+	.	.	.	.	.	.	.	.	.	.	
Hypnum bambergeri	Mr	.	.	.	r	+	1	.	+	.	.	.	.	.	.	.	.	.	
Hypnum callichroum	Mr	.	.	.	.	.	.	.	+	.	.	+	.	.	.	.	.	.	
Hypnum cupressiforme	Sc	.	.	.	.	.	r	.	.	.	.	.	.	.	.	.	.	.	
Meesia triquetra	Tt	.	.	.	.	.	.	.	.	+	.	1	.	.	.	.	.	.	
Meesia uliginosa	Ts	.	.	+	2	+	+	.	.	+	+	r	.	.	.	.	.	.	
Mesoptychia badensis	Sc	.	.	.	r	.	.	.	r	.	.	.	.	.	.	.	.	.	
Mesoptychia heterocolpos	Sc	.	.	+	+	.	.	+	+	+	+	+	.	.	.	.	.	.	
Myurella julacea	Sc	.	.	.	.	.	.	.	r	.	.	.	.	.	.	.	.	.	
Oncophorus wahlenbergii	Ts	.	.	.	+	.	.	.	.	.	.	.	.	.	.	.	.	.	
Orthothecium chryseum	Se	.	.	+	r	+	+	.	1	.	+	.	.	.	.	.	.	.	
Orthothecium rufescens	Sc	.	.	.	.	.	+	.	.	.	.	.	.	.	.	.	.	.	
Orthothecium strictum	Sc	.	.	r	.	+	.	1	.	.	.	.	.	.	.	.	.	.	
Plagiopus oederiana	Ts	.	.	+	.	.	.	.	.	.	.	.	.	.	.	.	.	.	
Platydictya jungermannioides	Ms	r	.	r	.	.	r	.	.	.	.	+	.	.	.	.	.	.	
Pohlia nutans	Ts	.	.	.	.	.	.	+	.	.	.	.	.	.	.	.	.	.	
Pohlia species	Ts	.	.	.	.	.	.	.	.	.	+	.	.	.	.	.	.	.	
Pseudocalliergon brevifolium	Mr	.	.	.	.	.	.	r	.	2	4	1	.	2	3	3	.	.	
Pseudocalliergon trifarium	Sc	.	.	.	.	.	.	.	r	.	.	.	.	.	.	.	.	.	
Pseudocalliergon turgescens	Se	.	.	.	.	.	r	.	1	1	+	.	.	.	.	.	.	.	
Pseudostereodon procerrimus	Mr	+	+	1	1	1	+	+	.	1	.	.	.	.	.	.	.	.	
Radula prolifera	Mr	.	.	1	.	+	.	.	.	.	.	.	.	.	.	.	.	.	
Rhizomnium andrewsianum	Se	.	.	.	.	r	.	.	.	.	.	.	.	.	.	.	.	.	
Rhytidium rugosum	Mr	+	r	.	.	.	.	.	.	.	.	.	.	.	.	.	.	.	
Scapania mucronata	Mr	.	.	.	.	.	.	+	.	.	.	.	.	.	.	.	.	.	
Scapania simmonsii	Ms	.	.	+	.	r	.	.	.	.	.	.	.	.	.	.	.	.	
Schljakovianthus quadrilobus	Sc	.	.	.	.	r	.	.	.	.	.	.	.	.	.	.	.	.	

Table A9.1 *(continued)*

Taxon	Life form	22-01 B1	22-02 B1	22-04 B2	22-05 B2	21-05 U3	21-21 U3	21-09 U4	21-34 U4	21-01 M2	21-16 M2	21-29 M2	21-03 M4	21-28 M4	21-31 E1,M4	21-35 E1,M4	22-11 E2	22-12 E2	Plot ID Veg type
Scorpidium revolvens	Mr	.	.	.	.	.	.	.	2	+	1	+	.	.	.	.	.	.	
Scorpidium scorpioides	Mr	.	.	.	.	.	.	.	.	2	.	1	2	2	1	2	4	5	
Splachnum vasculosum	Ts	.	.	.	.	.	.	.	+	.	.	.	.	.	.	.	.	.	
Syntrichia ruralis	Ts	r	r	.	.	.	.	.	.	.	.	.	.	.	.	.	.	.	
Timmia norvegica	Ts	.	.	.	.	.	.	.	+	.	.	.	.	.	.	.	.	.	
Tomentypnum nitens	Mr	.	+	1	1	3	2	1	3	+	+	.	.	.	+	.	.	.	
Tortella fragilis	Ts	.	.	.	.	.	.	+	.	.	.	.	.	.	.	.	.	.	
Tortella tortuosa var. *arctica*	Se	.	.	.	.	.	r	.	.	.	.	.	.	.	.	.	.	.	
Voitia hyperborea	Ts	.	.	+	.	.	.	.	.	.	.	.	.	.	.	.	.	.	

APPENDIX 10 Snow survey

Table A10.1. *Ground-based survey of snow depth, snow density, and snow water equivalent at permanent vegetation plots, NIRPO-Jorgenson-Colleen (NJC) Area, Prudhoe Bay, 28 April–3 May 2022.* ***Site:*** *Jorgenson (JS), Natual Ice-rich Permafrost Observatory (NIRPO), Colleen (CS), Airport (AS).* ***Snow depth: Mean:*** *average of five measurements taken at corners and center of 1-m^2 plots with a thaw probe and meter stick;* ***S.D.:*** *standard deviation (* denotes s.d. > 4 cm, indicating measurements may have been made outside the plot when plot boundaries were not apparent in the snow pit).* ***Core depth:*** *Depth of snow in snow-core-sampler tube placed at the edge of a snow pit and used to calculate snow density and snow water equivalent.* ***Snow density:*** *Snow mass/volume in g/cm^3.* ***SWE:*** *Snow water equivalent, equal to density x depth in cm. Note: Snow density and SWE data are not available at the Airport site, since no snow pits were dug there in 2022.*

Site	Plot ID	Tran-sect	Surface feature	Date	Snow depth Mean (cm)	Snow depth S.D. (cm)	Core depth (cm)	Snow density (g/cm³)	SWE (cm)	Field notes
JS	21A-01	JS	Pond	4/29/2022	50	2	52	0.29	15.1	
JS	21A-02	JS	Pond	4/29/2022	62	2	60	0.33	19.5	
JS	21A-03	JS	Pond	4/28/2022	61	4	56	0.29	16.4	PVC pole not visible
JS	21A-04	JS	Pond	4/28/2022	65	4	53	0.30	16.1	PVC pole not visible
JS	21A-05	JS	Pond	4/29/2022	60	1	50	0.32	15.8	
JS	21A-06	JS	Pond	4/28/2022	55	3	57	0.41	23.1	Pit between adjacent plots in same pond
JS	21A-07	JS	Pond	4/28/2022	52	3	57	0.41	23.1	Pit between adjacent plots in same pond
JS	21A-08	JS	Pond	4/29/2022	66	3	55	0.30	16.5	
JS	21A-09	JS	Pond	4/29/2022	74	3	67	0.31	20.5	
JS	21A-10	JS	Pond	4/29/2022	85	3	80	0.33	26.1	
JS	21A-11	JS	Pond	4/29/2022	70	3	51	0.25	12.5	Pit between adjacent plots
JS	21A-12	JS	Pond	4/29/2022	57	5	51	0.25	12.5	Pit between adjacent plots
JS	21A-13	JS	Pond	4/29/2022	67	3	68	0.30	20.3	PVC pole not visible
JS	21A-14	JS	Pond	4/29/2022	56	2	56	0.28	15.8	PVC pole not visible
JS	21A-15	JS	Pond	4/29/2022	81	9	88	0.29	25.7	
JS	21A-16	JS	Pond	4/29/2022	89	4	88	0.29	25.7	PVC pole not visible; found purple flagging
JS	21A-17	JS	Pond	4/29/2022	73	4	78	0.29	22.9	PVC pole not visible
JS	21A-18	JS	Pond	4/28/2022	73	8	68	0.28	18.9	Pit between adjacent plots in same pond
JS	21A-19	JS	Pond	4/28/2022	68	4	68	0.28	18.9	Pit between adjacent plots in same pond
NIRPO	21-05	T6	Center	4/30/2022	46	3	38	0.28	10.7	
NIRPO	21-06	T6	Center	4/30/2022	16	2	14	0.19	2.7	
NIRPO	21-07	T6	Center	4/30/2022	47	3	46	0.21	9.8	
NIRPO	21-08	T6	Center	4/30/2022	42	1	40	0.24	9.4	
NIRPO	21-09	T6	Center	4/30/2022	40	2	35	0.30	10.6	
NIRPO	21-10	T6	Center	4/30/2022	22	7	22	0.19	4.2	
NIRPO	21-11	T6	Trough	4/30/2022	63	2	64	0.28	18.2	
NIRPO	21-12	T6	Trough	4/30/2022	72	2	68	0.29	20.0	
NIRPO	21-13	T6	Trough	4/30/2022	61	3	60	0.30	17.8	
NIRPO	21-14	T6	Trough	4/30/2022	70	5	60	0.29	17.3	
NIRPO	21-15	T6	Trough	4/30/2022	84	4	84	0.31	25.7	
NIRPO	21-16	T6	Trough	4/30/2022	55	3	84	0.14	11.7	
NIRPO	21-01	T8	Featureless	4/30/2022	54	4	52	0.28	14.3	
NIRPO	21-02	T8	Featureless	4/30/2022	43	2	47	0.28	13.0	
NIRPO	21-03	T8	Featureless	4/30/2022	43	1	45	0.30	13.6	Plot is iced at bottom of snowpack
NIRPO	21-04	T8	Featureless	4/30/2022	44	1	45	0.26	11.9	Plot is iced at bottom of snowpack
NIRPO	21-17	T8	Rim	4/30/2022	31	3	32	0.23	7.5	
NIRPO	21-18	T8	Featureless	4/30/2022	48	2	53	0.28	14.8	
NIRPO	21-19	T9	Center	4/30/2022	43	3	38	0.24	9.3	
NIRPO	21-20	T9	Center	4/30/2022	26	1	30	0.27	8.0	
NIRPO	21-21	T9	Center	4/30/2022	18	2	23	0.21	4.9	
NIRPO	21-22	T9	Center	4/30/2022	37	5	35	0.25	8.6	
NIRPO	21-23	T9	Center	4/30/2022	50	4	53	0.28	14.8	
NIRPO	21-24	T9	Rim	4/30/2022	34	4	53	0.28	15.0	
NIRPO	21-25	T7	Marl pond	5/1/2022	39	2	38	0.27	10.2	Bottom and surface ice layer in snowpack
NIRPO	21-26	T7	Marl pond	5/1/2022	44	2	44	0.29	12.6	Bottom and surface ice layer in snowpack
NIRPO	21-27	T7	Center	5/1/2022	47	1	49	0.25	12.4	
NIRPO	21-28	T7	Center	5/1/2022	51	3	49	0.30	14.5	Plot is iced at bottom of snowpack
NIRPO	21-29	T7	Center	5/1/2022	36	2	39	0.27	10.4	

Table A10.1 *(continued)*

Site	Plot ID	Tran-sect	Surface feature	Date	Snow depth Mean (cm)	Snow depth S.D. (cm)	Core depth (cm)	Snow density (g/cm^3)	SWE (cm)	Field notes
NIRPO	21-30	T7	Rim	5/1/2022	30	3	32	0.27	8.5	
NIRPO	21-31	T7	Trough	5/1/2022	53	1	52	0.28	14.3	Plot is iced at bottom of snowpack
NIRPO	21-32	T7	Trough	5/1/2022	54	2	59	0.33	19.5	Plot is iced at bottom of snowpack
NIRPO	21-33	T7	Center	5/1/2022	52	2	57	0.29	16.7	
NIRPO	21-34	T7	Rim	5/1/2022	43	1	49	0.28	13.6	
NIRPO	21-35	T7	Trough	5/1/2022	53	4	59	0.31	18.2	Plot is iced at bottom of snowpack
NIRPO	21A-21	A/T6	Pond	5/3/2022	52	2	54	0.31	16.7	
NIRPO	21A-22	A/T6	Pond	5/3/2022	75	4	62	0.30	18.7	
NIRPO	21A-23	A/T6	Pond	5/3/2022	81	4	92	0.32	29.6	
NIRPO	21A-24	A/T6	Pond	5/3/2022	76	8*	92	0.32	29.6	
NIRPO	21A-25	A/T6	Pond	5/2/2022	58	1	56	0.27	15.1	
NIRPO	21A-26	A/T6	Pond	5/2/2022	65	2	61	0.30	18.2	Pit between adjacent plots in same pond
NIRPO	21A-27	A/T6	Pond	5/2/2022	57	1	61	0.30	18.2	Pit between adjacent plots in same pond
NIRPO	21A-28	A/T6	Pond	5/2/2022	72	1	65	0.29	18.6	
NIRPO	21A-29	A/T6	Pond	5/2/2022	69	2	73	0.29	21.2	Pit between adjacent plots in same pond
NIRPO	21A-30	A/T6	Pond	5/2/2022	72	1	73	0.29	21.2	Pit between adjacent plots in same pond
NIRPO	21A-31	A/T6	Pond	5/2/2022	50	2	54	0.31	16.5	
NIRPO	21A-32	A/T6	Pond	5/2/2022	66	2	72	0.28	20.3	
NIRPO	21A-33	A/T6	Pond	5/2/2022	77	1	84	0.27	22.9	
NIRPO	21A-34	A/T6	Pond	5/2/2022	80	2	80	0.29	23.4	
NIRPO	21A-35	A/T6	Pond	5/2/2022	84	3	84	0.32	27.0	
NIRPO	21A-36	A/T6	Pond	5/2/2022	88	1	84	0.30	25.1	
NIRPO	21A-37	A/T6	Pond	5/2/2022	73	2	88	0.29	25.3	Pit between adjacent plots in same pond
NIRPO	21A-38	A/T6	Pond	5/2/2022	82	2	88	0.29	25.3	Pit between adjacent plots in same pond
NIRPO	21A-39	A/T6	Pond	5/2/2022	63	2	62	0.29	18.0	
NIRPO	21A-40	A/T6	Pond	5/3/2022	63	1	66	0.28	18.2	
CS	T1-005-C	T1	Center	5/2/2022	68	2	70	0.28	19.9	Ice lens (20 cm diameter) at bottom of the pit; not fully iced as wet or aquatic plots
CS	T1-005-T	T1	Trough	5/2/2022	86	3	90	0.29	25.9	
CS	T1-010-C	T1	Center	5/2/2022	61	0	63	0.31	19.6	
CS	T1-010-T	T1	Trough	5/2/2022	73	2	59	0.30	17.8	
CS	T1-025-C	T1	Center	5/2/2022	22	2	22	0.17	3.8	
CS	T1-025-T	T1	Trough	5/2/2022	50	1	48	0.26	12.3	
CS	T1-050-C	T1	Center	5/2/2022	37	2	32	0.24	7.7	
CS	T1-050-T	T1	Trough	5/2/2022	61	1	58	0.29	16.5	
CS	T1-100-C	T1	Center	5/2/2022	26	2	28	0.25	6.9	
CS	T1-100-T	T1	Trough	5/2/2022	48	2	50	0.27	13.3	
CS	T1-200-C	T1	Center	5/2/2022	39	3	40	0.23	9.0	
CS	T1-200-T	T1	Trough	5/2/2022	58	4	69	0.29	20.2	Plot is iced at bottom of snowpack
CS	T2-005-C	T2	Center	5/1/2022	46	2	46	0.34	15.6	
CS	T2-005-T	T2	Trough	5/1/2022	68	3	70	0.43	30.3	
CS	T2-010-C	T2	Center	5/1/2022	28	13*	28	0.30	8.5	
CS	T2-010-T	T2	Trough	5/1/2022	58	2	61	0.33	20.3	
CS	T2-025-C	T2	Center	5/1/2022	17	2	27	0.27	7.2	
CS	T2-025-T	T2	Trough	5/1/2022	57	2	58	0.31	17.7	
CS	T2-050-C	T2	Center	5/1/2022	3	3	6	0.29	1.8	25% snow free, 2 photos
CS	T2-050-T	T2	Trough	5/1/2022	38	3	43	0.25	10.8	Plot is iced at bottom of snowpack
CS	T2-100-C	T2	Center	5/1/2022	32	2	28	0.20	5.5	
CS	T2-100-T	T2	Trough	5/1/2022	58	2	55	0.29	15.9	Plot is iced at bottom of snowpack
CS	T2-200-C	T2	Center	5/1/2022	18	2	17	0.13	2.2	
CS	T2-200-T	T2	Trough	5/1/2022	49	4	50	0.25	12.6	Plot is iced at bottom of snowpack
AS	T3-005-C	T3	Center	5/2/2022	109	1	n.d.	n.d.	n.d.	
AS	T3-005-T	T3	Trough	5/2/2022	165	5*	n.d.	n.d.	n.d.	Avalanche probe used to measure depth
AS	T3-010-C	T3	Center	5/2/2022	82	2	n.d.	n.d.	n.d.	
AS	T3-010-T	T3	Trough	5/2/2022	79	4	n.d.	n.d.	n.d.	
AS	T3-025-C	T3	Center	5/2/2022	21	3	n.d.	n.d.	n.d.	
AS	T3-025-T	T3	Trough	5/2/2022	78	3	n.d.	n.d.	n.d.	

Table A10.1 *(continued)*

Site	Plot ID	Tran-sect	Surface feature	Date	Snow depth Mean (cm)	Snow depth S.D. (cm)	Core depth (cm)	Snow density (g/cm³)	SWE (cm)	Field notes
AS	T3-050-C	T3	Center	5/2/2022	29	3	n.d.	n.d.	n.d.	
AS	T3-050-T	T3	Trough	5/2/2022	62	2	n.d.	n.d.	n.d.	
AS	T3-100-C	T3	Center	5/2/2022	22	2	n.d.	n.d.	n.d.	
AS	T3-100-T	T3	Trough	5/2/2022	80	1	n.d.	n.d.	n.d.	
AS	T4-005-C	T4	Center	5/2/2022	109	1	n.d.	n.d.	n.d.	
AS	T4-005-T	T4	Trough	5/2/2022	111	1	n.d.	n.d.	n.d.	
AS	T4-010-C	T4	Center	5/2/2022	75	1	n.d.	n.d.	n.d.	
AS	T4-010-T	T4	Trough	5/2/2022	83	0	n.d.	n.d.	n.d.	
AS	T4-025-C	T4	Center	5/2/2022	52	6*	n.d.	n.d.	n.d.	
AS	T4-025-T	T4	Trough	5/2/2022	65	1	n.d.	n.d.	n.d.	
AS	T4-050-C	T4	Center	5/2/2022	58	3	n.d.	n.d.	n.d.	
AS	T4-050-T	T4	Trough	5/2/2022	75	2	n.d.	n.d.	n.d.	
AS	T4-100-C	T4	Center	5/2/2022	38	1	n.d.	n.d.	n.d.	
AS	T4-100-T	T4	Trough	5/2/2022	37	2	n.d.	n.d.	n.d.	
AS	T5-025-C	T5	Center	5/2/2022	45	2	n.d.	n.d.	n.d.	
AS	T5-025-T	T5	Trough	5/2/2022	50	2	n.d.	n.d.	n.d.	
AS	T5-050-C	T5	Center	5/2/2022	31	1	n.d.	n.d.	n.d.	
AS	T5-050-T-A	T5	Trough	5/2/2022	34	3	n.d.	n.d.	n.d.	Only 1 stake for T5-050-T (no A and B)
AS	T5-050-T-B	T5	Trough	5/2/2022	n.d.	n.d.	n.d.	n.d.	n.d.	
AS	T5-100-C	T5	Center	5/2/2022	34	2	n.d.	n.d.	n.d.	
AS	T5-100-T	T5	Trough	5/2/2022	55	1	n.d.	n.d.	n.d.	

APPENDIX 11 Ground temperature loggers

Table A11.1. *Placement of ground temperature loggers, NIRPO and Jorgenson sites, Prudhoe Bay, August 2022.* ***Plot ID:*** *Two digit prefix indicates year plot was installed; A denotes aquatic plot.* ***Location:*** *T6-T9: NIRPO transects; JSA: Jorgenson aquatic plots; Pingo: Lemming pingo; Lakes: aquatic plots in vicinity of Lemming pingo.* ***Veg type:*** *See Table A2.2 for vegetation type codes and moisture gradient.* ***iBtn ID:*** *Temporary assigned ID number.* ***Stake ID:*** *Stake number or type.* ***Depth****: Distance from soil surface.* ***Serial no.****: Permanent factory ID.*

Plot ID	Loca-tion	Veg type	iBtn ID	Stake ID	Depth (cm)	Serial no.
21-01	T8	M2	144	16	0	CA0000003A59C621
21-01	T8	M2	194	16	-15	320000003A5CB021
21-01	T8	M2	259	16	-40	110000003A2D8221
21-02	T8	M2	166	17	0	080000003A2FE121
21-02	T8	M2	190	17	-15	FA0000003A1C1C21
21-02	T8	M2	265	17	-40	6D00000039EFEB21
21-03	T8	M4	192	18	0	F10000003A0D5621
21-03	T8	M4	105	18	-15	9100000036118321
21-03	T8	M4	273	18	-40	9F00000039FF3621
21-04	T8	M4	196	19	0	A40000003A084221
21-04	T8	M4	253	19	-15	C60000003A082A21
21-04	T8	M4	103	19	-40	C6000000360DDC21
21-05	T6	U3	239	24	0	3E0000003A1CCC21
21-05	T6	U3	125	24	-15	910000003613B121
21-05	T6	U3	136	24	-40	0200000039DCC521
21-09	T6	U4	177	22	0	A30000003A4EB221
21-09	T6	U4	129	22	-15	2A00000036126721
21-09	T6	U4	142	22	-40	CE00000039DF7221
21-11	T6	M2	209	23	0	570000003A5A3E21
21-11	T6	M2	120	23	-15	BA000000360C4C21
21-11	T6	M2	181	23	-40	120000003A367E21
21-16	T6	M2	261	25	0	6E0000003A08EB21
21-16	T6	M2	127	25	-15	1100000036131520
21-16	T6	M2	152	25	-40	480000003A254921
21-17	T8	U4	199	20	0	4E00000039DFD621
21-17	T8	U4	119	20	-15	7100000036127721
21-17	T8	U4	272	20	-40	A70000003A4CA621
21-21	T9	U3	242	10	0	680000003A2BFE21
21-21	T9	U3	210	10	-15	E70000003A579E21
21-21	T9	U3	169	10	-40	5B0000003A5C0221
21-23	T9	M2	175	21	0	AC0000003A04A221
21-23	T9	M2	126	21	-15	2B00000036098821
21-23	T9	M2	178	21	-40	F20000003A149821
21-28	T7	U4	180	26	0	110000003A387621
21-28	T7	U4	117	26	-15	D500000036182621
21-28	T7	U4	160	26	-40	F30000003A493721
21-29	T7	M2	111	28	0	D7000000361B1E21
21-29	T7	M2	110	28	-15	53000000360F7121
21-29	T7	M2	130	28	-40	350000003A187221
21-31	T7	M4/E1	227	30	0	B100000039EDDD21
21-31	T7	M4/E1	141	30	-15	1B0000003A148E21
21-31	T7	M4/E1	172	30	-40	190000003A1D4C21
21-34	T7	U4	122	29	0	1E0000003613E921
21-34	T7	U4	108	29	-15	1D000000361BB721
21-34	T7	U4	158	29	-40	9C00000039F8EF21
21-35	T7	M4/E1	146	27	0	EA0000003A59EF21
21-35	T7	M4/E1	112	27	-15	520000003608BB21
21-35	T7	M4/E1	163	27	-40	160000003A1F8221
21A-02	JSA	Em	222	3	0	FC0000003A257A21
21A-02	JSA	Em	207	3	-15	060000003A2E8121
21A-02	JSA	Em	184	3	-40	4A0000003A2D9221
21A-03	JSA	Ef	241	31	0	2E0000003A183021
21A-03	JSA	Ef	97	31	-15	2300000036033E21
21A-03	JSA	Ef	174	31	-40	310000003A0CB921
21A-14	JSA	Es	153	35	-40	5100000039DC9921
21A-15	JSA	Em	215	33	0	DA0000003A0BF321
21A-15	JSA	Em	200	33	-15	E60000003A199321
21A-15	JSA	Em	145	33	-40	A50000003A200421
21A-18	JSA	Em	263	32	0	ED0000003A2DAF21
21A-18	JSA	Em	155	32	-15	980000003A569821
21A-18	JSA	Em	134	32	-40	300000003A1E8721
21A-26	T6A	Em	264	7	0	FA0000003A3A4121
21A-26	T6A	Em	254	7	-15	570000003A5B2721
21A-26	T6a	Em	157	7	-40	B50000003A322721
21A-27	T6A	Es	138	34	-40	8C00000039E54B21
21A-28	T6A	Ef	248	6	0	2600000039E93521
21A-28	T6A	Ef	244	6	-15	1400000039D5B921
21A-28	T6A	Ef	147	6	-40	1D00000039E93521
22-01	Pingo	B1	246	1	0	8200000039ECE321
22-01	Pingo	B1	165	1	-15	D50000003A2D5221
22-01	Pingo	B1	235	1	-40	5D0000003A2E9121
22-02	Pingo	B1	203	2	0	DD0000003A121B21
22-02	Pingo	B1	173	2	-15	7E0000003A377621
22-02	Pingo	B1	257	2	-40	3C0000003A517C21
22-04	Pingo	B2	228	4	0	730000003A190C21
22-04	Pingo	B2	188	4	-15	780000003A23AE21
22-04	Pingo	B2	218	4	-40	D60000003A149721
22-05	Pingo	AIR	229	snow	~ 100	080000003A006D21
22-05	Pingo	B2	232	5	0	DC0000003A4C9F21
22-05	Pingo	B2	135	5	-15	140000003A0F1821
22-05	Pingo	B2	237	5	-40	AD0000003A227A21
22-08	Lakes	E1	230	8	0	D40000003A1E7E21
22-08	Lakes	E1	167	8	-15	E70000003A378321
22-08	Lakes	E1	267	8	-40	CF00000039E6A421
22-09	Lakes	E1	240	9	0	510000003A359121
22-09	Lakes	E1	168	9	-15	270000003A377521
22-09	Lakes	E1	204	9	-40	A90000003A148821
22-11	Lakes	E2	245	11	0	910000003A364C21
22-11	Lakes	E2	170	11	-15	0B0000003A141621
22-11	Lakes	E2	217	11	-40	D00000003A3A3721
22-12	Lakes	E2	268	12	0	6200000039EB7321
22-12	Lakes	E2	182	12	-15	1F0000003A004521
22-12	Lakes	E2	220	12	-40	D800000039E1C321
22-13	Pingo	AIR	225	snow	~ 100	700000003A127921
22-13	Pingo	U10	176	13	0	0B0000003A258D21
22-13	Pingo	U10	185	13	-15	0C0000003A3C6521
22-13	Pingo	U10	223	13	-40	480000003A0EA121
22-14	Pingo	U6	149	14	0	AE0000003A40C321
22-14	Pingo	U6	186	14	-15	640000003A2EE921
22-14	Pingo	U6	252	14	-40	E40000003A40CE21
22-15	T8	U10	161	15	0	550000003A227121
22-15	T8	U10	187	15	-15	D80000003A2DBD21
22-15	T8	U10	256	15	-40	5C00000039DE4421

APPENDIX 12 Thaw and water depths

Table A12.1. *Thaw depth and water depth at permanent vegeation plots, NIRPO, Jorgenson, Colleen and Airport sites, Prudhoe Bay, 27-29 August 2022. Measurements taken using small-diameter metal thaw probes and wooden meter sticks.* ***Site:*** *Natual Ice-rich Permafrost Observatory (NIRPO), Jorgenson (JS), Colleen (CS), Airport (AS).* ***Location:*** *Terrestrial plot transects (T1-T9); aquatic plots on transect T6 (T6A); Jorgenson aquatic plots (JSA); NIRPO Lemming pingo plots (pingo); NIRPO aquatic plots in vicinity of Lemming pingo (lake).* ***Veg type 2022:*** *See Table A2.2 for vegetation type codes.*

Site	Year surveyed	Plot ID	Location	Veg type 2022	Thaw depth (cm) 27–29 Aug 2022		Water depth (cm) 27–29 Aug 2022	
					Mean	S.D.	Mean	S.D.
NIRPO	2022	22-01	pingo	B1	120	5.7	0.0	0.0
NIRPO	2022	22-02	pingo	B1	120	1.0	0.0	0.0
NIRPO	2022	22-03	pingo	B1	99	6.4	0.0	0.0
NIRPO	2022	22-04	pingo	B2	73	14.4	0.0	0.0
NIRPO	2022	22-05	pingo	B2	94	8.3	0.0	0.0
NIRPO	2022	22-06	pingo	B2	87	3.9	0.0	0.0
NIRPO	2022	22-07	lake	E1	56	0.9	9.2	0.8
NIRPO	2022	22-08	lake	E1	37	5.4	17.4	3.1
NIRPO	2022	22-09	lake	E1	45	7.0	22.4	2.8
NIRPO	2022	22-10	lake	E2	45	2.5	47.8	4.1
NIRPO	2022	22-11	lake	E2	42	3.5	33.6	2.9
NIRPO	2022	22-12	lake	E2	37	2.9	33.8	4.9
NIRPO	2022	22-13	pingo	U10	58	11.2	0.0	0.0
NIRPO	2022	22-14	pingo	U6	99	4.2	0.0	0.0
NIRPO	2022	22-15	T8	U10	34	5.2	0.0	0.0
NIRPO	2021	21-01	T8	M2	43	2.1	2.2	2.2
NIRPO	2021	21-02	T8	M2	51	1.6	1.6	0.9
NIRPO	2021	21-03	T8	M4	46	1.1	11.2	1.3
NIRPO	2021	21-04	T8	M4	45	0.9	11.4	0.9
NIRPO	2021	21-05	T6	U3	54	1.5	0.0	0.0
NIRPO	2021	21-06	T6	U3	49	2.0	0.0	0.0
NIRPO	2021	21-07	T6	U4	48	1.5	0.0	0.0
NIRPO	2021	21-08	T6	U4	48	1.6	0.0	0.0
NIRPO	2021	21-09	T6	U4	53	0.8	0.0	0.0
NIRPO	2021	21-10	T6	U3	44	1.8	0.0	0.0
NIRPO	2021	21-11	T6	M2	53	0.8	2.4	1.7
NIRPO	2021	21-12	T6	U4	49	1.5	0.0	0.0
NIRPO	2021	21-13	T6	U4	53	2.6	0.0	0.0
NIRPO	2021	21-14	T6	M2	55	1.4	7.4	1.1
NIRPO	2021	21-15	T6	U4	44	3.6	0.0	0.0
NIRPO	2021	21-16	T6	M2	56	3.0	5.4	1.7
NIRPO	2021	21-17	T8	U4	46	2.9	0.0	0.0
NIRPO	2021	21-18	T8	U4	41	1.1	0.0	0.0
NIRPO	2021	21-19	T9	M2	53	0.5	1.7	1.0
NIRPO	2021	21-20	T9	U3	42	1.4	0.0	0.0
NIRPO	2021	21-21	T9	U3	43	1.3	0.0	0.0
NIRPO	2021	21-22	T9	U3	39	1.3	0.0	0.0
NIRPO	2021	21-23	T9	M2	51	2.8	0.8	1.1
NIRPO	2021	21-24	T9	U3	48	1.9	0.0	0.0
NIRPO	2021	21-25	T7	M4/Marl	56	1.1	0.5	0.5
NIRPO	2021	21-26	T7	M4/Marl	60	1.3	1.0	0.0
NIRPO	2021	21-27	T7	M2	59	0.9	0.3	0.4
NIRPO	2021	21-28	T7	M4	59	0.8	8.0	0.7
NIRPO	2021	21-29	T7	M2	63	3.6	3.2	1.3
NIRPO	2021	21-30	T7	U4	52	3.0	0.0	0.0
NIRPO	2021	21-31	T7	M4/E1	64	1.3	19.8	1.9
NIRPO	2021	21-32	T7	M4	55	3.1	10.0	2.0
NIRPO	2021	21-33	T7	M4	71	1.3	9.0	2.6
NIRPO	2021	21-34	T7	U4	50	1.6	0.0	0.0
NIRPO	2021	21-35	T7	M4/E1	68	1.3	20.4	3.1
NIRPO	2021	21A-21	T6A	Em	33	2.5	42.2	2.2
NIRPO	2021	21A-22	T6A	Ef	42	7.9	56.6	2.1
NIRPO	2021	21A-23	T6A	Em	39	7.3	55.0	6.0
NIRPO	2021	21A-24	T6A	Es	53	2.4	59.6	7.5
NIRPO	2021	21A-25	T6A	Ef	47	0.8	58.4	1.1
NIRPO	2021	21A-26	T6A	Em	27	3.2	60.2	3.5
NIRPO	2021	21A-27	T6A	Es	37	8.9	64.6	8.6
NIRPO	2021	21A-28	T6A	Ef	44	6.0	39.2	5.8
NIRPO	2021	21A-29	T6A	Em	43	6.8	45.2	3.8
NIRPO	2021	21A-30	T6A	Es	53	2.2	48.8	6.1
NIRPO	2021	21A-31	T6A	Es	48	3.7	44.6	6.5
NIRPO	2021	21A-32	T6A	Em	27	3.8	49.0	4.6
NIRPO	2021	21A-33	T6A	Em	38	6.1	31.8	5.4
NIRPO	2021	21A-34	T6A	Em	29	6.2	59.6	6.4
NIRPO	2021	21A-35	T6A	Es	47	3.6	52.4	5.0
NIRPO	2021	21A-36	T6A	Em	40	1.3	34.2	2.8

Table A12.1 (*continued*)

Site	Year surveyed	Plot ID	Location	Veg type 2022	Thaw depth (cm) 27–29 Aug 2022 Mean	Thaw depth (cm) 27–29 Aug 2022 S.D.	Water depth (cm) 27–29 Aug 2022 Mean	Water depth (cm) 27–29 Aug 2022 S.D.
NIRPO	2021	21A-37	T6A	Em	40	2.0	53.0	3.5
NIRPO	2021	21A-38	T6A	Es	43	6.3	61.8	8.7
NIRPO	2021	21A-39	T6A	Em	40	3.5	38.4	2.3
NIRPO	2021	21A-40	T6A	Ef	37	7.0	61.4	9.1
JS	2021	21A-01	JSA	Em	32	7.4	55.6	9.0
JS	2021	21A-02	JSA	Em	20	9.6	66.8	9.8
JS	2021	21A-03	JSA	Ef	45	6.2	61.8	5.9
JS	2021	21A-04	JSA	Em	46	2.1	75.2	2.9
JS	2021	21A-05	JSA	Em	23	14.3	59.0	4.4
JS	2021	21A-06	JSA	Em	36	3.5	62.0	2.9
JS	2021	21A-07	JSA	Ef	46	3.5	61.8	6.5
JS	2021	21A-08	JSA	Em	45	2.6	59.6	3.2
JS	2021	21A-09	JSA	Em	50	4.4	48.6	1.7
JS	2021	21A-10	JSA	Em	32	6.0	93.6	11.2
JS	2021	21A-11	JSA	Em	35	2.1	55.0	7.0
JS	2021	21A-12	JSA	Es	32	5.5	75.2	3.2
JS	2021	21A-13	JSA	Ef	24	4.1	83.2	7.4
JS	2021	21A-14	JSA	Es	31	7.4	81.0	6.0
JS	2021	21A-15	JSA	Em	25	4.0	78.0	6.0
JS	2021	21A-16	JSA	Es	45	5.7	58.0	12.5
JS	2021	21A-17	JSA	Es	38	5.0	65.0	8.9
JS	2021	21A-18	JSA	Em	34	2.9	67.4	2.5
JS	2021	21A-19	JSA	Es	28	2.3	73.0	3.7
CS	2014	T1-005-C	T1	M2d	66	1.3	0.0	0.0
CS	2014	T1-005-T	T1	M2d	52	3.4	0.0	0.0
CS	2014	T1-010-C	T1	M2d	60	2.2	0.0	0.0
CS	2014	T1-010-T	T1	M2d	52	6.1	3.0	3.1
CS	2014	T1-025-C	T1	U4d	60	2.2	0.0	0.0
CS	2014	T1-025-T	T1	M2d	50	1.8	15.2	1.6
CS	2014	T1-050-C	T1	M2d	59	1.8	0.0	0.0
CS	2014	T1-050-T	T1	E3d	34	17.4	34.2	5.1
CS	2014	T1-100-C	T1	M2d	54	1.3	0.0	0.0
CS	2014	T1-100-T	T1	E1d	44	4.5	12.4	4.7
CS	2014	T1-200-C	T1	U4d/M2d?	57	2.1	0.0	0.0
CS	2014	T1-200-T	T1	E1	41	5.9	29.4	5.7
CS	2014	T2-005-C	T2	M10d	80	2.5	0.0	0.0
CS	2014	T2-005-T	T2	E1d	69	1.3	3.6	3.0
CS	2014	T2-010-C	T2	M2d	66	1.5	0.0	0.0
CS	2014	T2-010-T	T2	E1d	53	12.9	61.6	7.1
CS	2014	T2-025-C	T2	M2d	61	2.5	0.0	0.0
CS	2014	T2-025-T	T2	E6d	62	4.2	43.6	6.9
CS	2014	T2-050-C	T2	U4d	51	3.3	0.0	0.0
CS	2014	T2-050-T	T2	E1/E6d	51	5.0	29.0	10.4
CS	2014	T2-100-C	T2	M2d	47	1.8	0.0	0.0
CS	2014	T2-100-T	T2	E1d	57	1.3	31.4	14.0
CS	2014	T2-200-C	T2	U4d	43	0.8	0.0	0.0
CS	2014	T2-200-T	T2	M2d	44	2.8	3.8	3.8
AS	2015	T3-5-C	T3	Barren	101	12.0	0.0	0.0
AS	2015	T3-5-T	T3	Barren	102	11.1	0.0	0.0
AS	2015	T3-10-C	T3	B16	70	1.5	0.0	0.0
AS	2015	T3-10-T	T3	W1	48	2.3	75.8	6.6
AS	2015	T3-25-C	T3	B17	62	1.2	0.0	0.0
AS	2015	T3-25-T	T3	M2d	60	6.5	10.1	10.3
AS	2015	T3-50-C	T3	M2d	55	1.2	0.0	0.0
AS	2015	T3-50-T	T3	E1d	48	5.5	28.4	13.7
AS	2015	T3-100-C	T3	U17	62	2.2	0.0	0.0
AS	2015	T3-100-T	T3	E1d	48	1.9	34.6	3.8
AS	2015	T4-5-C	T4	E1d	70	2.9	34.2	6.1
AS	2015	T4-5-T	T4	E1d	60	1.9	68.2	8.6
AS	2015	T4-10-C	T4	E1d	62	3.6	33.6	3.7
AS	2015	T4-10-T	T4	W1	70	7.0	93.6	7.8
AS	2015	T4-25-C	T4	E1d	110	2.1	27.3	1.2
AS	2015	T4-25-T	T4	W1	31	2.8	102.5	3.5
AS	2015	T4-50-C	T4	E1d	67	2.5	35.2	6.0
AS	2015	T4-50-T	T4	E1d	48	2.3	50.6	0.9
AS	2015	T4-100-C	T4	M4d	48	1.1	27.2	1.9
AS	2015	T4-100-T	T4	E1d	46	3.5	37.0	1.0
AS	2015	T5-25-C	T5	M2	62	0.8	0.0	0.0
AS	2015	T5-25-T	T5	M4d	51	3.5	5.5	5.9
AS	2015	T5-50-C	T5	M2d	52	2.2	0.0	0.0
AS	2015	T5-50-T	T5	M2d	49	6.8	4.0	5.5
AS	2015	T5-100-C	T5	M2d	55	0.8	0.0	0.0
AS	2015	T5-100-T	T5	E1d	40	3.4	19.4	2.9

APPENDIX 13 Trace gas fluxes

Table 13.1. *Sampling dates of trace-gas flux measurements, NIRPO and Colleen sites, Prudhoe Bay, July 2021 to November 2022.* ***Site:*** *Natural Ice-rich Permafrost Observatory (NIRPO), Colleen (CS). Net ecosystem exchange (NEE), gross ecosystem productivity (GEP), and ecosystem respiration (ER) were derived fom CO_2 and CH_4 fluxes measured in summer 2021 and 2022. Ecosystem respiration (ER) was derived from from the CO_2 concentration below the snow pack and from snow depth, snow density, and snow and air temperature measured in late and early winter 2022. See Section 2.5 Greenhouse Gas Fluxes for a summary of methods and results.*

		Mid-summer 2021			Late-winter 2022		Mid-summer 2022				Early-winter 2022	
Site	**Plot ID**	**July 16**	**July 18**	**July 18**	**Apr 30**	**May 1**	**Jul 15**	**Jul 16**	**Jul 17**	**Jul 18**	**Nov 28**	**Nov 29**
NIRPO	21-01	X			X							X
NIRPO	21-01B	X			X							X
NIRPO	21-02	X			X							X
NIRPO	21-03	X			X							X
NIRPO	21-04	X			X							X
NIRPO	21-04B	X			X							X
NIRPO	21-05		X		X							X
NIRPO	21-06		X		X							X
NIRPO	21-07		X		X							X
NIRPO	21-08		X		X							X
NIRPO	21-09			X	X							X
NIRPO	21-10			X	X							X
NIRPO	21-11			X	X							X
NIRPO	21-12			X	X							X
NIRPO	21-13		X		X							X
NIRPO	21-14		X		X							X
NIRPO	21-15		X		X							X
NIRPO	21-16		X		X							X
NIRPO	21-28			X	X							X
NIRPO	21-28B			X	X							X
NIRPO	21-30			X	X							X
NIRPO	21-30B			X	X							X
NIRPO	21-31			X	X							X
NIRPO	21-32			X	X							X
NIRPO	21-33			X	X							X
NIRPO	21-34			X	X							X
NIRPO	21-35			X	X							X
CS	T1-5-C					X		X			X	
CS	T1-5-T					X		X			X	
CS	T1-10-C					X		X			X	
CS	T1-10-T					X		X			X	
CS	T1-25-C					X				X	X	
CS	T1-25-T					X			X		X	
CS	T1-50-C					X			X		X	
CS	T1-50-T					X			X		X	
CS	T1-100-C					X			X		X	
CS	T1-100-T					X			X		X	
CS	T1-200-C					X			X		X	
CS	T1-200-T					X			X		X	
CS	T2-5-C					X		X			X	
CS	T2-5-T					X		X			X	
CS	T2-10-C					X			X		X	
CS	T2-10-T					X	X				X	
CS	T2-25-C					X	X				X	
CS	T2-25-T					X	X				X	
CS	T2-50-C					X	X				X	
CS	T2-50-T					X	X				X	
CS	T2-100-C					X	X				X	
CS	T2-100-T					X	X				X	
CS	T2-200-C					X	X				X	
CS	T2-200-T					X	X				X	

APPENDIX 14 Permafrost boreholes

Table A14.1. *Thicknesses of frozen protective layers above massive-ice bodies in thermokarst ponds, Transect 6, NIRPO site, Prudhoe Bay, August-September 2021 and 2022.* ***Water depth and Thaw depth (ALT)****: Measured at the borehole location (ALT = active-layer thickness).* ***Transient layer (TL), Intermediate layer (IL), Depth to massive ice, and TL+IL (PL2):*** *Measured on core samples.*

Borehole ID	Plot ID	Date	Borehole depth (cm)	Water depth (cm)	Thaw depth (ALT) (cm)	Transient layer (TL) (cm)	Intermediate layer (IL) (PL3) (cm)	Depth to massive ice (cm)	TL+IL (PL2) (cm)	Notes and results
T6-21A-31	21A-31	8/31/2021	99	45	49	5	7	61	12	1.8 m S of 21A-31
T6-21A-29	21A-29	8/31/2021	95	46	50	6	0	56	6	1.5 m NW of 21A-29
T6-21A-39	21A-39	8/31/2021	82	39	46	6	0	52	6	1.6 m W of 21A-39
T6-21A-37	21A-37	8/31/2021	97	46	48	0	4	52	4	1.5 m N of 21A-37
T6-21A-36	21A-36	8/31/2021	79	45	41	6	9	56	15	1.6 m N of 21A-36
T6-21A-35&34	21A-35,-34	9/1/2021	90	55	42	8	13	63	21	Between 21A-35 and 21A-34
T6-21A-33	21A-33	9/1/2021	89	35	41	0	0	41	0	1.6 m E of 21A-33; actively degrading ice wedge; fresh cracks around the pond
T6-21A-32	21A-32	9/1/2021	77	30	45	6	7	58	13	1.6 m W of 21A-32
T6-21A-26&27	21A-26,-27	8/26/2022	69	55	41	8	7	56	15	Between 21A-26 and 21A-27, aquatic moss
T6-21A-25	21A-25	8/26/2022	71	57	45	8	3	56	11	1.2 m W of 21A-25; aquatic moss; 45-56 cm destroyed and/or lost core
T6-21A-25A (excl.)	21A-25	8/26/2022	77	56	47	7	3	57	10	0.3 m W of 21A-25 borehole; aquatic moss; 57-65 cm ice-wedge boundary, soil from 65 cm
T6-21A-22	21A-22	8/26/2022	80	47	53	7	3	63	10	1.2 m S of 21A-22; aquatic moss
T6-21A-23&24	21A-23,-24	8/26/2022	66	61	39	12	3	54	15	Between 21A-23 and 21A-24; some aquatic moss
T6-21A-28	21A-28	8/26/2022	71	41	41	6	11	58	17	1.0 m E of 21A-28; aquatic moss; 41-43 cm destroyed
T6-21A-30	21A-30	8/26/2022	83	55	48	8	0	56	8	1.2 m W of 21A-30; no aquatic moss. (See 21A-29, in the same pond)
T6-21A-38	21A-38	8/26/2022	74	51	47	3	0	50	3	1.3 m E of 21A-38; no aquatic moss
T6-21A-21	21A-21	8/27/2022	73	35	41	7	13	61	20	1.2 m E of 21A-21; very thick aquatic moss; 41-44 cm destroyed
T6-21A-40	21A-40	8/27/2022	73	52	46	9	0	55	9	1.2 m E of 21A-40; some aquatic moss; 46-54 cm destroyed (gravel)
Mean (n=8)		**2021**	**88.5**	**42.6**	**45.3**	**4.6**	**5**	**54.9**	**9.6**	**Only one ice wedge (T6-21A-33) was degrading in 2021**
Mean (n=9)		**2022**	**73.3**	**50.4**	**44.6**	**7.6**	**4.4**	**56.6**	**12**	**No degrading ice wedges in 2022; T6-21A-25A excluded from analysis.**
Mean (n=17)		**2021-2022**	**80.5**	**46.8**	**44.9**	**6.2**	**4.7**	**55.8**	**10.9**	**One ice wedge was degrading in 2021; six ice wedges were vulnerable in 2021-2022 (PL2<10 cm). T6-21A-25A excluded from analysis.**

Table A14.2. *Thicknesses of frozen protective layers above massive-ice bodies in thermokarst ponds, Jorgenson site, Prudhoe Bay, July 2019, September 2021, and August 2022.* ***Water depth and Thaw depth (ALT)****: Measured at the borehole location (ALT = active-layer thickness).* ***Transient layer (TL), Intermediate layer (IL), Depth to massive ice, and TL+IL (PL2):*** *Measured on core samples.*

Borehole ID	Plot ID	Date	Borehole depth (cm)	Water depth (cm)	Thaw depth (ALT) (cm)	Transient layer (TL) (cm)	Intermediate layer (IL) (PL3) (cm)	Depth to massive ice (cm)	TL+IL (PL2) (cm)	Notes and results
DA2/19	21A-08	7/11/2019	117	42	40		10	98		Significant stabilization since 2011 (probably slightly different locations of 2011 and 2019 boreholes)
DA3/19	21A-06	7/11/2019	93	49	34		0	66		Stabilization since 2011
DA1/19	21A-14	7/11/2019	90	65	33		4	58		Stabilization since 2011
SI3/19	21A-10	7/11/2019	85	65	35		0	50		Degradation since 2011 (new deep pond); this ice wedge was vulnerable in 2019
SI5/19	21A-11	7/13/2019	82	20	42		3	60		Some degradation (indicated by deeper pond) and then some stabilization since 2012
JS-21A-01	21A-01	9/3/2021	81	49	49	7	1	58	8	1.5 m NW of 21A-01
JS-21A-02	21A-02	9/3/2021	76	49	46	9	0	55	9	1.6 m S of 21A-02
JS-21A-03	21A-03	9/3/2021	71	63	46	13	0	59	13	1.6 m E of 21A-03
JS-21A-15	21A-15	9/3/2021	81	34	54	6	0	60	6	1.5 m E of 21A-15
JS-21A-05	21A-05	8/27/2022	71	47	38	8	21	67	29	1.2 m N of 21A-05; thick aquatic moss
JS-21A-09	21A-09	8/27/2022	77	52	46	3	0	49	3	1.2 m S of 21A-09
JS-21A-12	21A-12	8/28/2022	72	60	42	5	2	49	7	Between 21A-12 and 21A-11; similar to 21A-12, not much vegetation
JS-21A-13	21A-13	8/28/2022	61	63	39	10	3	52	13	1.0 m N of 21A-13; not much vegetation; TCI from 52
JS-21A-18&19	21A-18,-19	8/28/2022	73	59	40	9	0	49	9	Between 21A-18 and 21A-19; average conditions, vegetation
JS-21A-07	21A-07	8/28/2022	74	60	44	8	8	60	16	1.2 m N of 21A-07, between 21A-07 and 21A-06; thick aquatic moss
JS-21A-04	21A-04	8/28/2022	65	62	39	9	17	>65	>26	1.4 m E of 21A-04; aquatic moss; refusal at 65 cm (gravel)
JS-21A-17	21A-17	8/29/2022	80	52	55	8	0	63	8	1.2 m S of 21A-17; aquatic moss; active layer (AL) mostly mineral
JS-21A-16	21A-16	8/29/2022	76	49	52	5	4	61	9	1.2 m S of 21A-16; bare bottom; gravel at 76 cm (ice-wedge boundary)
Mean (n=4)		**2019**	**87.5**	**49.8**	**36**	**?**	**1.8**	**58.5**	**?**	**DA2 excluded from analysis; only one ice wedge (SI3/19, pond 21A-10) was vulnerable in 2019**
Mean (n=4)		**2021**	**77.3**	**48.8**	**48.8**	**8.8**	**0.3**	**58**	**9**	**No degrading ice wedges in 2021**
Mean (n=9)		**2022**	**72.1**	**56**	**43.9**	**7.2**	**6.1**	**57.2**	**13.3**	**No degrading ice wedges in 2022**
Mean (n=13)		**2021-2022**	**73.7**	**53.8**	**45.4**	**7.7**	**4.3**	**57.5**	**12**	**No degrading ice wedges in 2021 and 2022**

Table A14.3. *Thicknesses of frozen protective layers above massive-ice bodies in thermokarst ponds, Transect 2, Colleen site, Prudhoe Bay, 29-30 August 2022 and comparison with 10-14 August 2014 cores.* ***Water depth and Thaw depth (ALT):*** *Measured at the borehole location (ALT = active-layer thickness).* ***Transient layer (TL), Intermediate layer (IL), Depth to massive ice, and TL+IL (PL2):*** *Measured on core samples.*

Borehole ID	Date	Borehole depth (cm)	Water depth (cm)	Thaw depth (ALT) (cm)	Transient layer (TL) (cm)	Intermediate layer (IL) (PL3) (cm)	Depth to massive ice (cm)	TL+IL (PL2) (cm)	Notes and results
T2-10T-1	8/10/2014	89	0	53	6	7	66	13	1.0 m W of T2-10T-1; no significant changes since 2914; no clear TL/IL boundary
T2-10T-1/22	8/29/2022	73	18	55	6	4	65	10	
T2-25T-1	8/10/2014	102	35	45	0	19	64	19	0.6 m N of T2-25T-1; refusal at 67 cm (gravel); no significant changes
T2-25T-1/22	8/29/2022	67	43	52	4	11	>67	>15	
T2-50T-1	8/11/2014	77		48	10	1	59	11	0.6 m N of T2-50T-1; refusal at 64 cm (gravel); some stabilization
T2-50T-1/22	8/29/2022	64	0	51	0	13	>64	>13	
T2-50T-3	8/11/2014	68	35	46	8	2	56	10	1.0 m W of T2-50T-3; no clear TL/IL boundary; aquatic vegetation; some stabilization since 2014
T2-50T-3/22	8/29/2022	73	33	50	8	8	66	16	
T2-100T-1	8/11/2014	65	8	43	8	6	57	14	0.6 m N of T2-100T-1; no clear TL/IL boundary; no significant changes
T2-100T-1/22	8/29/2022	71	19	42	11	5	58	16	
T2-200T-1	8/12/2014	49	70	28	8	0	36	8	0.6 m W of T2-200T-1; aquatic vegetation; some stabilization since 2014
T2-200T-1/22	8/30/2022	75	60	48	7	7	62	14	
T2-200T-3	8/12/2014	98		68	0	5	73	5	0.6 m S of T2-200T-3; refusal (gravel) at 71 cm; no clear TL/IL boundary; some stabilization since 2014
T2-200T-3/22	8/30/2022	71		54	8	8	>71	16	
T2-200T-4	8/12/2014	92		55	0	5	60	5	0.6 m S of T2-200T-4, some stabilization since 2014, no clear TL/IL boundary
T2-200T-4/22	8/30/2022	71		45	5	11	61	16	
T2-200T-8	8/13/2014	75	27	44	5	0	49	5	0.6 m N of T2-200T-8, aquatic vegetation, some degradation since 2014, then stabilization
T2-200T-8/22	8/30/2022	71	44	45	4	9	58	13	
Mean (n=9)	**2014**	**79**	**29.2**	**47.8**	**5**	**5**	**57.8**	**10**	**No degrading ice wedges in 2014; four wedges were vulnerable (PL2<10 cm)**
Mean (n=9)	**2022**	**71**	**31**	**49.1**	**5.9**	**8.4**	**63.6**	**14.3**	**No degrading or vulnerable ice wedges in 2022; PL2>10 cm for all the ice wedges**

ALASKA GEOBOTANY CENTER

The Alaska Geobotany Center (AGC) is dedicated to understanding northern ecosystems through the use of geographic information systems, remote sensing, field experiments, and cooperative team research projects. We share a commitment to excellence in field research and teaching with the goal of inspiring an appreciation of northern ecosystems and making our research and teaching relevant to societal issues and concerns, particularly issues relevant to the state of Alaska.

Alaska Geobotany Center
Institute of Arctic Biology
University of Alaska Fairbanks

P.O. Box 757000
Fairbanks, AK 99775-7000
Phone (907) 474-2459

www.geobotany.uaf.edu